Mathematics of Dengue Transmission Dynamics and Assessment of Wolbachia-based Interventions

by

Rahim Taghikhani

A Thesis Presented in Partial Fulfillment
of the Requirements for the Degree
Doctor of Philosophy

Approved July 2020 by the
Graduate Supervisory Committee:

Abba Gumel, Chair
Sharon Crook
Malena Espanol
Yang Kuang
Matthew Scotch

ARIZONA STATE UNIVERSITY

August 2020

ABSTRACT

Dengue is a mosquito-borne arboviral disease that causes significant public health burden in many trophical and sub-tropical parts of the world (where dengue is endemic). This dissertation is based on using mathematical modeling approaches, coupled with rigorous analysis and computation, to study the transmission dynamics and control of dengue disease. In Chapter 2, a new deterministic model was designed and used to assess the impact of local fluctuation of temperature and mosquito vertical (transvasorial) transmission on the population abundance of dengue mosquitoes and disease in a population. The model, which takes the form of a deterministic system of nonlinear differential equations, was parametrized using data from the Chiang Mai province of Thailand. The disease-free equilibrium of the model was shown to be globally-asymptotically stable when a certain epidemiological quantity is less than unity. Vertical transmission was shown to only have marginal impact on the disease dynamics, and its effect is temperature-dependent. Dengue burden in the province is maximized when the mean monthly temperature lie in the range [26-28] °C. A new deterministic model was designed in Chapter 3 to assess the impact of the release of *Wolbachia*-infected mosquitoes on curtailing the mosquito population and dengue disease in a population. The model, which stratifies the mosquito population in terms of sex and *Wolbachia*-infection status, was rigorously analysed to characterize the bifurcation property of the model as well as the asymptotic stability of the various disease-free equilibria. Simulations, using *Wolbachia*-based mosquito control from Queensland, Australia, showed that the frequent release of mosquitoes infected with the bacterium can lead to the effective control of the local wild mosquito population, and that such effective control increases with increasing number of *Wolbachia*-infected mosquitoes released (up to 90% reduction in the wild mosquito population, from their baseline values, can be achieved). It was also shown that the well-known feature of cytoplas-

mic incompatibility has very little effect on the effectiveness of the *Wolbachia*-based mosquito control.

ACKNOWLEDGMENTS

I would like to express my sincere gratitude to my advisor Professor Abba B. Gumel of the School of Mathematical and Statistical Sciences, Arizona State University, for the continuous supports, motivations and management for this dissertation. I am sincerely grateful for his comments and immense knowledge. I would also like to thank the rest of my thesis committee members: Professor Sharon Crook, Professor Malena Espanol, Professor Yang Kuang and Professor Matthew Scotch, for their insightful comments, suggestions and encouragement. My sincere thanks also goes to Ms. Joelle Park (Graduate Program Coordinator, SoMSS, ASU) for her continued support and kindness.

I am grateful to my family, Hadi (my father), Zahra (my mother) and Tahereh (my sister). I would like to express my deepest gratitude to my partner Blasina for her supports.

All with Love.

TABLE OF CONTENTS

CHAPTER Page

LIST OF TABLES

LIST OF FIGURES

Figure Page

Figure Page

Figure Page

Figure Page

Chapter 1

PRELIMINARIES

1.1 Mathematical Biology

Mathematical scientists (modelers, applied mathematicians, statisticians, computational mathematicians etc.) and biologists (e.g., public health practitioners, clinicians, epidemiologists etc.) have a long history of successful collaborations aimed at gaining insight into the transmission dynamics and control of emerging and re-emerging diseases of humans and non-human primates. These collaborations typically entail the design, analysis, parameterizations and simulations of robust mathematical models for studying the transmission dynamics and control of emerging and re-emerging diseases of public health importance (see, for instance, the pioneering works of Daniel Bernouli [17], Sir Ronald Ross [170] and Kermack-Mckenrick [94]). Various types of models, such as deterministic, stochastic, network, agents-based, spatial etc. [15; 52; 73; 109; 141; 174], have been designed and used for these settings. This dissertation is based on the use of mathematical modeling approaches to study the transmission dynamics and control of dengue fever, one of the most important vector-borne diseases affecting mankind [42; 69].

1.1.1 Vector-borne Diseases

A disease is a particular abnormal condition that negatively affects the structure or function of all or part of an organism, and that is not due to any immediate external injury [162]. Vectors (such as mosquitoes, sandflies etc.) are living organisms that can transmit infectious pathogens between humans, or from animals to humans [65; 171]. Many of these vectors are bloodsucking insects, which ingest disease producing

microorganisms during a blood meal from an infected host (human or animal) and later transmit it into a new host, after the pathogen has replicated [42; 69]. Often, once a vector becomes infectious, it is capable of transmitting the pathogen for the rest of its natural life during each subsequent bite/blood meal [195].

Vector-borne diseases (VBDs) are human illnesses caused by parasites, viruses and bacteria that are transmitted by vectors. Historically, malaria, dengue, yellow fever, plague, filariasis, louseborne typhus, trypanosomiasis, leishmaniasis, and other vector-borne diseases were responsible for more human disease and death in the 17th through the early 20th centuries than all other causes combined [42; 69]. The burden of these diseases is highest in tropical and subtropical areas, and they disproportionately affect the poorest populations [66; 161].

Since 2014, major outbreaks of dengue, malaria, chikungunya, yellow fever and Zika have affected numerous populations, claimed lives, and overwhelmed health systems in many countries [65; 171]. Other VBDs, such as Chikungunya, leishmaniasis and lymphatic filariasis, cause chronic diseases, life-long morbidity, disability and occasional stigmatisation [42]. In terms of human morbidity and mortality, malaria and dengue are the most important of these reemerging VBDs [66; 161]. Mosquito-borne diseases causes a huge burden on human societies. Recent vector control campaigns have resulted in promising declines in the incidence and prevalence of these diseases, notably malaria, but resistance to insecticides and drugs are on the rise, threatening to overturn these gains [10; 117; 119; 171].

VBDs can be classified into two categories, namely emerging (newly-emerging) or re-emerging. Emerging (or newly-emerging) diseases are infections that have newly appeared in the population, or have existed but are rapidly increasing in disease incidence or geographic range [120; 121]. Kilbourne [95] and Morse [121] state that a disease is new when its symptoms are distinct from any disease that has previously existed (and they are usually caused by preexisting zoonotic agents).

Re-emerging VBDs are diseases that were under control through the use of vector habitat modification and insecticides, but have re-emerged in recent times, and are spreading (including in geographical areas in which they have not been previously found) [65]. This category of VBDs are the most abundant form of VBDs, some of which are believed to have existed since 16th-18th century [65]. Since the focus of this dissertation is dengue, a mosquito-borne disease, it is instructive to provide some basic background on mosquito life cycle.

1.2 Mosquito Life Cycle

Mosquitoes involve a group of about 3,500 species of small insects that are flies that constitute the family *Culicidae* [10; 48]. The mosquito life cycle consists of four development stages, namely egg, larva, pupa, and adult stages [119; 134]. These are described in some detail below.

1. **Egg**: Eggs are laid one at a time or attached together to form rafts. They float on the surface of the water. Most eggs hatch into larvae within 48 hours; others might withstand subzero winters before hatching. Water is a necessary part of their habitat.

2. **Larva**: The larva (plural - larvae) lives in the water and comes to the surface to breathe. Larvae shed (molt) their skins four times, growing larger after each molt. Most larvae have siphon tubes for breathing and hang upside down from the water surface. The larvae feed on microorganisms and organic matter in the water. During the fourth molt the larva changes into a pupa. This stage takes 5-7 days, on average, (depending on temperature [48]).

3. **Pupa**: The pupal stage is a resting, non-feeding stage of development, but pupae are mobile, responding to light changes and moving (tumble) with a flip of their tails towards the bottom or protective areas. This is the time the mosquito

changes into an adult. This process is similar to the metamorphosis seen in butterflies when the butterfly develops-while in the cocoon stage from a caterpillar into an adult butterfly. In Culex species in the southern United States this takes about two days in the summer. When development is complete, the pupal skin splits and the adult mosquito emerges. Pupa stage takes 2-3 days, on average, (depending on temperature [48]).

4. **Adult**: The newly emerged adult rests on the surface of the water for a short time to allow itself to dry and all its body parts to harden. The wings have to spread out and dry properly before it can fly. Blood feeding and mating does not occur for a couple of days after the adults emerge. Adult mosquitoes survive 20-50 days, on average.

As stated earlier, the duration of each stage depends on both temperature and species characteristics. For instance, *Culex tarsalis*, a common mosquito in State of California, might go through its life cycle in 14 days at 70° F and take only 10 days at 80° F [10; 48]. On the other hand, some species have naturally adapted to go through their entire life cycle in as little as four days or as long as one month [119; 134]. Figure 1.3 depicts the life cycle of the *culex* mosquito.

While adult male mosquitoes feed on plant liquids, such as nectar, honeydew, fruit juices and other sources of sugar for energy, the adult female mosquitoes, in addition to feeding on sugar sources (for energy), feed on the blood of human and other animals solely to acquire the proteins needed for eggs development [139]. Once a blood meal is taken successfully (and eggs are developed), the adult female mosquito moves to a convenient breeding site where it lays its eggs. The chances of survival of the female adult mosquitoes depend on temperature and humidity, as well as their ability to successfully obtain a bloodmeal while avoiding host defenses [119; 134; 139].

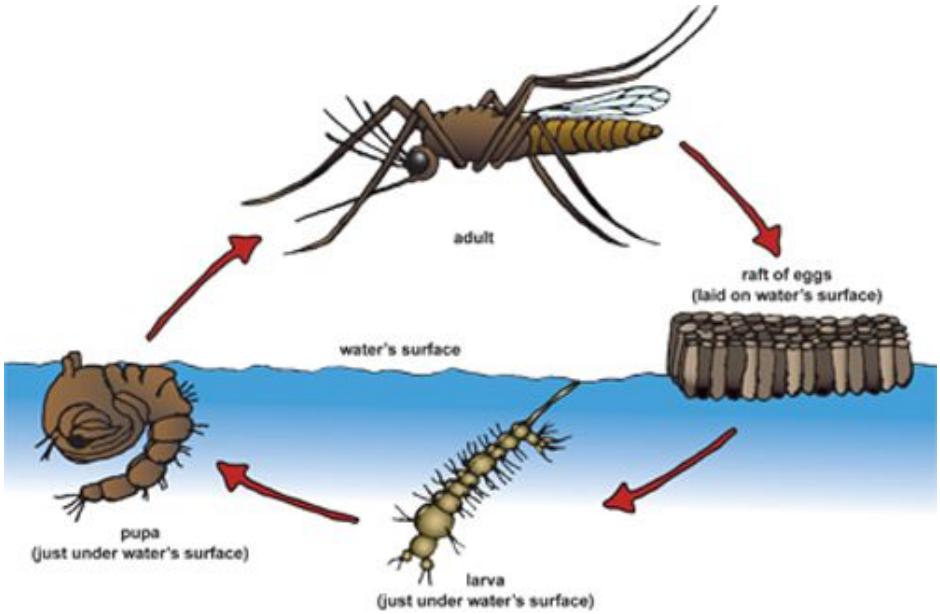

Figure 1.1: Life Cycle of *culex* Mosquito [122].

1.3 Dengue Fever

Dengue, caused by dengue virus (DENV), is a mosquito-borne, single positive-stranded RNA virus of the family *Flaviviridae*; genus *Flavivirus* [68; 131]. Four serotypes of the virus have been found [67; 154], all of which can cause the full spectrum of disease. Dengue virus has increased dramatically within the last 20 years, becoming one of the worst mosquito-borne human pathogens [33; 142]. Current estimates indicate that as many as 50-100 million infections occur each year [74] and causing over 20,000 deaths, especially among children under the age of 15. Dengue remains endemic in over 100 countries [41; 136; 151; 168; 180] (see Figure 1.2 for global distribution of dengue disease).

Dengue fever (DF) is an acute illness when left untreated and can lead to severe case of dengue called the dengue hemorrhagic fever (DHF) or dengue shock syndrome (DSS), which are more common after a secondary infection with dengue virus [63; 151].

Infection with one serotype enhance long-term protective immunity to reinfection with the serotype but the individual remains susceptible (or gain only a short-term

immunity) to all other serotypes [47; 63; 41; 180]. In addition, an important characteristic of DF and DHF/DSS is its properties of antibody-dependent enhancement (ADE), whereby dengue infection becomes more severe in individual who have acquired dengue antibodies after recovering from a previous dengue infection [47; 78; 96; 173].

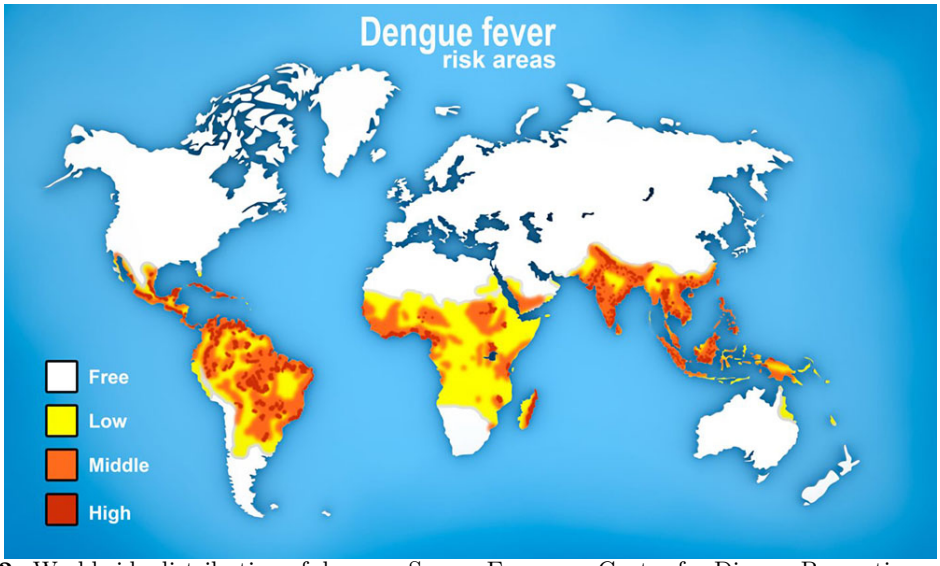

Figure 1.2: Worldwide distribution of dengue. Source European Center for Disease Prevention and Control [50].

Aedes aegypti mosquito is largely responsible for the transmission of dengue viruses that cause disease in humans. The virus is taken up with an infected blood meal from which it will first infect the mosquito gut tissue [40].

Figure 1.3: *Aedes-aegypti* mosquito. Source: Centers for Disease Control and Prevention [32].

1.3.1 Control Strategies Against Dengue Disease

The control of dengue has been based on a number of strategies [10; 117; 149], including source reduction (locating and destroying mosquitoes breeding places), larvicides, ultra-low volume (ULV) application of aerosol adulticides [10; 117; 149]. The first two strategies have been applied with varying degrees of success. However, there is still considerable controversy over the efficacy of the current methods for controlling adult mosquitoes [10; 117; 149]. At the time of the advent of DDT (*Dichloro-Diphenyl-Trichloroethane*), *Aedes aegypti* was highly susceptible to this agent [149]. DDT is a colorless, tasteless, and almost odorless crystalline chemical compound, an organochlorine. Originally developed as an insecticide, it became infamous for its environmental impacts [10; 117]. DDT was first synthesized in 1874 by the Austrian chemist Othmar Zeidler [10; 117]. The successful application of DDT resulted in the eradication of *Aedes aegypti* from 22 countries in the Americas in 1962 and from all countries in the Mediterranean region in 1972 [149]. DDT was abandoned due to the evolution of resistant insects and due to the environmental impacts of the insecticide [10; 117].

Therefore, the control of dengue disease shifted to the use og other approaches, such as, source reduction, larvicides and adulticides from other chemical families [10; 117]. From a theoretical perspective, significant advances were made by George Macdonald in the 1950s [110], who proposed that the most effective control strategy against vector-borne infections is to kill adult mosquitoes.

Additionally, control effort have also been emphasized on public-health programs that promote and encourage communal understanding of the vector specie and the disease, to enhance community vector control and practice of personal protection [68; 149; 151]. However, these substantial vector control efforts have not stopped the rapid emergence and global spread of DENV [68; 131]. A vaccine for DENV (*Dengvaxia* by Sanofi Pasteur) was released in 2015 [183]. However, the ADE property of the DENV plays an important factor for the development of dengue vaccine as "ADE suggest that dengue vaccines must induce protective neutralizing antibodies to all 4 serotypes simultaneously, rather than sequentially, to avoid enhancement of dengue illness after subsequent infection" [47]. As a result, the manufacturer (Sanofi) issued a press release in 2017 stating that "for individuals who have not been previously infected by dengue virus, vaccination should not be recommended" [156].

Over the years, a range of alternative biological control measures, aimed at suppressing or replacing the mosquito vector *via* the mass release of genetically-modified mosquitoes, have been proposed [3; 60; 88]. These modifications include the sterilization of adult male mosquitoes (SIT) to reduce the reproduction of adult wild female mosquitoes [3; 23], genetic modification to introduce lethal genes [60; 160] or introduction of genes that reduce disease transmission [88; 89] into wild adult female mosquito population and the infection of mosquitoes by a second agent, such as the bacterium *Wolbachia*, aimed at suppressing pathogen transmission [89].

1.3.2 Mathematical Preliminaries

This section introduces some of the key mathematical theories and methodologies relevant to the dissertation. Consider the equation below

$$\frac{d\mathbf{x}}{dt} = f(\mathbf{x}),\ x \in \mathbb{R}^n. \tag{1.3.1}$$

The equation (1.3.1) is an *ordinary differential equation (ODE)* and the right-hand side function, $f(\mathbf{x})$, is called a *vector field*. ODEs that explicitly depend on time are called *non-autonomous*, while those that are independent of time are called *autonomous*. This dissertation focuses on autonomous ODEs.

Definition 1.3.1 *([140]). An equilibrium solution of* (1.3.1) *is given by* $\mathbf{x} = \bar{\mathbf{x}} \in \mathbb{R}^n$ *where* $f(\bar{\mathbf{x}}) = 0$. *The point* $\bar{\mathbf{x}}$ *is called an equilibrium point.*

Definition 1.3.2 *([140]). The class* C^1 *consists of all differentiable functions whose derivative is continuous; such functions are called continuously differentiable.*

Theorem 1.3.1 *(Fundamental Existence-Uniqueness Theorem [140]). Let* E *be an open subset of* $\mathbb{R}^n$ *containing* $\mathbf{x}_0$ *and assume that* $f \in C^1(E)$. *Then there exists an* $a > 0$ *such that the initial value problem (IVP)*

$$\frac{d\mathbf{x}}{dt} = f(\mathbf{x}),\ \ \mathbf{x}(\mathbf{0}) = \mathbf{x}_0\,,$$

has a unique solution $\mathbf{x}(t)$ *on the interval* $[-a, a]$.

1.3.3 Stability of Solutions

The following are standard definitions and theorems required to analyze the asymptotic stability of an equilibrium of an autonomous system. Let $\bar{\mathbf{x}}(t)$ be any solution of (1.3.1). Then, $\bar{\mathbf{x}}(t)$ is stable if solutions starting "close" to $\bar{\mathbf{x}}(t)$ at a given time remain

close to $\bar{\mathbf{x}}(t)$ for all later times. It is asymptotically stable if nearby solutions converge to $\bar{\mathbf{x}}(t)$ as $t \to \infty$. These concepts are formally defined below.

Definition 1.3.3 *([192]) The equilibrium $\bar{\mathbf{x}}(t^*)$ is said to be stable if given $\epsilon > 0$, there exists a $\delta = \delta(\epsilon) > 0$ such that, for any solution $\mathbf{y}(t)$ of (1.3.1) satisfying $|\bar{\mathbf{x}}(t^*) - \mathbf{y}(t_0)| < \delta$, it follows $|\bar{\mathbf{x}}(t^*) - \mathbf{y}(t)| < \epsilon$ for $t > t^*$, $t^* \in \mathbb{R}$.*

Definition 1.3.4 *([192]) The equilibrium $\bar{\mathbf{x}}(t^*)$ is said to be asymptotically stable if it is stable and, in addition, there exists $\delta_0 > 0$ such that whenever $|\bar{\mathbf{x}}(t^*) - \mathbf{y}(t_0)| < \delta_0$, then $\lim_{t\to\infty} |\bar{\mathbf{x}}(t^*) - \mathbf{y}(t)| = 0$.*

Definition 1.3.5 *A solution which is not stable is said to be unstable.*

Theorem 1.3.2 *[140]. Suppose all the eigenvalues of $Df(\bar{\mathbf{x}})$ have negative real parts. Then the equilibrium solution $\mathbf{x} = \bar{\mathbf{x}}$ of the system (1.3.1) is locally-asymptotically stable, and unstable if at least one of the eigenvalues has positive real part.*

Definition 1.3.6 *([192]). A function $V : \mathbb{R}^n \to \mathbb{R}$ is said to be a positive-definite function if*

- *$V(\mathbf{x}) > 0$ for all $\mathbf{x} \neq 0$,*
- *$V(\mathbf{x}) = 0$ if and only if $\mathbf{x} = 0$,*
- *$V(\mathbf{x}) \to \infty$ as $\mathbf{x} \to \infty$.*

The general Lyapunov Function Theorem is given below.

Theorem 1.3.3 *([192]) Let $\bar{\mathbf{x}}$ be an equilibrium solution of the system (1.3.1) and $V : U \to \mathbb{R}$ be a C^1 function defined on some neighbourhood U of $\bar{\mathbf{x}}$ such that*

1. *V is positive definite*
2. *$\dot{V}(\mathbf{x}) \leq 0$ in $U \setminus \{\bar{\mathbf{x}}\}$.*

Then $\bar{\mathbf{x}}$ is stable. Moreover, if

3. $\dot{V}(\mathbf{x}) < 0$ *in* $U \setminus \{\bar{\mathbf{x}}\}$

then $\bar{\mathbf{x}}$ *is asymptotically stable. Any function that satisfies the above items is called Lyapumov function. If* $U = \mathbb{R}^n$*, then* $\bar{x}$ *is globally-asymptotically stable (GAS) whenever Items 1 and 3 of Theorem 1.3.3 hold.*

The equilibrium $\bar{\mathbf{x}}$ is GAS if it attracts all solutions in the feasible region of the system.

Compartmental mathematical models have been widely used to gain insight into the spread and control of emerging and re-emerging human diseases, dating back to the pioneering work of Bernoulli (on modelling the transmission dynamics of smallpox) in 1760 and the likes of Ross, Kermack and McKendrick and others (see [6; 81; 152] and the references therein). The dynamics of these models tend to generally be completely characterized by a threshold quantity, known as the *basic reproduction number* (denoted by $\mathcal{R}_0$), which measures the average number of new cases an index case can generate in a completely susceptible population [81; 152]. Typically, when $\mathcal{R}_0$ is less than unity, a small influx of infected individuals will not generate large outbreaks, and the disease dies out in time (in this case, the corresponding disease-free equilibrium (DFE) is LAS). On the other hand, the disease will persist if $\mathcal{R}_0$ exceeds unity, where a stable endemic equilibrium point (EEP) exists. This phenomenon, where the DFE and an EEP exchange their stability at $\mathcal{R}_0 = 1$, is known as forward bifurcation (or transcritical bifurcation).

The forward bifurcation phenomenon was first noted by Kermack and McKendrick [94], and has been observed in many disease transmission models. In general, for models that exhibit forward bifurcation, the requirement $\mathcal{R}_0 < 1$ is necessary and sufficient for disease elimination (i.e., the number of infectives at steady-state depends continuously on $\mathcal{R}_0$ [6; 81; 152]).

A number of studies have shown that whilst $\mathcal{R}_0 < 1$ is necessary for disease elimination, this requirement may not be sufficient. This is owing to the phenomenon

of backward bifurcation, where a stable endemic equilibrium co-exists with a stable disease- free equilibrium for $\mathcal{R}_0 < 1$ [81; 152]. This phenomenon has been observed in numerous disease transmission models such as those in [26; 73; 94; 129]. The phenomenon of backward bifurcation has important public health implication, since it renders the classical requirement of reproduction number being less than unity to be insufficient (in general) for disease elimination.

1.4 Outline of the Dissertation

The research work in this dissertation is based on use of mathematical approaches, together with rigorous analysis (using theories and techniques from nonlinear dynamical systems) and computations (including statistics and data analysis) to gain the insights into the population ecology of the dengue mosquito (*Aedes aegypti* and disease in a community. In particular, I studied the impact of local temperature fluctuation and mosquito vertical transmission on the population abundance of *Aedes aegypti* mosquito and dengue disease in Chiang Mai province of Thailand. I also studied the impact of the release of *Wolbachia*-infected mosquitoes on the control of dengue mosquitoes and disease in Queensland, Australia. Chapter 1 provides a detailed introduction of the dissertation, as well as brief review of some of the mathematical tools (theories, techniques, concepts etc.) used in the dissertation.

In Chapter 2, a new deterministic model is designed and used to assess the combined impact of local temperature fluctuation and vector vertical transmission on dengue transmission dynamics and control. The model, which incorporates many pertinent aspects of dengue disease (such as immature mosquito structure, vector vertical transmission, larval mortality, effects of temperature variability and dengue ecology and epidemiology in the vector and human hosts populations) is rigorously analyzed. In particular, theoretical results for the local and global asymptotic stability of the associated disease-free equilibria are provided.

In Chapter 3, I studied the potential impact of *Wolbachia*-based intervention on the population abundance of dengue mosquitoes and and disease in a population. I designed a new model, which incorporates numerous crucial aspects of the *Wolbachia*-vector-pathogen dynamics (such as fitness cost of *Wolbachia* infection, sex structure in the vector, dynamics of the aquatic stages of vector life cycle, vertical and horizontal transmission of *Wolbachia*, the effect of *Wolbachia* infection in mosquitoes and dengue epidemiology in humans). The model which takes the form of an impulsive deterministic system of nonlinear differential equations, is also rigorously analyzed.

Chapter 2

MATHEMATICS OF DENGUE TRANSMISSION DYNAMICS: ROLES OF VECTOR VERTICAL TRANSMISSION AND TEMPERATURE FLUCTUATIONS

2.1 Introduction

Dengue, a viral disease caused by one of the four closely-related *Flavivirus* (DENV 1-4), is endemic in many tropical and subtropical regions of the world with over 2.5 billion people at risk of acquiring dengue infection [194]. Annually, the disease accounts for approximately 50 million cases and $20,000$ fatalities [131; 194]. Dengue and dengue haemorrhagic fever are on the rise in the Americas [68; 138]. In Latin America, about 78% of the population (around 81 million people) live in urban areas, and the incidence of the rise has been on the increase in the past decade [64; 137]. In Puerto Rico, for example, almost 10,000 dengue fever cases are reported annually (dengue outbreaks are recorded in almost all Caribbean countries and Mexico [68; 138]).

Dengue has also been periodically endemic in Texas over the past 20 years [68; 138]. The disease, which is transmitted to humans by female *Aedes aegypti* mosquito (following taking a blood meal, needed for eggs laying), threatens other non-endemic countries in Europe. For instance, the first local transmission of the disease in France and Croatia was recorded in 2010 [127; 153] (outbreaks were also recorded in Madeira islands of Portugal in 2012, imported cases (mainly from Portugal) were also detected in three other European countries [153; 194]). Furthermore, in 2013, dengue outbreaks were recorded in Miami, USA and Yunnan province of China [45; 201].

Dengue causes life-threatening complications (such as Dengue Hemorrhagic fever and Dengue Shock syndrome [77]), often triggered by immune responses to secondary infections [184].

The incidence of dengue has significantly increased globally over the last few years [45; 153; 194]. This is due to a number of factors [64] (notably the geographic expansion, enhanced transmission intensity in endemic areas, variability in local weather and habitat conditions). Furthermore, vertical (transovarial) transmission, which has been observed in dengue transmission dynamics [38; 135], is believed to retain dengue viral disease in nature during inter-epidemic periods of dengue [8].

Changes in local temperature is known to significantly affect the dynamics of vector-borne diseases, including dengue [64; 187]. In particular, temperature variability affects the maturation, survival, biting rate and abundance of dengue-competent mosquitoes [64]. As the global temperature is increasing due to greenhouse-gas effects (daily average temperature in southern borders of USA have increased by 0.4°C over the past 30 years [93]; and it is estimated that global temperature will rise by $1.0 - 3.5$°C over the next 100 years [64; 187]), it is imperative to carry out detailed modeling studies to analyse the potential impact of such increases on the dynamics of vector-borne diseases (it should be mentioned that health risks due to these climate changes differ between countries, depending on the level of infrastructure and economic development [93]).

Vertical transmission (i.e., disease transmission from an infected mother to a child) is also another factor affecting the dynamics of many pathogens and diseases including dengue [2; 8; 39; 92; 98]. For instance, evidence for vertical transmission has been established in the dynamics of VBDs such as, La Crosse virus [115], St Louis Encephalitis virus ([124]), West Nile virus [14] and Yellow fever [44]. Vertical transmission of dengue virus has been demonstrated in the lab in *Aedes aegypti*, *Aedes albopictus* and *Aedes scutellaris* mosquitoes [57; 91; 116; 154; 164] (including in the wild [8; 92; 98]). It should also be mentioned that local temperature affects vertical transmission in the vector population. In subtropical regions, for example, dengue disease shows a resurgent pattern with yearly epidemics (which starts typically in the months with heavy rains and heat, peaking some 3 or 4 months after the beginning

of the rainy season) [118]. In the dry months, the number of dengue cases typically drops essentially to zero (because the disease (vector) has virtually disappeared during this period) [118]. Dengue continues to re-emerge for many years in some regions [39; 64]. This (re-emergence) is attributed to many factors, such as the survival of long-lived infected adult female mosquitoes, infected eggs (laid by infected adult female mosquitoes, vertically) that remain infected during the dry season (and their hatching during the beginning of the raining season) [39; 64; 118].

Although numerous climate variables such as temperature, precipitation and humidity [34; 64; 93; 101] affect the transmission dynamics of vector-borne diseases, this dissertation focuses on the singular effects of temperature. Consequently, the purpose of the current chapter is to use mathematical modeling approaches to gain insight into the role of temperature variability, and vertical transmission in the vector population, on the transmission dynamics of dengue disease in the community.

A new deterministic model, which includes the dynamics of both the immature (i.e., modeling the eggs-larvae-pupae lifecycle stages) and adult female *Aedes aegypti* mosquitoes, as well as the effect of vector vertical transmission and temperature variability, will be designed. The chapter is organized as follows. The model is designed in Section 2.2. The case of the model where temperature is fixed (i.e., the *autonomous* equivalent of the *non-autonomous* model) is rigorously analysed (for the existence and asymptotic stability of some of its equilibria, as well as to characterize bifurcation types) in Section 2.3. Uncertainty and sensitivity analysis of the parameters of this version of the model, as well as numerical simulations of the effect of temperature variability, are also carried out. The (full) non-autonomous model, which accounts for daily fluctuations in local temperature, is rigorously analysed in Section 2.4.

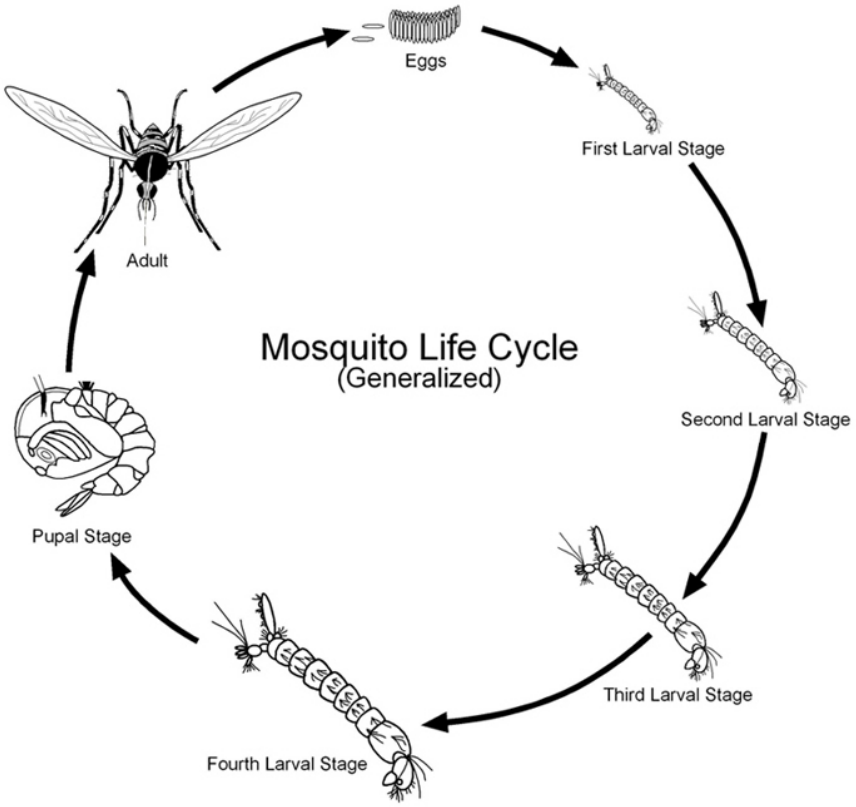

Figure 2.1: Schematic Description of the Lifecycle of the *Aedes Aegypti* Mosquito [48].

2.2 Model Formulation

This study is motivated by dengue transmission dynamics in Chiang Mai province of Thailand [36; 142; 176]. Although there are four dengue serotypes (DENV 1-4), serological data from this province (for 2004 to 2010) shows that one of the four serotypes typically dominates the others each year [142] (for example, in the year 2004, the percentage prevalence of DENV-1, DENV-2, DENV-3 and DENV-4 were 56.4%, 28.2%, 5.1% and 10.3%, respectively [142]). Consequently, this chapter will consider only one dengue serotype in the community (this simplifying assumption allows for the tractability of the mathematical analysis to be carried out; a number of models for dengue transmission dynamics also use a single dengue serotype, such as those in [2; 39; 49; 61; 67; 77]).

The model to be designed is based, first of all, on splitting the total immature mosquito population at time t (denoted by $N_{VI}(t)$) into compartments of susceptible eggs ($S_E(t)$), infected eggs ($I_E(t)$), susceptible larvae ($S_L(t)$), infected larvae ($I_L(t)$), susceptible pupae ($S_P(t)$) and infected pupae ($I_P(t)$), so that

$$N_{VI}(t) = S_E(t) + I_E(t) + S_L(t) + I_L(t) + S_P(t) + I_P(t).$$

Furthermore, the total adult female mosquito population at time t (denoted by $N_{VA}(t)$) is split into the sub-populations of susceptible adult female mosquitoes ($S_M(t)$) and infected adult female mosquitoes (($I_M(t)$). Thus,

$$N_{VA}(t) = S_M(t) + I_M(t).$$

Finally, the total human population at time t (denoted by $N_H(t)$) is sub-divided into susceptible ($S_H(t)$), exposed ($E_H(t)$), symptomatic ($I_H(t)$) and recovered ($R_H(t)$) humans. Hence,

$$N_H(t) = S_H(t) + E_H(t) + I_H(t) + R_H(t).$$

The model to be designed in this chpater incorporates the effect of variability in ambient (air) temperature (denoted by $T(t)$) on the dynamics of the mosquito-borne disease in a community. It is assumed that $T(t)$ is non-negative, continuous and bounded periodic functions of t (it is also assumed, for mathematical convenience, that air temperature and the temperature near the surface of the water are approximately the same; so that we can use $T(t)$ to approximate the temperature near the surface of the water where the development process of the immature mosquitoes occurs [8]).

The weather-driven model for the transmission dynamics of dengue, with vertical transmission in the vector, is given by the following deterministic system of non-linear differential equations (the state variables and parameters of the model are described in Table 3.2, their ranges and values are given in Table 2.3; a flow diagram of the model

is depicted in Figure 2.2):

$$
\begin{aligned}
\frac{dS_E(t)}{dt} &= \phi_V(T)\left[1-\frac{N_{VA}(t)}{K_V(t)}\right]_+ [S_M(t)+(1-r)I_M(t)] - [\sigma_E(T)+\mu_E(T)]\,S_E(t),\\
\frac{dI_E(t)}{dt} &= r\phi_V(T)\left[1-\frac{N_{VA}(t)}{K_V(t)}\right]_+ I_M(t) - [\sigma_E(T)+\mu_E(T)]\,I_E(t),\\
\frac{dS_L(t)}{dt} &= \sigma_E(T)S_E(t) - \{\sigma_L(T)+\mu_L(T)+\delta_L(T)\,[S_L(t)+I_L(t)]\}\,S_L(t)\\
\frac{dI_L(t)}{dt} &= \sigma_E(T)I_E(t) - \{\sigma_L(T)+\mu_L(T)+\delta_L(T)\,[S_L(t)+I_L(t)]\}\,I_L(t),\\
\frac{dS_P(t)}{dt} &= \sigma_L(T)S_L(t) - [\sigma_P(T)+\mu_P(T)]\,S_P(t),\\
\frac{dI_P(t)}{dt} &= \sigma_L(T)I_L(t) - [\sigma_P(T)+\mu_P(T)]\,I_P(t),\\
\frac{dS_M(t)}{dt} &= f_V\sigma_P(T)S_P(t) - [\lambda_{HV}(T,N_H(t),N_{VA}(t))+\mu_V(T)]\,S_M(t),\\
\frac{dI_M(t)}{dt} &= f_V\sigma_P(T)I_P(t) + \lambda_{HV}(T,N_H(t),N_{VA}(t))S_M(t) - \mu_V(T)I_M(t),\\
\frac{dS_H(t)}{dt} &= \Pi_H - [\lambda_{VH}(T,N_H(t),N_{VA}(t))+\mu_H]\,S_H(t),\\
\frac{dE_H(t)}{dt} &= \lambda_{VH}(T,N_H(t),N_{VA}(t))S_H(t) - (\sigma_H+\mu_H)E_H(t),\\
\frac{dI_H(t)}{dt} &= \sigma_H E_H(t) - (\gamma_H+\mu_H)I_H(t),\\
\frac{dR_H(t)}{dt} &= \gamma_H I_H(t) - \mu_H R_H(t),
\end{aligned}
\tag{2.2.1}
$$

where,

$$
\begin{aligned}
\lambda_{HV}(T,N_H(t),N_{VA}(t)) &= \frac{a_V(T)\beta_V(T)I_H(t)}{N_H(t)},\\
\lambda_{VH}(T,N_H(t),N_{VA}(t)) &= \frac{a_V(T)\beta_H(T)I_M(t)}{N_H(t)}.
\end{aligned}
\tag{2.2.2}
$$

In the model (2.2.1), eggs are laid by adult female *Aedes aegypti* mosquitoes at a logistic growth rate $\phi_V(T)\left[1-\frac{N_{VA}(t)}{K_V(t)}\right]_+$, where $\phi_V(T)$ is the temperature-dependent egg oviposition rate, $K_V(t)$ is the carrying capacity of the breeding habitats for adult female mosquitoes to lay eggs. The notation $(m)_+$, where $m_+ = \max\{0, m\}$ with

$m > 0$, is used to ensure that the term $\left(1 - \frac{N_{VA}(t)}{K_V(t)}\right) \geq 0$ for all t. The parameter r (with $0 \leq r < 1$) represents the proportion of mosquito offsprings that are born infected (due to vertical transmission). Table 2.1 shows the average proportion of eggs laid that are infected, for various subtypes of dengue fever, based on laboratory experiments [67; 154].

Table 2.1 Proportion of Infected Eggs (r) for Various Dengue Subtypes.

Species	Dengue subtype	Proportion of infected eggs (r) *per* $1,000$	Reference
Ae. aegypti	DENV-1-4	[0.61-15]	[67; 154]
Ae. albopictus	DENV-1	[1.7-14]	[67]
	DENV-2	[0.91-2.5]	[67]
	DENV-3	[0.23-0.78]	[67]
	DENV-4	[0.22-5.2]	[67]

Eggs hatch into larvae at a temperature-dependent rate $\sigma_E(T)$, larvae mature into pupae at a temperature-dependent rate $\sigma_L(T)$, and pupae become adult female mosquitoes at a temperature-dependent rate $f_V\sigma_P(T)$ (where $0 < f_V < 1$ is the proportion of new adult mosquitoes that are females). Eggs, larvae and pupae suffer natural mortality loss at temperature-dependent rates $\mu_E(T), \mu_L(T)$ and $\mu_P(t)$, respectively. Larvae suffer additional density-dependent mortality at a temperature-dependent rate $\delta_L(T)\left(S_L(t) + I_L(t)\right)$ [109].

Susceptible adult female mosquitoes acquire dengue infection, following effective contact with an infected human (after taking a blood meal), at a rate λ_{HV} (given in (2.2.2)), where $a_V(T)$ is the temperature-dependent effective contact (biting) rate of adult female mosquitoes on humans (regardless of infectious status of the vector or the host), $\beta_V(T)$ is the temperature-dependent probability that a bite from a susceptible adult female mosquito to an infected human results in an infection. Adult mosquitoes suffer natural death at a temperature-dependent rate ($\mu_V(T)$). The parameter Π_H represents the *per capita* recruitment rate of humans into the community (by birth or immigration). Susceptible humans acquire dengue infection, following effective contact

with an infected adult female mosquito, at a rate λ_{VH} (given in (2.2.2)), where $a_V(T)$ is as defined above, and $\beta_H(T)$ is the temperature-dependent probability of infection from an infected mosquito to a susceptible human *per* bite. Exposed humans develop clinical symptoms of the disease at a rate σ_H. Infectious humans recover at a rate γ_H (it is assumed that recovery induces permanent immunity against reinfection). Natural death occurs in all human compartments at a rate μ_H. Since dengue-induced mortality in humans is generally negligible [35; 53; 61; 104; 157] (for instance, there were only 126 dengue-induced fatalities in Thailand in 2017 [157]), no human disease-induced mortality is assumed in the model. Furthermore, no disease-induced mortality is assumed in the adult mosquito population.

The model (2.2.1) is an extension of numerous dengue transmission models that include vertical transmission in the vector population (such as those in [2; 39; 49; 61; 67; 77]) by (*inter alia*):

(i) adding the dynamics of immature mosquitoes (this was not included in [49; 61; 77]);

(ii) incorporating the effect of temperature variability (this was not considered in [2; 49; 61]);

(iii) including the effects of temperature on vertical transmission in the vector population and on the dynamics of dengue disease (this was not considered in [39; 49; 77]).

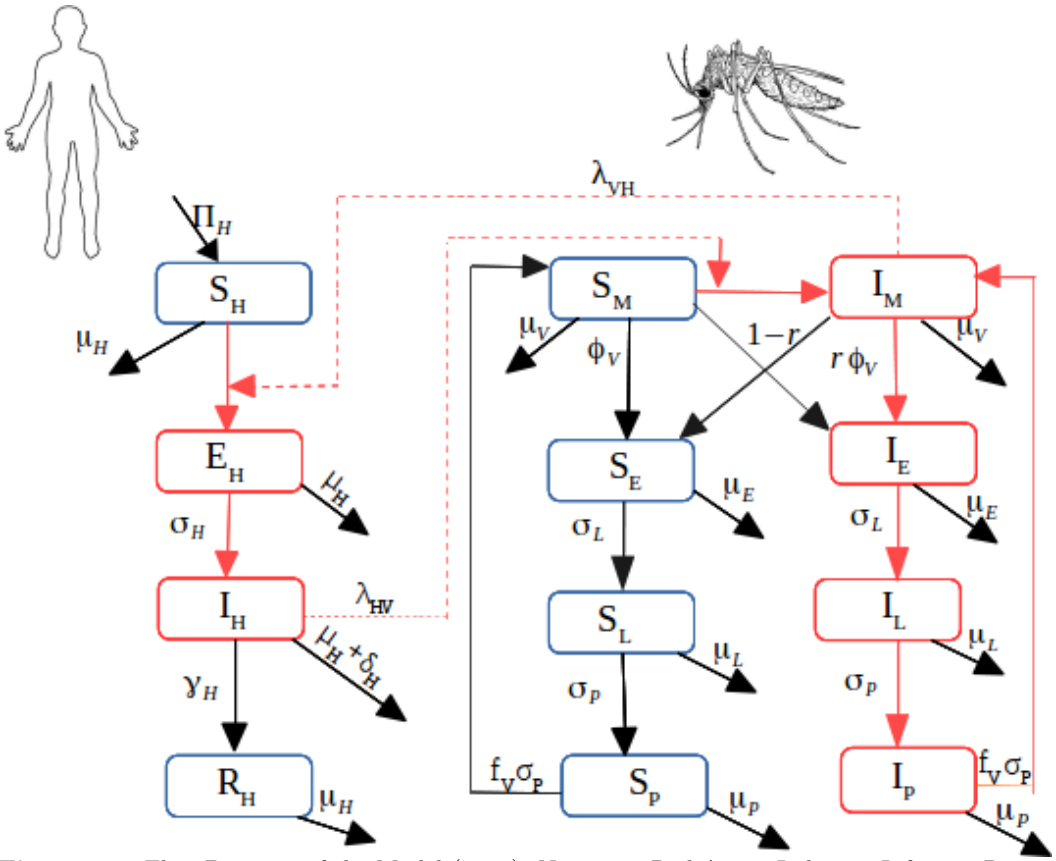

Figure 2.2: Flow Diagram of the Model (2.2.1). Notation: Red Arrow Indicates Infection Route.

Table 3.2. Description of Variables and Parameters of the Model (2.2.1)

Symbol	**Description**
Variables	
S_E	Population of susceptible eggs
I_E	Population of infected eggs
S_L	Population of susceptible larvae
I_L	Population of infected larvae
S_P	Population of susceptible pupae
I_P	Population of infected pupae
S_M	Population of susceptible adult female mosquitoes
I_M	Population of infected adult female mosquitoes
S_H	Population of susceptible humans
E_H	Population of latently-exposed humans
I_H	Population of symptomatically-infected humans
R_H	Population of recovered humans

N_{VI}	Total population of immature mosquitoes
N_{VA}	Total population of adult female mosquitoes
N_H	Total population of humans
Parameters	
$\sigma_E(T)$	Hatching rate of eggs into larvae
$\mu_E(T)$	Natural mortality rate of eggs
$\sigma_L(t)$	Maturation rate of larvae to pupae
$\mu_L(T)$	Natural mortality rate of larvae
$\delta_L(T)$	Density-dependent mortality rate of larvae
$\sigma_P(T)$	Maturation rate of pupae to adult mosquito
$\mu_P(T)$	Natural mortality rate of pupae
$\lambda_{HV}(T, N_H, N_{VA})$	Transmission rate from infected humans to susceptible mosquitoes
$\lambda_{VH}(T, N_H, N_{VA})$	Transmission rate from infected mosquitoes to susceptible humans
$a_V(T)$	*Per capita* contact (biting) rate of adult female mosquitoes on humans
$\phi_V(T)$	*Per capita* egg oviposition rate
$\mu_V(T)$	Natural mortality rate of adult mosquitoes
$K_V(t)$	Carrying capacity of breeding habitats for adult female mosquitoes to lay eggs
f_V	Proportion of new adult mosquitoes that are females
μ_H	Natural mortality rate of humans
σ_H	Rate of development of disease symptoms in humans
γ_H	Recovery rate for humans
Π_H	Recruitment rate (by birth and immigration) into the community
β_V	Probability of infection of a susceptible mosquito *per* bite on an infected human
β_H	Probability of infection of a susceptible human *per* bite by an infected mosquito
r	Proportion of infected eggs laid by infected adult female mosquitoes (due to vertical transmission)

2.2.1 *Functional Forms of Temperature-dependent Parameters for Adult Mosquitoes*

The functional forms of the temperature-dependent parameters of the model related to adult mosquitoes *Aedes aegypti* (namely, $a_V(T)$, $\beta_H(T)$, $\beta_V(T)$,$\phi_V(T)$ and $\mu_V(T)$) are defined as follows (for $12.4°\text{C} < T(t) < 32°\text{C}$):

1. The biting rate of adult female mosquitoes on the human host (a_V) is given by (see [159], Figure 5):

$$a_V(T) = 0.0943 + 0.0043T. \tag{2.2.3}$$

2. The probability of infection from an infected mosquito to a susceptible human (β_H) *per* bite is given by (see [103], Supporting Information) :

$$\beta_H(T) = 0.001044T(T - 12.286)\sqrt{32.461 - T}. \tag{2.2.4}$$

3. The probability of infection from an infected human to a susceptible mosquito *per* bite (β_V) is given by (see [103], Supporting Information):

$$\beta_V(T) = -0.9037 + 0.0729T. \tag{2.2.5}$$

4. The oviposition rate (ϕ_V) is given by ([103]):

$$\phi_V(T) = -15.837 + 1.2897T - 0.0163T^2. \tag{2.2.6}$$

5. The mortality rate μ_V of the *Aedes aegypti* mosquito is given by [198]:

$$\mu_V(T) = 0.8692 - 0.159T + 0.01116T^2 - 3.408 \times 10^{-4}T^3 + 3.809 \times 10^{-6}T^4. \tag{2.2.7}$$

The aforementioned functional forms are depicted in Figure 2.3. Furthermore, typically, a sinusoidal function of the following form is used to account for hourly fluctuations in local ambient temperature [130]:

$$T(t) = T_0 - \frac{\Delta_T}{2} \sin\Big[\frac{2\pi}{24}\Big(t_h + 14\Big)\Big], \tag{2.2.8}$$

where T_0 is the mean daily air temperature, Δ_T captures variation about the mean (i.e., Δ_T is the diurnal temperature range), and t_h denotes for time in hour for any given day. If a formulation such as (2.2.8) is used for the temperature-dependent functional forms, then the parameters defined in Equations (2.2.3)-(2.2.7) are time-dependent. Hence, the model (2.2.1) is *non-autonomous*. However, if fixed temperature values are used (e.g., using the mean daily or mean monthly temperature), then each of the parameters defined in Equations (2.2.3)-(2.2.7) is constant. Hence, the model (2.2.1) is *autonomous* in this case. In the absence of good data to realistically derive the functional forms for the other temperature-dependent parameters related to the immature *Aedes aegypti* mosquitoes (i.e., $\sigma_E(T)$, $\mu_E(T)$, $\sigma_L(T)$, $\mu_L(T)$, $\sigma_P(T)$ and $\mu_P(T)$), numerical simulations of the model (2.2.1) will be carried out using fixed (constant) values for these parameters (available in the literature).

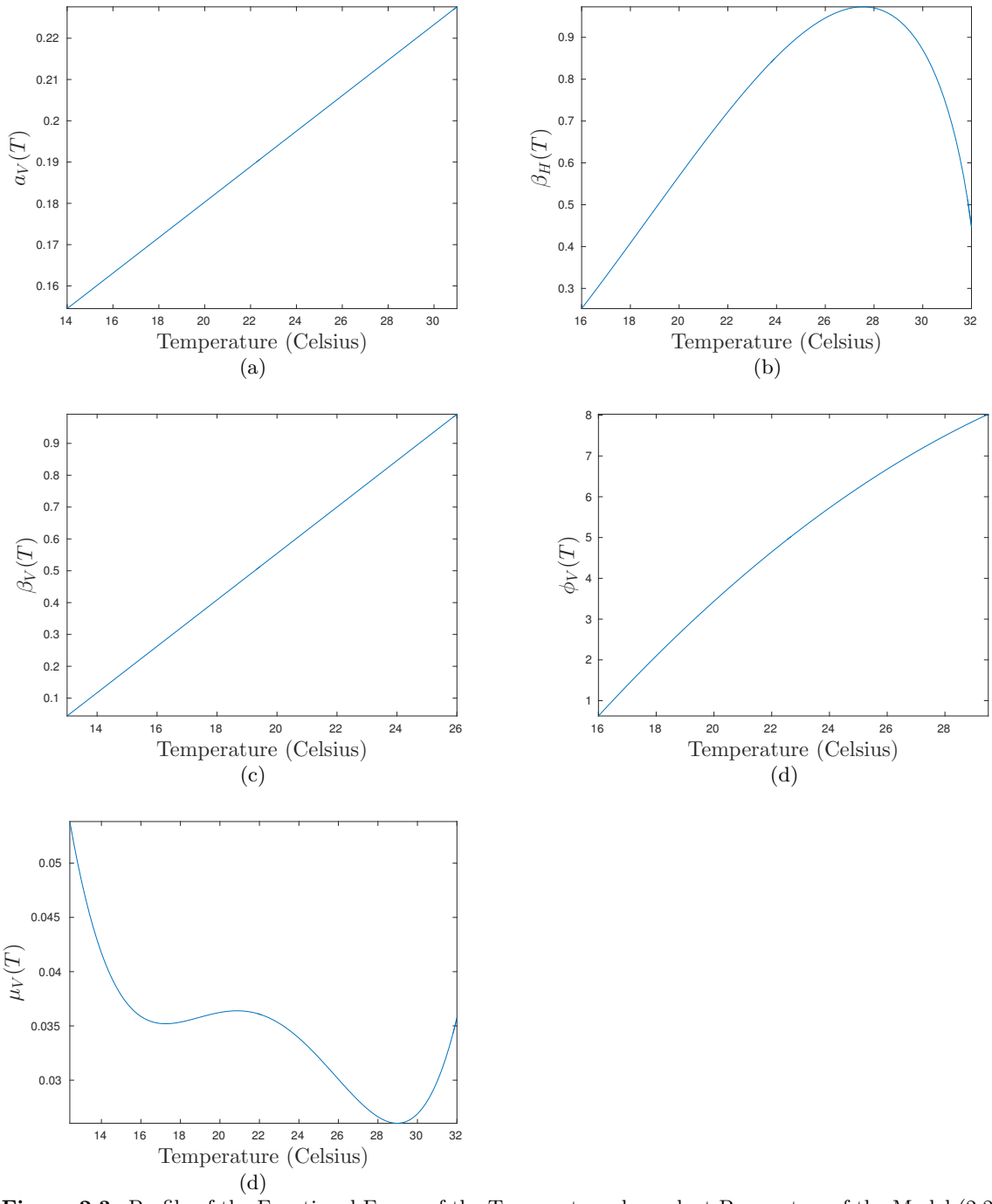

Figure 2.3: Profile of the Functional Forms of the Temperature-dependent Parameters of the Model (2.2.1) Related to the Adult *Aedes Aegypti* Mosquito. (a) Probability of Infection from an Infected Mosquito to a Susceptible Human *per* Bite ($\beta_h(T)$). (b) the Biting Rate of Adult Female Mosquitoes ($a_v(T)$). (c) Probability of Infection from an Infected Human to a Susceptible Mosquito *per* Bite ($\beta_v(T)$). (d) Egg Oviposition Rate ($\phi_v(T)$). (e) Mortality Rate of Adult Female Mosquito ($\mu_v(T)$).

2.2.2 Data Fitting

The model (2.2.1) is, first of all, fitted using available epidemiological and weather data relevant (see Tables 2.3, 2.4 and 2.5) to dengue transmission dynamics in the Chiang Mai province of Thailand [25; 176] (using least square regression). In particular, both the temperature data (provided by Thai Meteorological Department [176]) and incidence data (provided by Thailand Bureau of Epidemiology [25]; see also Appendix A) are given for monthly periods between 2005-2016. The mean monthly temperature for Chiang Mai (given in Table 2.4) is plotted alongside the average monthly dengue incidence (given in Table 2.5) in Figure 2.4 (a). This figure shows that peak dengue incidence is attained for temperatures between 26°C and 28°C, which are recorded in the Chiang Mai province during the period between June and August annually.

Furthermore, the model (2.2.1) is fitted using the aforementioned mean monthly temperature and incidence data (Tables 2.4 and 2.5) using the baseline parameter values given in Table 2.3, where the temperature-dependent biting rate ($a_V(T)$) is chosen as a fitting parameter (and the remaining temperature-dependent parameters of the model are computed using their respective functional forms given in Section 2.2.1). The result obtained, depicted in Figure 2.4 (b), shows a reasonably good fit. Plots of the fitted biting rates (using the data in Table 2.3) and the incidence data (given in Table 2.5) are depicted in Figure 2.4 (c), from which it follows that the dengue incidence positively correlates with increasing biting rate.

Table 2.3. Values and Ranges of the Parameters of Autonomous Version of the Model (2.2.1).

Parameter	Range	Baseline value	Reference
σ_E	(0.1,0.5)/day	0.4/day	[37; 55]
μ_E	(0.07,0.3)/day	0.2/day	[37; 55]
σ_L	(0.08,0.35)/day	0.14/day	[37; 55]
μ_L	(0.07,0.3)/day	0.18/day	[37; 55]

σ_P	(0.1,0.5)/day	0.3/day	[37; 55]
μ_P	(0.07,0.25)/day	0.17/day	[37; 55]
a_V	(0,1)/day	0.12/day	[7]
μ_V	(0.047,0.071)/day	0.05/day	[35; 53; 104]
μ_H	(0.00003,0.000042)/day	0.00005/day	[181]
σ_H	(0,1)/day	0.15/day	[61]
γ_H	(0,1)/day	0.1428/day	[61]
Π_H	(60,300)/day	66/day	[36]
β_V	(0.3,0.75)	0.5	[55; 61]
β_H	(0.1,0.75)	0.4	[55; 61]
r	(0,0.3)	0.007	[22; 57; 164]
f_V	(0.4,0.6)	0.55	[108]
K_V	$(10^4, 10^6)$	40,000	[53; 104]
ϕ_V	(1,500)	1.84/day	[35; 53; 104]

Table 2.4. Mean Monthly Temperature (in °C) for Chiang Mai Province of Thailand for the Period 2005-2016 [176].

Month	Jan	Feb	Mar	Apr	May	Jun	Jul	Aug	Sep	Oct	Nov	Dec
High	28.9	32.2	34.9	36.1	34.1	32.3	31.7	31.1	31.3	31.1	29.8	28.3
Mean	20.5	22.9	26.4	28.7	28.1	27.3	27.0	26.6	26.5	25.8	23.8	21.0
Low	13.7	14.9	18.2	21.8	23.4	23.7	23.6	23.4	23.0	21.8	19.0	15.0

Table 2.5. Average Monthly Dengue Incidence Data for Chiang Mai Province of Thailand, for the Period 2005-2016 [33].

Month	Dengue cases *per* 100,000 People
January	3.8
February	2.3
March	3.5
April	7.5
May	21.4
June	51.63
July	73.33
August	72.61
September	45.14
October	23.82
November	17.44
December	7.38

Table 2.6. Fitted Values of Monthly Biting Rates (Obtained from Fitting the Model with Data).

Month	Jan	Feb	Mar	Apr	May	Jun	Jul	Aug	Sep	Oct	Nov	Dec
Biting rate (a_V)	0.05	0.01	0.01	0.09	0.15	0.12	0.15	0.1	0.05	0.03	0.02	0.02

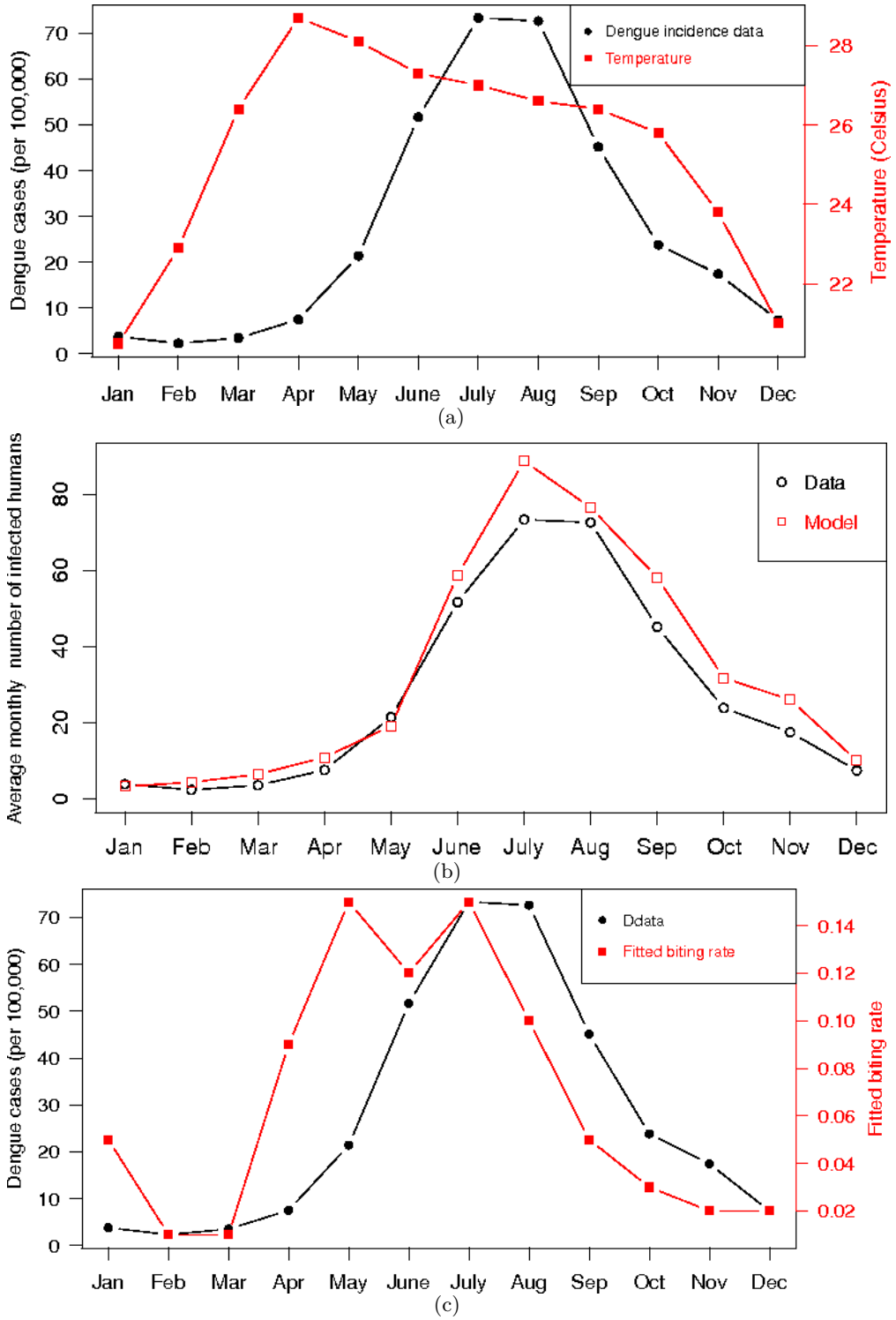

Figure 2.4: Data Fittings of the Autonomous Version of the Model (2.2.1). (a) Plot of the Average Monthly Temperature (In °C) for Chiang Mai (Table 2.4) Superimposed with the Monthly Dengue Incidence Data (Table 2.5). (b) Data Fitting of the Model (2.2.1) Using the Average Monthly Incidence Data in Table 2.5 (And the Fitted Monthly Biting Rates in Table 2.6). (c) Fitted Biting rate (a_V) Used to Fit the Model with the Data. Plots Are Generated Using the Baseline Parameter Values in Table 2.3.

2.2.3 Basic Qualitative Properties

Since the model (2.2.1) monitors the temporal dynamics of mosquitoes (immature and mature) and humans, all parameters of the model are assumed to be non-negative. Define the region

$$\mathcal{D} = \left\{(S_E, I_E, S_L, I_L, S_P, I_P, S_M, I_M, S_H, E_H, I_H, R_H) \in \mathbb{R}^{12}_{+} \cup \{\mathbf{0}\}\right\}. \tag{2.2.9}$$

Theorem 2.2.1 *If the initial values of the system* (2.2.1) *lie in the region* $\mathcal{D}$*, then there exists a unique positive solution for* (2.2.1)*, such that*

$$\Gamma = \{(S_E, I_E, S_L, I_L, S_P, I_P, S_M, I_M, S_H, E_H, I_H, R_H) \in \mathcal{D} : N_V(t) \leq m_1, N_H(t) \leq m_2, t \geq 0\},$$

is positively-bounded and invariant for the model (2.2.1)*, where* $0 \leq m_1, m_2 < \infty$.

2.3 Analysis of Autonomous Version of the Model

The model (2.2.1) will, first of all, be analysed for the case when fixed temperature values are used (i.e., the *autonomous* equivalent/version of the model (2.2.1) will be considered first).

2.3.1 Disease-free Equilibria

It is convenient to define the quantity:

$$\mathtt{r}_0 = \frac{\phi_V f_V \sigma_E \sigma_L \sigma_P}{\mu_V(\sigma_E + \mu_E)(\sigma_L + \mu_L)(\sigma_P + \mu_P)}. \tag{2.3.10}$$

The autonomous version of the model (2.2.1) has two disease-free equilibria, described below:

1. Trivial (mosquito-free) disease-free equilibrium (TDFE):

$$\begin{aligned}\mathcal{T}_0 &= (S_E^*, I_E^*, S_L^*, I_L^*, S_P^*, I_P^*, S_M^*, I_M^*, S_H^*, E_H^*, I_H^*, R_H^*)\\ &= (0,0,0,0,0,0,0,0,0,\frac{\Pi_H}{\mu_H},0,0,0).\end{aligned}$$

2. Non-trivial (mosquito-present) disease-free equilibrium (NDFE):

$$\begin{aligned}\mathcal{T}_1 &= (S_E^\dagger, I_E^\dagger, S_L^\dagger, I_L^\dagger, S_P^\dagger, I_P^\dagger, S_M^\dagger, I_M^\dagger, S_H^\dagger, E_H^\dagger, I_H^\dagger, R_H^\dagger)\\ &= (S_E^\dagger, 0, S_L^\dagger, 0, S_P^\dagger, 0, S_M^\dagger, 0, \frac{\Pi_H}{\mu_H}, 0, 0, 0),\end{aligned}$$

where,

$$S_M^\dagger = \frac{k_1}{k_2+\delta_L k_3^2}(\mathtt{r}_0 - 1), \quad S_E^\dagger = \frac{\phi_V}{\sigma_E+\mu_E}\left(1-\frac{S_M^\dagger}{K_V}\right)_+ S_M^\dagger, \quad S_P^\dagger = \frac{\sigma_L S_L^\dagger}{\sigma_P+\mu_P}, \tag{2.3.11}$$

$$S_L^\dagger = \frac{-(\sigma_L+\mu_L)+\sqrt{(\sigma_L+\mu_L)^2+4\sigma_E\delta_L S_E^\dagger}}{2\delta_L},$$

with $k_1 = \dfrac{\mu_V(\sigma_P+\mu_P)(\sigma_L+\mu_L)}{f_V\sigma_P\sigma_L}$, $k_2 = \dfrac{\phi_V\sigma_E}{K_V(\sigma_E+\mu_E)}$, $k_3 = \dfrac{\mu_V(\sigma_P+\mu_P)}{f_V\sigma_L\sigma_P}$ and $K_V > S_M^\dagger$ in $\mathcal{D}$. It follows from (2.3.11) that $\mathcal{T}_1$ exists if and only if $\mathtt{r}_0 > 1$. The quantity $\mathtt{r}_0$ represents the average number of new adult female mosquitoes generated by a single susceptible adult female mosquito that has successfully taken a blood meal. It is the product of the rate at which eggs are laid eggs by an adult female mosquito (ϕ_V), the proportion of eggs survived to become larvae ($\frac{\sigma_E}{\sigma_E+\mu_E}$), proportion of larvae survived and matured into pupae ($\frac{\sigma_L}{\sigma_L+\sigma_L}$), proportion of pupae survived and become adult female mosquitoes ($\frac{\sigma_P f_V}{\sigma_P+\mu_P}$), and the average lifespan of a susceptible adult female mosquito ($\frac{1}{\mu_V}$).

2.3.1.1 Local asymptotic stability of TDFE ($\mathcal{T}_0$)

The TDFE ($\mathcal{T}_0$), which always exists, corresponds to the case without mosquitoes. It can be shown, by linearizing the autonomous version of the model (2.2.1) around $\mathcal{T}_0$, that the associated eigenvalues of the linearization have negative real part whenever

$$r_{VH}^{v} = \max\{\mathtt{r}_0, r\mathtt{r}_0\} < 1, \tag{2.3.12}$$

where, $\mathtt{r}_0$ is given in (2.3.10). Since we assumed $0 \leq r < 1$, it follows that $r_{VH}^{v} = \mathtt{r}_0$ in this case. The following result can be established using standard linearization of the autonomous version of the model (2.2.1) around the TDFE ($\mathcal{T}_0$).

Theorem 2.3.1 *The TDFE point ($\mathcal{T}_0$) is locally-asymptotically stable (LAS) whenever $r_{VH}^{v} < 1$, and unstable if $r_{VH}^{v} > 1$.*

It is worth noting that, since the quantity $\mathtt{r}_0$ is the average number of new susceptible adult female mosquitoes generated by a single susceptible adult female mosquito that has successfully taken a blood meal, the quantity $r\mathtt{r}_0$ measures the average number of new infected adult female mosquitoes generated by a single infected adult female mosquito that has successfully taken a blood meal. It is worth noting, from the expression (2.3.12), the threshold quantity r_{HV}^{v} increases with increasing values of r. That is, as expected, increasing the vertical transmission rate ($0 \leq r < 1$) increase the disease burden (by increasing in r_{VH}^{v}).

2.3.1.2 Local asymptotic stability of NDFE ($\mathcal{T}_1$)

The local asymptotic stability of $\mathcal{T}_1$ can be established using the next generation operator method [46; 182]. The non-negative matrix $\mathcal{F}$ of new infection terms and the matrix $\mathcal{V}$ of the transition terms associated with the autonomous case of the model

(2.2.1) are, respectively, given by:

$$\mathcal{F}=\begin{bmatrix} 0 & 0 & 0 & \phi_V r(1-\frac{S_M^\dagger}{K_V})_+ & 0 & 0 \\ 0 & 0 & 0 & 0 & 0 & 0 \\ 0 & 0 & 0 & 0 & 0 & 0 \\ 0 & 0 & 0 & 0 & 0 & \frac{\beta_V a_V S_M^\dagger}{N_H^\dagger} \\ 0 & 0 & 0 & \beta_H a_V & 0 & 0 \\ 0 & 0 & 0 & 0 & 0 & 0 \end{bmatrix}, \mathcal{V}=\begin{bmatrix} g_1 & 0 & 0 & 0 & 0 & 0 \\ -\sigma_E & g_2 & 0 & 0 & 0 & 0 \\ 0 & -\sigma_L & g_3 & 0 & 0 & 0 \\ 0 & 0 & -f_V\sigma_P & g_4 & 0 & 0 \\ 0 & 0 & 0 & 0 & g_5 & 0 \\ 0 & 0 & 0 & 0 & -\sigma_H & g_6 \end{bmatrix}, \tag{2.3.13}$$

where, $g_1=\sigma_E+\mu_E$, $g_2=\sigma_L+\mu_L$, $g_3=\sigma_P+\mu_P$, $g_4=\mu_V$, $g_5=\sigma_H+\mu_H$, and $g_6=\gamma_H+\mu_H$. It follows, from [182], that the basic reproduction number ($\mathbb{R}_{0V}$) of autonomous case of the model (2.2.1) is given by (where ρ is the spectral radius):

$$\mathbb{R}_{0V}=\rho(\mathcal{F}\mathcal{V}^{-1})=\frac{1}{2}\left[\mathbb{R}_V^v+\sqrt{(\mathbb{R}_V^v)^2+4\mathbb{R}_0}\right], \tag{2.3.14}$$

with, $\mathbb{R}_V^v=r\mathtt{r}_0\left(1-\dfrac{S_M^\dagger}{K_V}\right)_+$ and $\mathbb{R}_0=\frac{a_V^2\beta_V\beta_H S_M^\dagger}{\mu_V(\sigma_H+\mu_H)(\gamma_H+\mu_H)N_H^\dagger}$. It is worth noting from (2.3.14) that, in the absence of vertical transmission, the reproduction threshold ($\mathbb{R}_{0V}$) reduces to

$$\mathbb{R}_{0V}|_{r=0}=\sqrt{\mathbb{R}_0}\,.$$

The result below follows from Theorem 2 of [182].

Theorem 2.3.2 *The NDFE ($\mathcal{T}_1$) is LAS whenever $\mathbb{R}_{0V}<1$, and unstable if $\mathbb{R}_{0V}>1$.*

The epidemiological implication of Theorem 2.3.2 is that a small influx of infected individuals or vectors into the population will not generate a large outbreak in the community if $\mathbb{R}_{0V}<1$. Hence, the disease may be effectively-controlled if $\mathbb{R}_{0V}$ can be brought to (and maintained at) values less than unity. A plot of $\mathbb{R}_{0V}$, as a function of fixed mean monthly temperature (for $T(t)\in[14-32]^\circ$C) for the Chiang Mai province of Thailand [176], is depicted in Figure 2.5. This figure shows, that the profile of $\mathbb{R}_{0V}$

lies in the range $[0.18, 1.6]$. Furthermore, the values of $\mathbb{R}_{0V}$ increase with increasing temperature values in the range $[18 - 28]^{\circ}$C (and decrease thereafter, for increasing temperatures above the peak temperature of 28°C). Thus, disease burden increases with increasing temperature values in the range $[18-28]^{\circ}$C, and decreases for increasing temperature values thereafter.

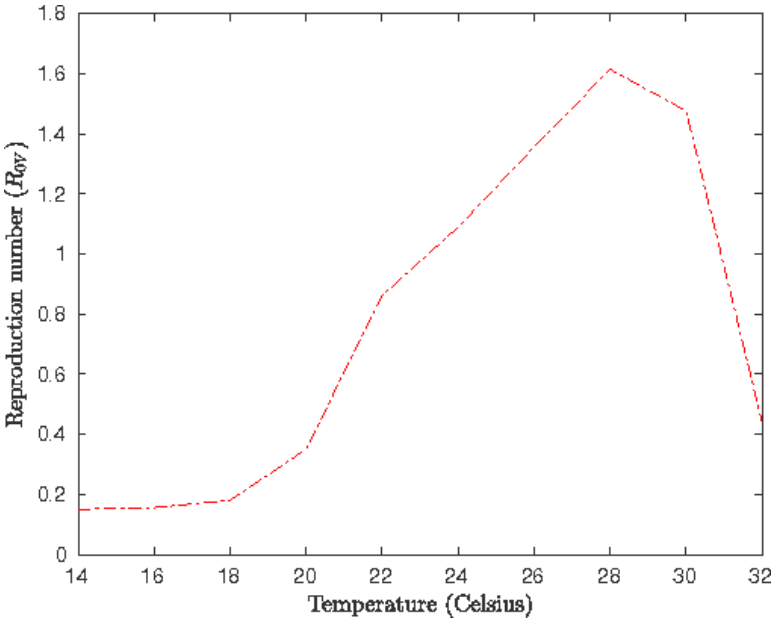

Figure 2.5: Profile of the Reproduction Number ($\mathbb{R}_{0V}$) as a Function of Mean Monthly Temperature for Chiang Mai Thailand. Parameters Values Used as given by the Baseline Values in Table 2.3.

2.3.1.3 Effects of vertical transmission on the reproduction number

The effect of vertical transmission in the vector population (i.e., $r \neq 0$) on the reproduction number ($\mathbb{R}_{0V}$) is assessed by using the approach in [165] as follows. Let $K = \mathcal{F}\mathcal{V}^{-1}$ (recall that the matrices $\mathcal{F}$ and $\mathcal{V}$ are given by Equation (2.3.13)) be the

next-generation matrix of the autonomous version of the model (2.2.1) [46], given by:

$$K = \begin{bmatrix} K_{11} & K_{12} & K_{13} & K_{14} & 0 & 0 \\ 0 & 0 & 0 & 0 & 0 & 0 \\ 0 & 0 & 0 & 0 & 0 & 0 \\ 0 & 0 & 0 & 0 & K_{45} & K_{46} \\ K_{51} & K_{52} & K_{53} & K_{54} & 0 & 0 \\ 0 & 0 & 0 & 0 & 0 & 0 \end{bmatrix},$$

where, $K_{11} = \frac{rf_V\sigma_E\sigma_L\sigma_P\phi_V}{g_1g_2g_3g_4}\left(1-\frac{S_M^\dagger}{K_V}\right)_+$, $K_{12} = \frac{rf_V\sigma_L\sigma_P\phi_V}{g_2g_3g_4}\left(1-\frac{S_M^\dagger}{K_V}\right)_+$, $K_{13} = \frac{rf_V\sigma_P\phi_V}{g_3g_4}\left(1-\frac{S_M^\dagger}{K_V}\right)_+$, $K_{14} = \frac{r\phi_V}{g_4}\left(1-\frac{S_M^\dagger}{K_V}\right)_+$, $K_{45} = \frac{a_V\beta_V\sigma_H S_M^\dagger}{g_5g_6N_H^\dagger}$, $K_{46} = \frac{a_V\beta_V S_M^\dagger}{g_6N_H^\dagger}$, $K_{51} = \frac{a_Vf_V\beta_H\sigma_E\sigma_L\sigma_P}{g_1g_2g_3g_4}$, $K_{52} = \frac{a_Vf_V\beta_H\sigma_L\sigma_P}{g_2g_3g_4}$, $K_{53} = \frac{a_Vf_V\beta_H\sigma_P}{g_3g_4}$, $K_{54} = \frac{a_V\beta_H}{g_4}$. The notion of *target reproduction number* (as introduced by Shuai *et al.* [46; 165]) will be used. Using the notation in [165], the entries K_{ij} $(i,j=1,\ldots,6)$ of the matrix K represent the average number of new cases of infections in humans (vectors) generated by an average infected (immature and mature) vector (humans). In particular, the entry K_{51} is the effect of infected eggs $(j=1)$ on the generation of new infected (exposed) humans (i.e., $i=5$). Furthermore, following [165], let $S=\{(i,j)=(5,1)\}$ be the set of target entries and $S_1=\{5\}$ and $S_2=\{1\}$.

Following [165], it is convenient to define the following projection matrices associated with the autonomous case of the model (2.2.1). Let I be the 6×6 identity matrix, E_{S_1}, P_{S_1} and P_{S_2} be 6×6 matrices with entries $(E_{S_1})_{kk}=1$ if $k\in S_1$ and $(E_{S_1})_{ij}=0$ otherwise, and P_{S_1} and P_{S_2} are 6×6 projection matrices (e.g., $(P_{S_1})_{kk}=1$ if $k\in S_1$ and $(P_{S_1})_{ij}=0$ otherwise) [165]. It follows that the target reproduction number (denoted by $T_S=T_r^H$) with respect to the set S is given by [165]:

$$T_r^H = \rho(E_{S_1}P_{S_1}KP_{S_2}(I-K+P_{S_1}KP_{S_2})^{-1}E_{S_1}),$$

provided the spectral radius $\rho(K - P_{S_1} K P_{S_2}) < 1$. Hence,

$$T_r^H = \frac{\sigma_H \mathbb{R}_0}{1 - r\mathtt{r}_0 \left(1 - \frac{S_M^\dagger}{K_V}\right)_+} = \frac{\sigma_H \mathbb{R}_0}{1 - \mathbb{R}_V^v}, \tag{2.3.15}$$

provided $\rho(K - P_{S_1} K P_{S_2}) = r\mathtt{r}_0 \left(1 - \frac{S_M^\dagger}{K_V}\right)_+ < 1$. It is worth noting that, the expression $\dfrac{\sigma_H \mathbb{R}_0}{1 - r\mathtt{r}_0 (1 - \frac{S_M^\dagger}{K_V})_+}$ in Equation (2.3.15) accounts for the average number of infected humans caused by an infected egg (after maturation to adulthood). Figure 2.6 compares the target reproduction number (T_r^H) with the basic reproduction number ($\mathbb{R}_{0V}$) of the autonomous version of the model (2.2.1) for various values of r, from which it follows that T_r^H is always less than $\mathbb{R}_{0V}$ for $r \in [0, 1)$.

Furthermore, for the range of the vertical transmission rate for *Aedes aegypti* mosquitoes given in Table 2.1 (where $r \in (0.0025, 0.13)$), it follows from Figure 2.6 that vertical transmission has very marginal population-level impact on the disease dynamics (vertical transmission becomes relevant far larger values of r, outside the aforementioned realistic range). This result is consistent with the numerical simulation results reported in [2].

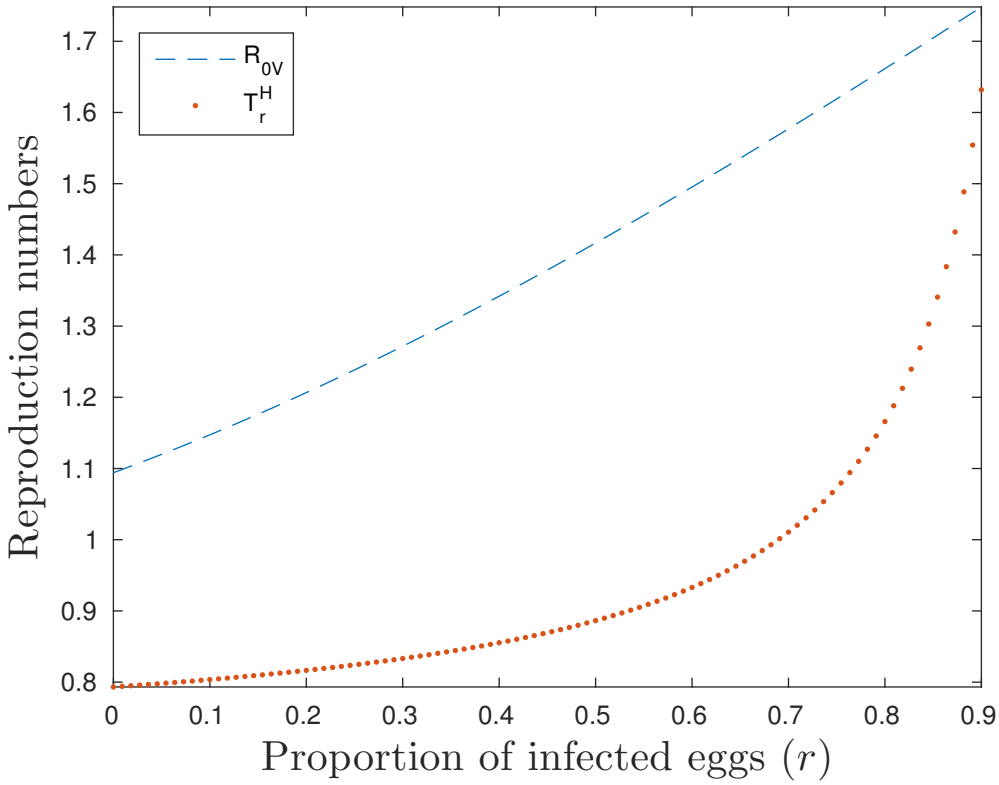

Figure 2.6: Plot of $\mathbb{R}_{0V}$ and T_r^H as function of r. Parameters values used are as given by the baseline values in Table 2.3.

Figure 2.7 shows that, in the absence of human-mosquito interaction (i.e., no mosquito bites on humans), vertical transmission (r) has very marginal effect on the abundance of infected adult female mosquitoes (Figure (2.7a)). However, when the human-mosquito interaction is slightly increased (such as by setting the biting rate to $a_V = 0.1$), the number of infected adult female mosquitoes significantly increases with increasing values of the proportion of new infected eggs (Figure (2.7b)). Figure (2.7 b) clearly shows that vertical transmission in the vector population has little or no effect on the number of infected adult female mosquitoes (this result supports the finding in Figure 2.6).

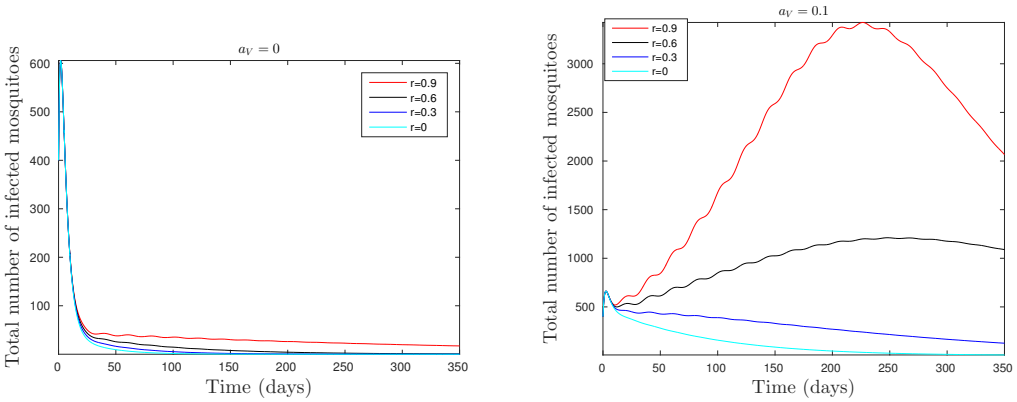

Figure 2.7: Simulations of the Model (2.2.1) Showing the Effect of the Proportion of Infected Eggs (r) on the Disease Dynamics for (a) Mosquito-human Interaction Set at $a_V = 0$, (b) Mosquito-human Interaction Set at $a_V = 0.1$. Parameter Values Used Are as given in Table 2.3.

2.3.2 Endemic Equilibria

In this section, conditions for the existence of endemic equilibria will be derived. Let $\mathcal{E}_1 = (S_E^{**}, I_E^{**}, S_L^{**}, I_L^{**}, S_P^{**}, I_P^{**}, S_M^{**}, I_M^{**}, S_H^{**}, E_H^{**}, I_H^{**}, R_H^{**})$ be any arbitrary endemic equilibrium of autonomous version of the model (2.2.1). Furthermore, let

$$\lambda_{VH}^{**} = \frac{a_V \beta_H I_M^{**}}{N_H^{**}}, \quad \text{and} \quad N_H^{**} = S_H^{**} + E_H^{**} + I_H^{**} + R_H^{**}. \tag{2.3.16}$$

It is convenient to define

$$\mathbb{R}_{0V}^{*} = \mathbb{R}_0 + \mathbb{R}_V^{v}, \tag{2.3.17}$$

where, $\mathbb{R}_0$ and $\mathbb{R}_V^v$ are as defined in Section 2.3.1.2. It can be shown that $\mathbb{R}_{0V}^{*} < 1$ (> 1) if and only if $\mathbb{R}_{0V} < 1$ (> 1) (so that $\mathbb{R}_{0V}^{*}$ behaves like the *target reproduction number* discussed in [166]). It can be shown, by solving for the variables of the autonomous version of the model (2.2.1) at steady-state, that the solutions of the autonomous model satisfy the following linear equation in terms of λ_{VH}^{**}:

$$b_1 \lambda_{VH}^{**} + b_0 = 0, \tag{2.3.18}$$

where, $b_1 = \mu_H\left((1-r)\mu_V g_5 g_6 + a_V\beta_V\mu_H\sigma_H\right) > 0$, $b_0 = g_5 g_6(1-\mathbb{R}^*_{0V})$. It follows from (2.3.18) that $\lambda^{**}_{VH} = \frac{-b_0}{b_1}$, (so that $\lambda^{**}_{VH} > 0$ (< 0) if $\mathbb{R}^*_{01} > 1$ (< 1)). The components of the positive equilibrium of autonomous version of the model (2.2.1) can then be obtained by solving for λ^{**}_{VH} from (2.3.18), and substituting the result into the steady-state expressions for each of the state variables in (2.2.1). It follows that the autonomous case of the model (2.2.1) has a unique endemic equilibrium whenever $\mathbb{R}^*_{0V} > 1$. Thus, the autonomous version of the model (2.2.1) will not have an endemic equilibrium point if $\mathbb{R}^*_{0V} < 1$. Hence, the model will not undergo the usual phenomenon of backward bifurcation [35; 53; 104; 61]. A global asymptotic stability result is given below for the NDFE ($\mathcal{T}_1$). It is convenient, first of all, to define the threshold quantity:

$$\mathbb{R}_G = \frac{1}{2}\left[r\mathtt{r}_0 + \sqrt{r\mathtt{r}_0^2 + 4\mathbb{R}_0}\right],$$

where, $\mathtt{r}_0$ and $\mathbb{R}_0$ are as defined in Sections 2.3.1 and 2.3.1.2, respectively. We claim the following result.

Theorem 2.3.3 *The NDFE ($\mathcal{T}_1$) of the autonomous version of the model* (2.2.1) *is GAS in $\mathcal{D}$ whenever $\mathtt{r}_0 > 1$ and $\mathbb{R}_G < 1$.*

The proof of Theorem 2.3.3, based on using the approach in [86; 87], is given in Appendix B. The epidemiological significance of Theorem 2.3.3 is that, for the autonomous version of the model (2.2.1), reducing (and maintaining) the threshold quantity ($\mathbb{R}_G$) to a value less than unity is necessary and sufficient for the effective control or elimination of the disease in the community.

2.3.3 Simulations: Effect of Temperature Variability

The effect of temperature variability on the disease dynamics, as a function of vertical transmission in the vector (r), is monitored by simulating the model (2.2.1) with various fixed temperature values in the range 16°C to 32°C. In the absence of vertical

transmission (i.e., $r = 0$), Figure 2.8 (a) shows that the disease burden, as measured in terms of the number of new infected humans, increases with increasing temperature values until 28°C (where the maximum peak is attained). The disease burden then decreases for increasing temperatures thereafter. Similar pattern is observed when 10% vertical transmission is assumed (Figure 2.8 (b)), although an increase in the number of new cases in humans is observed as expected. Furthermore, the number of infected mosquitoes exhibit similar pattern (that is, the number of infected adult female mosquitoes increases with increasing temperature until 28°C, and decreases for increasing temperatures thereafter), although oscillatory dynamics, due to the assumed logistic eggs oviposition rate ($\phi_V(T)$), was observed (Figures 2.8 (c) and (d)).

The overall effect of temperature on disease dynamics is assessed by simulating the model (2.2.1) using various values of temperature in the range $[16 - 32]$°C (for Chiang Mai province of Thailand [176]). The results obtained (depicted in Figure 2.9) show that the total number of new dengue cases (in both the human and mosquito populations) reaches a peak during the period June to August (which correspond to the temperature range of 26°C- 28°C). The potential impact of temperature variability on the burden of disease caused by vertical transmission (r) is monitored by simulating the non-autonomous model (2.2.1) using various value of r and temperature. Figure 2.10 shows that the effect of r in generating new infected cases is more pronounced for temperature values in the range $[16 - 26]$°C (Figures 2.10 (a) and (b)) and decreases thereafter (Figures 2.10 (d) and (e)). Thus, this study shows that the ability of vertical transmission to cause significant increase in disease burden is temperature-dependent.

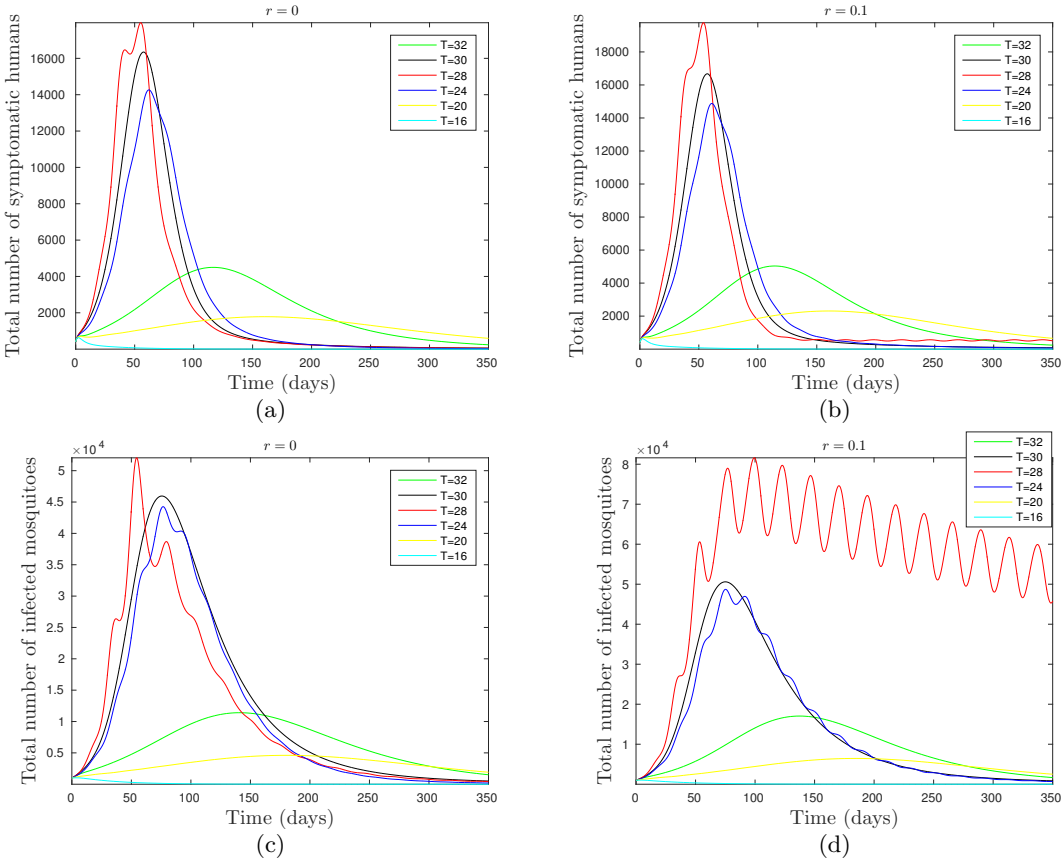

Figure 2.8: Simulations of the Model (2.2.1), for the Effect of Temperature and Vertical Transmission on Disease Dynamics. (a) Total Number of Symptomatic Humans (I_H) as a Function of Time for $r = 0$. (b) Total Number of Symptomatic Humans (I_H) as a Function of Time for $r = 0.1$. (c) Total Number of Infected Adult Mosquitoes (I_M) as a Function of Time for $r = 0$. (d) Total Number of Infected Adult Mosquitoes (I_M) as a Function of Time for $r = 0.1$. Parameters Values Used Are given in Table 2.3. The Functional Forms for the Temperature-dependent Parameters ($a_V(T)$, $\beta_H(T)$, $\beta_V(T)$, $\phi_V(T)$ and $\mu_V(T)$), given in Section 2.2, Are Used.

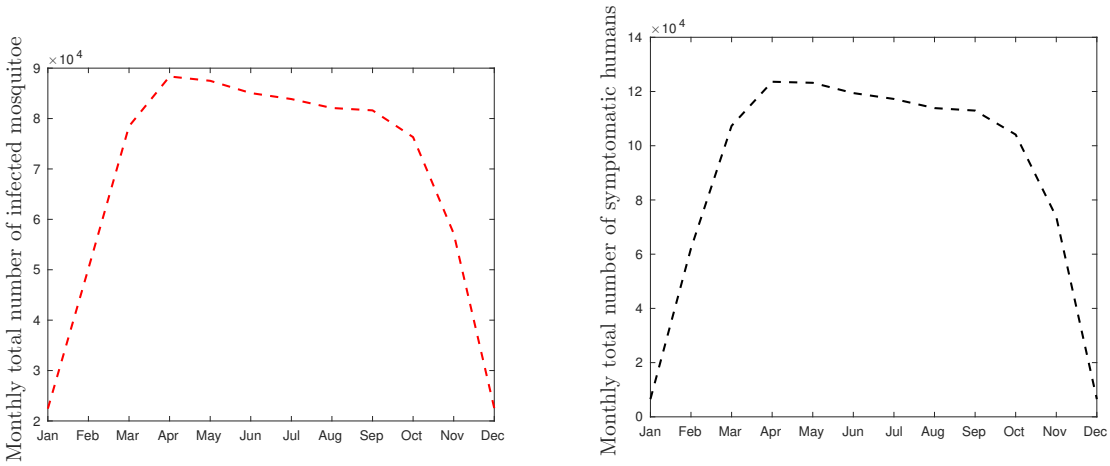

(a) (b)

Figure 2.9: Simulation of the Model 2.2.1 for the Disease Dynamics in Chiang Mai, Thailand. (a) Monthly Total Number of Infected Mosquitoes. (b) Monthly Total Number of Infected Humans. Parameters Values Used Are given in Table 2.3. The Functional Forms for the Temperature-dependent Parameters ($a_V(T)$, $\beta_H(T)$, $\beta_V(T)$, $\phi_V(T)$ and $\mu_V(T)$), given in Section 2.2, Are Used, Using Mean Monthly Temperature (T) given in Table 2.4.

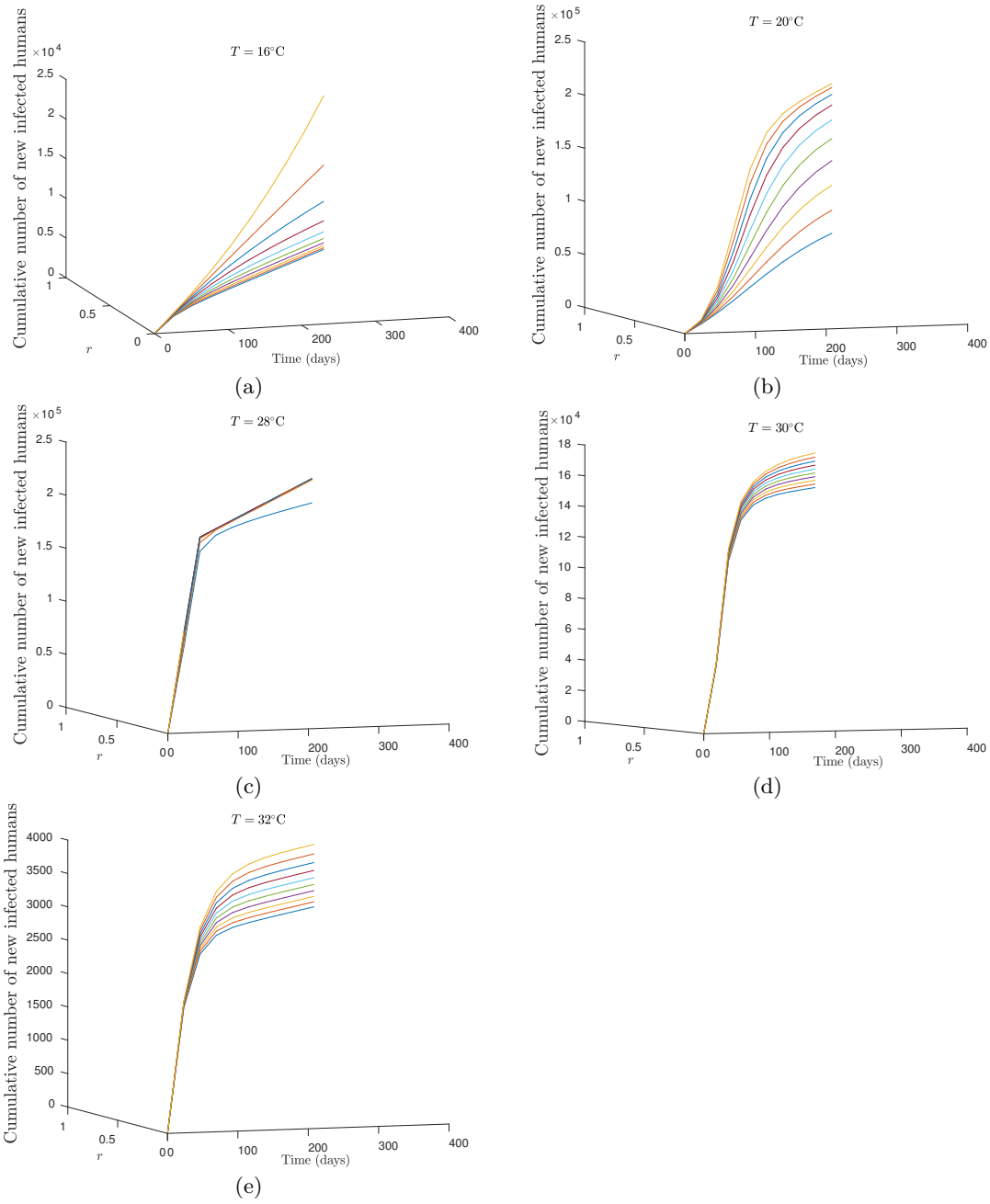

Figure 2.10: Cumulative Number of Infected Humans for Various Values of the Proportion of Infected Eggs Laid by an Infected Mosquito ($0 \leq r < 1$) and Temperature (T): (a) $T = 16$, (b) $T = 20$, (c) $T = 28$, (d) $T = 30$, (e) $T = 32$. Color Notation from Blue ($r = 0$) to Gold ($r = 0.9$) Represent Varying Values of r, from 0 to 0.9, in Steps of Length 0.1.

2.3.4 Uncertainty and Sensitivity Analysis

The autonomous version of the model (2.2.1), with fixed temperature values, contains 19 parameters, and uncertainty in their estimates are expected to arise. The effect of such uncertainties is assessed using uncertainty and sensitivity analysis [29]. In particular, Latin Hypercube Sampling (LHS) and Partial Rank Correlation Coefficients (PRCC) is used for this model, as below. The purpose of sensitivity analysis is to assess the effects of parameters on the outcomes of the simulations of the model [29]. A highly-sensitive parameter should be more carefully estimated, since a small change in that parameter can cause a large quantitative change in the result [29]. On the other hand, a parameter that is not sensitive does not require as much attempt to estimate (because a small change in that parameter will not cause a large variation to the quantity of interest) [21; 29; 111]. The analyses will be carried out using data (temperature, demographic and epidemiological) relevant to dengue transmission dynamics in the Chiang Mai province of Thailand [36; 103; 159; 198]. The total population of the Chiang Mai province is estimated to be 1.7 million, and the average lifespan is 65-72 years [36] (so that $\mu_H \in [0.000037 - 0.000042]$ *per* day with a mean of $\mu_H^* = 0.000039$). Thus, $\frac{\Pi_H}{\mu_H^*} = 1.7$ million. Hence, $\Pi_H \approx 66$ *per* day. The analysis will be carried out using the baseline values and ranges tabulated in Table 2.3.

Using the population of infectious humans (I_H) as the response function, it is shown in Table 2.7 that the top PRCC-ranked parameters of the model (i.e., parameters with PRCC values greater or equal to 0.5) are the mosquito biting rate (a_V) and the transmission probability *per* contact for susceptible human (β_H). Similarly, using the population of infectious mosquitoes (I_M) as the response function, the top PRCC-ranked parameters are the egg deposition rate (ϕ_V), maturation rate of pupae to adult mosquito (σ_P) and the environmental carrying capacity of immature mosquitoes (K_V). Furthermore, using the population of infected pupae (I_P) as the response function,

the top PRCC-ranked parameters of the model are the egg deposition rate (ϕ_V),the environmental carrying capacity (K_V) and the maturation rate of larvae to pupae (σ_L). Considering the population of infected larvae (I_L) as the response function, the top PRCC-ranked parameters of the model are egg deposition rate (ϕ_V) and maturation rate of eggs to larvae (σ_E). Finally, using the population of infected eggs (I_E) as the response function, the top PRCC-ranked parameters of the model are egg deposition rate (ϕ_V), the environmental carrying capacity (K_V) and the natural death rate of adult female mosquitoes (μ_V).

In summary, We identified four parameters that dominate the transmission dynamics of the autonomous version of the model (2.2.1), namely the environmental carrying capacity of immature mosquitoes (K_V), biting rate (a_V), probability of infection of a susceptible human (β_H) and the egg oviposition rate (ϕ_V). It is worth noting from Table 2.7 that the parameter related to vertical transmission in the vector (r) does not have significant PRCC values, suggesting that vertical transmission plays a marginal (if at all) role on the transmission dynamics of the disease.

Table 2.7. PRCC Values for the Parameters of Autonomous Case of the Model (2.2.1) Using the Total Number of Infected Eggs (I_E), Larvae (I_L), Pupae (I_P), Adult Mosquitoes (I_M) and Infectious Humans (I_H) as Response Functions (with PRCC $\geq$ .5). The Top Parameters That Affect the Model with Respect to Each of the Six Response Functions Are Highlighted in Bold Font.

Parameters	I_E	I_L	I_P	I_M	I_H
σ_E	-0.21966	**+0.8402**	**+0.5515**	**0.6804**	-0.1074
μ_E	-0.0241	+0.1490	-0.1112	+0.0171	-0.0313
σ_L	-0.0334	-0.2195	**+0.5821**	+0.4081	+0.0458
μ_L	+0.2574	-0.3229	-0.0120	-0.0845	-0.0513
σ_P	+0.3572	+0.0673	-0.2042	**+0.7500**	-0.0245
μ_P	+0.2973	+1453	-0.3415	+0.0376	+0.0100
a_V	-0.1988	+0.3124	-0.1143	+0.281	**+0.9463**
μ_V	-0.4202	-0.0292	0.0854	+0.1701	-0.1462
μ_H	-0.3149	-0.3936	+0.2996	+0.2687	0.0856
σ_H	+0.0409	-0.1667	+0.0184	+0.2364	-0.0995
γ_H	+0.0475	+0.0176	-0.0262	+0.1769	-0.4349
Π_H	0.0506	+0.1099	+0.2162	-0.0028	-0.2039
β_V	-0.1364	-0.1257	+0.0843	+0.4012	+0.1832
β_H	-0.1176	-0.2754	-0.2405	-0.0476	**+0.8009**
r	-0.2010	+0.1766	-0.3528	+0.0543	-0.0186
f_V	+0.2057	+0.1517	+0.1094	+0.3173	-0.0903
K_V	**+0.5157**	+0.4100	**+0.6001**	**+0.7446**	+0.0310
ϕ_V	**+0.8603**	**+0.8999**	**+0.7805**	**+0.8113**	-0.0185

2.4 Analysis of Non-autonomous Model

Consider, now, the full non-autonomous model (2.2.1), where the function (2.2.8), for the daily temperature fluctuations is used (so that the temperature-dependent parameters, given in Equations (2.2.3)-(2.2.7), are now functions of t). Although the concept of basic reproduction number has been extensively addressed for autonomous models for disease transmission over the decades, such a concept has only been recently extended to disease transmission models with periodic coefficients (see, for instance, [11; 12; 13; 186]). In this section, the methodology in [186] will be used to compute the reproduction number associated with the non-autonomous model (2.2.1) with (2.2.8). Although the non-autonomous model (2.2.1) has two disease-free solutions, namely the trivial disease-free equilibrium and a non-trivial disease-free periodic solution, only the non-trivial disease-free periodic solution will be analyzed (since the former, associated with the absence of mosquitoes in the population, is ecologically unrealistic). It is convenient to define the functional threshold quantity

$$\mathtt{r}_0(t) = \frac{\phi_V(t) f_V \sigma_E(t) \sigma_L(t) \sigma_P(t)}{\mu_V(t)[\sigma_E(t) + \mu_E(t)][\sigma_L(t) + \mu_L(t)][\sigma_P(t) + \mu_P(t)]}.$$

The non-trivial disease-free solution (NDFS), obtained by setting $I_E = I_L = I_P = I_M = E_H = I_H = R_H = 0$ in (2.2.1), has the form

$$\varepsilon_{0n}(t) = (S^*_{nE}(t), 0, S^*_{nL}(t), 0, S^*_{nP}(t), 0, S^*_{nM}(t), 0, \frac{\Pi_H}{\mu_H}, 0, 0, 0),$$

(recalling that $T = T(t)$) with $(S^*_{nE}(t), S^*_{nL}(t), S^*_{nP}(t), S^*_{nM}(t), S^*_{nH}(t))^T$ being the unique periodic solution (for $\mathtt{r}_0(t) > 1$ for all $t \geq 0$) satisfying:

$$\begin{aligned}
\frac{dS^*_{nE}(t)}{dt} &= \phi_V(t) \left[1 - \frac{S^*_{nM}(t)}{K_V(t)}\right]_+ S^*_{nM}(t) - [\sigma_E(t) + \mu_E(t)] S^*_{nE}(t), \\
\frac{dS^*_{nL}(t)}{dt} &= \sigma_E(t) S^*_{nE}(t) - [\sigma_L(t) + \mu_L(t) + \delta_L(t) S^*_{nL}(t)] S^*_{nL}(t),
\end{aligned} \tag{2.4.19}$$

$$\frac{dS^*_{nP}(t)}{dt} = \sigma_L(t)S^*_{nL}(t) - [\sigma_P(t) + \mu_P(t)]\, S^*_{nP}(t),$$
$$\frac{dS^*_{nM}(t)}{dt} = f_V\sigma_P(t)S^*_{nP}(t) - \mu_V(t)S^*_{nM}(t),$$
$$\frac{dS^*_{nH}(t)}{dt} = \Pi_H - \mu_H S^*_{nH}(t).$$

The next generation matrix $F(t)$ (of the new infection terms) and the M -Matrix $V(t)$ (of the remaining transfer terms), associated with the non-autonomous model (2.2.1) with (2.2.8), are given, respectively, by

$$F(t) = \begin{bmatrix} 0 & 0 & 0 & \phi_V(t)r(1 - \frac{S^*_{nM}(t)}{K_V(t)})_+ & 0 & 0 \\ 0 & 0 & 0 & 0 & 0 & 0 \\ 0 & 0 & 0 & 0 & 0 & 0 \\ 0 & 0 & 0 & 0 & 0 & \frac{\beta_V(t)a_V(t)S^*_{nM}(t)}{N^*_H} \\ 0 & 0 & 0 & \beta_H(t)a_V(t) & 0 & 0 \\ 0 & 0 & 0 & 0 & 0 & 0 \end{bmatrix}, \tag{2.4.20}$$

and,

$$V(t) = \begin{bmatrix} v_1(t) & 0 & 0 & 0 & 0 & 0 \\ -\sigma_E(t) & v_2(t) & 0 & 0 & 0 & 0 \\ 0 & -\sigma_L(t) & v_3(t) & 0 & 0 & 0 \\ 0 & 0 & -f_V\sigma_P(t) & v_4(t) & 0 & 0 \\ 0 & 0 & 0 & 0 & v_5 & 0 \\ 0 & 0 & 0 & 0 & -\sigma_H & v_6 \end{bmatrix}, \tag{2.4.21}$$

where, $v_1(t) = \sigma_E(t)+\mu_E(t)$, $v_2(t) = \sigma_L(t)+\mu_L(t)$, $v_3(t) = \sigma_P(t)+\mu_P(t)$, $v_4(t) = \mu_V(t)$, $v_5 = \sigma_H + \mu_H$, and $v_6 = \gamma_H + \mu_H$, $N^*_H = \frac{\Pi_H}{\mu_H}$. Let $\mathbf{h} = (h_1, h_2, h_3, h_4)^T$ be the vector

field in the right-hand sides of Equation (2.4.19) and $\mathbf{x}(t) = (x_1(t), x_2(t), x_3(t), x_4(t))^T$ $= (S^*_{nE}(t), S^*_{nL}(t), S^*_{nP}(t), S^*_{nM}(t))^T$.

Following [186], let Φ_M be the monodromy matrix of the linear ω-periodic system

$$\frac{dZ}{dt} = M(t)Z,$$

where, $M(t) = \left(\frac{\partial h_i(\mathbf{x}(\mathbf{t}), t)}{\partial x_j}\right)_{1\leq i,j\leq 4}$. Further, let $Y(t,s)$ $t \geq s$, be the evolution operator of the linear ω-periodic system

$$\frac{dy}{dt} = -V(t)y,$$

that is, for each $s \in \mathbb{R}$, the 6×6 matrix $Y(t,s)$ satisfies

$$\frac{dY(t,s)}{dt} = -V(t)Y(t,s), \qquad \forall t \geq s, Y(s,s) = \mathbb{I}_6,$$

where, $\mathbb{I}_6$ is the 6×6 identity matrix. Suppose that $\phi(s)$ (ω - periodic in s) is the initial distribution of infectious individuals. Thus, $F(s)\phi(s)$ is the rate at which new infections are produced by infected individuals who were introduced into the population at time s [186]. Since $t \geq s$, it follows that $Y(t,s)F(s)\phi(s)$ is the distribution of those infected individuals who were newly-infected at time s, and remain infected at time t. Hence, the cumulative distribution of new infections at time t, produced by all infected individuals ($\phi(s)$) introduced at a prior time $s = t$, is given by [186]

$$\Psi(t) = \int_{-\infty}^{t} Y(t,s)F(s)\phi(s)ds = \int_0^{\infty} Y(t,t-a)F(t-a)\phi(t-a)da.$$

Let C_ω be the ordered Banach space of all ω-periodic functions from $\mathbb{R}$ to $\mathbb{R}^6$, which is equipped with maximum norm and positive cone $C^+_\omega = \{\phi \in C_\omega : \phi(t) \geq 0, \forall t \in \mathbb{R}\}$.

Define a linear operator $L : C_\omega^+ \to C_\omega^+$ given by [186]

$$L(\phi)(t) = \int_0^\infty Y(t, t-a)F(t-a)\phi(t-a)da, \qquad \forall t \in \mathbb{R}^+, \phi \in C_\omega^+.$$

The basic reproduction ratio for non-autonomous model (2.2.1) (denoted by $\mathcal{R}_{0n}$) is then given by the spectral radius of the linear operator L, denoted by $\rho(L)$ [186]. That is, $\mathcal{R}_{0n} = \rho(L)$. It can be verified that the assumptions $A1 - A7$ in [186] are valid for the model (2.2.1) with periodic parameters. Therefore, the below fllows from Theorem 2.2 in [186].

Theorem 2.4.1 *Let* $\mathtt{r}_0(t) \geq 1$ *for all* $t \geq 0$. *The NDFS* $(\varepsilon_{0n}(t))$, *of the non-autonomous model* (2.2.1), *is LAS if* $\mathcal{R}_{0n} < 1$, *and unstable if* $\mathcal{R}_{0n} > 1$.

We claim the following result.

Theorem 2.4.2 *Let* $\mathtt{r}_0(t) > 1$. *The NDFS* $(\varepsilon_{0n}(t))$ *of the special case of the non-autonomous model* (2.2.1) *is GAS in* $C([0], \mathbb{R}_+^{12}) \setminus \{\mathcal{T}_0, \mathcal{T}_1\}$ *if* $\mathcal{R}_{0n} < 1$.

The proof of Theorem 2.4.2 is given in Appendix C. Theorem 2.4.2 shows that the disease can be effectively-controlled or eliminated if the threshold quantity $\mathcal{R}_{0n}$ can be brought to and maintained at, a value less than unity. In other words, the prospects of such effective control in the Chiang Mai province is promising if the control measures implemented in the province can bring, and maintain, $\mathcal{R}_{0n}$ to a value less than unity.

2.5 Discussion and Conclusions

This chapter is based on the design and analysis of a new deterministic model for assessing the impact of vertical transmission, in the vector population, and temperature variability on the transmission dynamics and control of dengue disease. Although dengue is primarily transmitted horizontally (*via* the vector-host-vector transmission cycle), vertical transmission has also been observed in the two main dengue-competent

Aedes mosquitoes (namely *Aedes albopictus* and *Aedes aegypti* [67; 154]) and the human host population [38].

The consequence of the vertical transmission process is that infected vectors continue to emerge (during favorable temperature and habitat conditions) even when there are no infected hosts, since the infected eggs can survive the dry season and re-emerge as infected adult mosquitoes [2; 135]. Temperature affects the dynamics of both immature and adult stages of the dengue-competent mosquito lifecycle by generally affecting vector dynamics (e.g., survival, development, etc.) and mosquito-host interactions (e.g., biting) [4].

The new model designed, which incorporates the dynamics of the aquatic stages of the mosquito (including logistic eggs oviposition and density-dependent larval mortality), vertical transmission effects in the vector, was rigorously analysed to gain insight into its dynamical features. It was further shown that, for small enough dengue mortality rate, the non-trivial disease-free equilibrium of autonomous version of the model is globally-asymptotically stable if the associated reproduction number of the model is less than unity. The epidemiological implication of this result is that the disease can be effectively-controlled if the control strategies implemented in the community can bring (and maintain) the reproduction number to a value less than unity. In other words, this result shows that bringing (and maintaining) the reproduction number to a value less than unity is necessary and sufficient for the effective control of the disease in the community.

The model was used to assess the population-level impact of vertical transmission. It should be recalled from Table 2.1 that proportion of dengue-competent vector born infected (r) is quite small (with $r \in (0.0025, 0.13)$). Numerical simulations of the autonomous version of the model (Figure 2.6(a)) show that vertical transmission has very marginal effect on the disease dynamics. However, when temperature effects are incorporated, simulations of the resulting model show that the effect of vertical

transmission is more pronounced for temperature values in the range [16−26]°C (Figure 2.10). This effect decreases for temperature values greater than 28°C.

The model designed in this chapter contains numerous parameters, and the effect of the associated uncertainties of the parameters on the numerical simulations of the model was assessed using Latin Hypercube Sampling (LHS) and Partial Rank Correlation Coefficients (PRCC) [21; 29; 111], based on parameter values and ranges relevant to dengue transmission dynamics in the Chiang Mai province of Thailand [176]. These analyses reveal some of the parameters of the model that play a dominant role on the disease transmission dynamics, including the mosquito carrying capacity, biting rate and eggs oviposition rate. Hence, effective dengue control is dependent on the design of strategies that reduce the values of these parameters (e.g., using larviciding and adulticiding to reduce the egg oviposition rate and mosquito carrying capacity, using insecticide-treated bednets and insect repellents to minimize the biting rate).

Furthermore, simulations of the model show that vertical transmission has very marginal (if at all) impact on the disease transmission dynamics in the community. Finally, it is shown that dengue-associated burden, as measured in terms of the total number of new dengue cases in humans, increases with increasing mean monthly temperature in the recorded range for Chiang Mai ($[16 - 28]^{\circ}C$). Further, such burden is maximized when the mean monthly temperature lie in the range $[16 - 28]^{\circ}C$. This range is recorded in Chiang Mai province during 3-4 months of the year (between June and August). Thus, this study suggests that anti-dengue control efforts should be intensified in the Chiang Mai province of Thailand during these months (this result supports the finding in [1]). Furthermore, dengue-associated burden decreases with decreasing mean monthly temperature below 15°C and above 32°C and this result supports the finding in [36; 61; 73; 103; 159; 198].

Some of the relevant computer codes for this chapter (and next chapter) are appended in Appendix J. I plan to work on converting the codes into an easy-to-use Decision Support System for members of the general public (including public health and other researchers) to use to run scenario analysis.

Although the model we developed in this chapter accounts for many important features of mosquito dynamics (such as the detailed mosquito lifecycle, at both immature and and adult stages) and dengue dynamics in humans, in addition to the roles of temperature fluctuations and vertical transmission, the model has a number of limitations. These include not explicitly accounting for mosquito dispersal (e.g., using a diffusion or metapopulation model to account for the effect of the mobility of mosquitoes within the community), and the effect of land use changes and human mobility on the disease dynamics. Furthermore, the homogeneous mixing assumption (where every resident of the community is assumed to have equal chance of being bitten- and infected - by a mosquito) can be relaxed, since people in certain neighbourhoods are less likely to encounter mosquitoes than people in other neighbourhoods (i.e., aspects of socioeconomic and health disparities need to be incorporated into the model). The model can also be extended to explicitly account for the dynamics of all four serotypes of dengue disease (as against considering only one dengue serotype).

Chapter 3

DYNAMICS OF A TWO-SEX MODEL FOR THE POPULATION ECOLOGY OF DENGUE MOSQUITOES IN THE PRESENCE OF WOLBACHIA

3.1 Introduction

Mosquito-borne diseases (MBDs) are infections transmitted to humans *via* the bite of infected adult female mosquitoes. MBDs, such as chikungunya, dengue, malaria, West Nile and Zika, continue to pose major public health challenges globally (particularly in the tropical and sub-tropical regions [18; 70; 72; 90]). There are over 3,500 species of mosquitoes, of which about 200 are known to be competent vectors of human diseases [9; 71]. Dengue fever, chikungunya and Zika, the most significant and widely spread arthropod-borne viral diseases [62; 79; 197], are vectored by *Aedes* mosquitoes (with the world's prevalent *Aedes aegypti* as the primary vector and the now-expanding *Aedes albopictus* as the secondary vector) [99; 197]. Of the aforementioned three arboviral diseases, dengue poses the heaviest burden (accounting for 390 million cases and 300,000 mortality annually in over 120 countries) [100; 191].

Unfortunately, there is no specific therapy available against dengue fever. Furthermore, the world's first anti-dengue vaccine (Sanofi's *Dengvaxia* licensed in 2016 [193]) proved to be ineffective and had to be withdrawn from the market [54]. Other traditional methods for controlling mosquito population abundance, such as the use of chemical insecticides to kill immature (larvicide) and adult (adulticiding *via* indoor residual spraying IRS) and/or the use of long-lasting insecticidal nets (LLINs), insect repellents etc, have also generally proved to be ineffective, largely due to adult mosquito resistance to the chemicals used in each of the insecticide-based preventive control measures mentioned above [10; 117]. In the context of dengue fever, traditional

measures (focused on reducing the population abundance of *Aedes aegypti* mosquitoes) have failed to significantly reduce or slow dengue outbreaks. Xue *et al.* [102] noted that, there has been about 30-fold increase in dengue fever cases over the last 50 years.

The failure of traditional mosquito control methods necessitate a paradigm shift in the effort to control MBDs. Over the years, a range of alternative biological control measures, aimed at suppressing or replacing the mosquito vector *via* the mass release of genetically-modified mosquitoes, have been proposed [3; 60; 88; 132; 163]. These modifications include the sterilization of adult male mosquitoes (sterile insect technology, (SIT)) to reduce the reproduction of adult wild female mosquitoes [3; 23], genetic modification to introduce lethal genes [60; 160] or introduction of genes that reduce disease transmission [88; 89; 113] into wild adult female mosquito population and the infection of mosquitoes by a second agent, such as the bacterium *Wolbachia*, aimed at suppressing pathogen transmission [132]. As noted by Segoli *et al.* [163], although these alternative methods have potential effect, their success solely depend on the ability of the released modified mosquitoes to survive and reproduce in the field. For instance, the success of SIT is crucially dependent on the ability of the released sterile male mosquitoes to be competitive and attractive to wild adult female mosquitoes [80]. Similarly, transgenic mosquitoes need to be able to survive and mate in the field in order to induce their novel genes into the wild mosquito population [112].

The release of lab-reared mosquitoes that are infected with the bacterium *Wolbachia pipientis* is considered to be a promising development for the control of dengue [51; 163]. *Wolbachia* is a maternally-transmitted intracellular parasitic infection naturally found in over 60% of insect species, including mosquitoes [150; 178]. Although *Wolbachia* is rarely found in *Aedes aegypti* (the primary vector of dengue), *Wolbachia* strains derived from *Drosophila Melanogaster* artificially introduced into *Aedes* mosquitoes (*via* embryo microinjection) was shown to suppress the development of the dengue virus [5; 58; 163].

Furthermore, *Wolbachia* induces cytoplasmic incompatibility (CI) by disrupting the reproductive cycle between the sperm and the eggs, resulting in the development failure of offsprings in the cross between *Wolbachia*-infected males and uninfected females [188; 189]. In other words, CI occurs when *Wolbachia*-infected males mate with *Wolbachia*-uninfected females to produce fewer or no offspring [188; 189]. This phenomenon causes embryos from *Wolbachia*-uninfected females to die when the females mate with *Wolbachia*-infected males (*Wolbachia*-infected females are not affected in this manner).

The overall ecological consequence of CI is that it increases the relative success of *Wolbachia*-infected females in the population, thereby enhancing the spread of the bacterium [163; 179]. In other words, since *Wolbachia* is maternally inherited, the CI effect provides a transmission advantage for the symbiont, resulting in the rapid invasion of the uninfected wild mosquito population [150; 178]. Successful invasion depends on the CI overcoming incomplete maternal transmission of the *Wolbachia* infection, as well as overcoming a loss of fitness of infected hosts [82].

In summary, *Wolbachia* induces resistance to dengue virus in *Aedes aegypti* (and limits transmission of dengue virus in *Aedes albopictus*) [19; 123; 197]. As noted by Xue *et al.* [197], *Wolbachia*-based mosquito control primarily focus on the release of *Wolbachia*-infected mosquitoes aimed at creating sustaining *Wolbachia* infection in the wild (*Wolbachia*-uninfected) mosquito population. If such (*Wolbachia*) infection is sustained, then, the wild *Wolbachia*-infected mosquitoes will be less effective in transmitting dengue virus to humans [89; 113]. Studies have shown that maintaining *Wolbachia* infection in a wild mosquito population requires continually introducing new *Wolbachia*-infected mosquitoes into the wild population [126].

Furthermore, a recent large-scale release of *Wolbachia*-infected mosquitoes in Cairns, Australia, showed that the infected mosquitoes successfully invade and spread through the wild population [89]. On the other hand, smaller releases of *Wolbachia*-infected mosquitoes resulted in the failure of infected mosquitoes to invade (owing to the immi-

gration of *Wolbachia*-free mosquitoes from surrounding areas [89]). At least 12 countries, (namely Australia, Brazil, Colombia, Fiji, India, Indonesia, Kiribati, Mexico, New Caledonia, Sri Lanka, Vanuatu and Vietnam) have been using *Wolbachia*-based strategy to control the abundance of dengue mosquitoes and disease [133].

A number of mathematical models, typically of the form of deterministic systems of nonlinear ordinary differential equations (ODEs), have been developed and used to gain insight into the dynamics and impact of large scale release of *Wolbachia*-infected mosquitoes on the control dengue virus in a population. Caspari and Watson [31] developed the first mathematical model for assessing the dynamics of CI-causing infections, and showed that the frequency of release *Wolbachia*-infected mosquitoes should always tend to increase for infections that impose no fitness cost. Qu and Hyman [144] presented a hierarchy of reduced ODE models for the spread of *Wolbachia* in mosquitoes. Numerical simulations of the ODE models developed by Qu *et al.* [145] and by Xue *et al.* [197] show that, although a small *Wolbachia* infection will die out with time, *Wolbachia* epidemic can be sustained if the fraction of *Wolbachia*-infected mosquitoes exceed a certain threshold (this result, which is supported by a recent large scale field trial in Australia [59; 82], is owing to the presence the phenomenon of backward bifurcation [61; 128]).

Koiller *et al.* [97] presented a 13-dimensional ODE model that included each aquatic stage of the mosquito and fitness cost from *Wolbachia* infection.

Zheng *et al.* [203] presented a delay differential equations model for studying the population biology of *Wolbachia*-infected mosquitoes in a community. This study shows that when the *Wolbachia* infection does not alter the mean lifespan of the *Wolbachia*-infected mosquito, the bacterium can spread into the entire population (of wild adult mosquitoes) as long as the infection frequency stays strictly above a certain threshold for a period no less than the pre-productive time τ. Furthermore, Zheng *et al.* [199] developed a diffusion model to asses the impact mosquito mobility on

the effectiveness of the *Wolbachia*-based mosquito control strategy. Their study shows that diffusion is able to lower threshold value of the *Wolbachia* infection frequency over which *Wolbachia* can invade the whole population. They also studied the impact of imperfect maternal transmission (of *Wolbachia*) on the population ecology of the *Wolbachia*-infected mosquitoes [204].

Li and Liu [106] presented an impulsive differential equation model for *Wolbachia* infection, and showed that factors such as birth and death rates and *Wolbachia* strain type play crucial roles on the persistence of *Wolbachia*-infected mosquitoes in the wild population. Hughes and Britton [85] showed that *Wolbachia* has excellent potential for dengue control in areas where the basic reproduction number for dengue-infected mosquitoes (denoted by $\mathcal{R}_0$) is not too large. Ndii *et al.* [125], using an ODE model that incorporates seasonal forcing, showed that a significant reduction in dengue cases can be achieved *via* the release of wMel strain of *Wolbachia*. Similarly, Ferguson *et al.* [56] showed that wMel *Wolbachia* strain can reduce the basic reproduction number of dengue virus by 66-70%.

In this chapter, a mathematical model will be designed and used to gain realistic insight into the population-level impact of the large-scale release of *Wolbachia*-infected mosquitoes on the control of dengue disease and mosquitoes. The central objective of this project is to determine whether or not a *Wolbachia*-based strategy will lead to the effective control of dengue virus. To achieve this objective, a new mathematical model is designed. The new two-sex model, which takes the form of a deterministic system of nonlinear differential equations is designed> The model incorporates numerous pertinent aspects of *Wolbachia*-vector-pathogen dynamics, such as the fitness cost of *Wolbachia* infection, dynamics of the aquatic stages of the vector, vertical and horizontal transmission of *Wolbachia* infection and the effects of *Wolbachia* infection in mosquitoes and humans infected with dengue disease. The chapter is organized as follows. The model is formulated in Section 3.2. Its basic qualitate features are also

explored. The model is rigorously analysed in Section 3.3.1. Numerical simulations are reported in Section 3.3.5.

3.2 Model Formulation

The total population of immature *Aedes aegypti* mosquitoes at time t, denoted by $N_A(t)$, is subdivided into mutually exclusive compartments of *Wolbachia*-uninfected (denoted by $A_U(t)$) and *Wolbachia*-infected ($A_W(t)$) immature *Aedes aegypti* mosquitoes, so that,

$$N_A(t) = A_U(t) + A_W(t).$$

Similarly, the total population of adult *Aedes aegypti* mosquitoes at time t, denoted by $N_V(t)$, is subdivided into subpopulation of *Wolbachia*-uninfected (i.e., wild or susceptible) adult female ($F_U(t)$), *Wolbachia*-uninfected adult male ($M_U(t)$), *Wolbachia*-infected adult female ($F_W(t)$), *Wolbachia*-infected adult male ($M_W(t)$) and adult female mosquitoes infected with dengue ($F_D(t)$). Hence,

$$N_V(t) = F_U(t) + M_U(t) + F_W(t) + M_W(t) + F_D(t).$$

Finally, the total human population at time t, denoted by $N_H(t)$, is subdivided into the compartments of susceptible ($S_H(t)$), exposed ($E_H(t)$), infectious ($I_H(t)$) and recovered ($R_H(t)$) humans, so that

$$N_H(t) = S_H(t) + E_H(t) + I_H(t) + R_H(t).$$

3.2.1 Birth Functions of Mosquitoes

After emergence, adult female *Aedes aegypti* mosquitoes seek male partners to mate. Let $B_{UU}(t)$ be the rate at which offsprings are produced following the mating of

Wolbachia-uninfected female and *Wolbachia*-uninfected male mosquitoes. The rate $B_{UU}(t)$ is modelled using the logistic growth rate function:

$$B_{UU}(t) = (\phi_u \psi_u) \left(\frac{1 + M_U}{1 + M_U + M_W} \right) \left(1 - \frac{N_A}{K_A} \right)_+ F_U. \tag{3.2.1}$$

In (3.2.1), ϕ_u represents the number of eggs laid *per* oviposition, while ψ_u is the oviposition rate of mated *Wolbachia*-uninfected adult female *Aedes aegypti* mosquitoes (F_U). The term $\dfrac{1 + M_U}{1 + M_U + M_W}$ represents the probability that the mating partner is a *Wolbachia*-uninfected male mosquito. The offspring growth rate is modulated by the the logistic term

$$\left(1 - \frac{N_A}{K_A} \right)_+,$$

where $K_A > N_A(t)$, for all $t > 0$, is the carrying capacity of immature mosquitoes. The notation $(x)_+ = \max\{0, x\}$ is used to ensure the non-negativity of the logistic term. Similarly, let B_{WU} represents the rate at which offsprings are produced following mating of *Wolbachia*-infected adult female mosquitoes and a *Wolbachia*-uninfected adult male mosquito. Hence,

$$B_{WU}(t) = (\phi_w \psi_w) \left(\frac{1 + M_U}{1 + M_U + M_W} \right) \left(1 - \frac{N_A}{K_A} \right)_+ F_W, \tag{3.2.2}$$

where, ϕ_w is the number of eggs laid *per* oviposition by F_W mosquito and ψ_w is the oviposition rate of mated F_W mosquito. Let B_{WW} represents the birth rate of offsprings between *Wolbachia*-infected adult female and *Wolbachia*-infected adult male mosquitoes. It follows that:

$$B_{WW}(t) = (\phi_w \psi_w) \left(\frac{M_W}{1 + M_U + M_W} \right) \left(1 - \frac{N_A}{K_A} \right)_+ F_W. \tag{3.2.3}$$

Let $B_{DU}(t)$ represents the rate at which offsprings are produced following the mating of dengue-infected adult female mosquito (F_D) and *Wolbachia*-uninfected adult male

mosquito (M_U). Hence,

$$B_{DU}(t) = (\phi_u \psi_u) \left(\frac{1 + M_U}{1 + M_U + M_W} \right) \left(1 - \frac{N_A}{K_A} \right)_+ F_D \tag{3.2.4}$$

Let B_{UW} represents the rate at which uninfected offsprings are produced following mating of *Wolbachia*-uninfected female and *Wolbachia*-infected male mosquitoes. It follows that

$$B_{UW}(t) = (1 - c_i)(\phi_w \psi_w) \left(\frac{M_W}{1 + M_U + M_W} \right) \left(1 - \frac{N_A}{K_A} \right)_+ F_U,$$

where, ϕ_w and ψ_w are as defined before, and $0 \leq c_i \leq 1$ denotes for proportion of eggs that failed to hatch due to cytoplasmic incompatibility (resulting from the mating between a *Wolbachia*-uninfected female and a *Wolbachia*-infected male mosquito). Finally, let

$$B_{DW}(t) = (1 - c_i)(\phi_w \psi_w) \left(\frac{M_W}{1 + M_U + M_W} \right) \left(1 - \frac{N_A}{K_A} \right)_+ F_D,$$

be the rate at which offsprings are produced following the mating of *Wolbachia*-infected adult male mosquitoes and dengue-infected adult female mosquitoes.

It is worth noting that, in dengue-endemic areas, adult dengue-competent (*Aedes*) mosquitoes (particularly adult wild mosquitoes) always exist. Hence, it is reasonable to assume, in the formulation of the mating probabilities above, that $M_U(t) \geq 1$ and $M_W(t) \geq 0$ for all $t \geq 0$. In other words, $M_U(t)$ is never zero in dengue-endemic areas. On the other hand, the population of *Wolbachia*-infected adult male mosquitoes ($M_W(t)$) can certainly be zero (e.g., in a dengue-endemic area where the *Wolbachia*-infected mosquitoes are not released or are released in small quantities that they failed to ultimately survive in the community). Hence, based on the assumption that $M_U(t) \geq 1$ and $M_W(t) \geq 0$, our formulation of the mating probabilities guarantee that an adult female mosquito has a higher probability of mating with the adult male

mosquito type (wild or *Wolbachia*-infected) that has higher population-level abundance in the community. For example (noting that $M_U(t) > 1$ and $M_W(t) \geq 0$), if $M_W(t) - M_U(t) - 1 > 0$, then an adult female mosquito has a higher probability of mating with an adult *Wolbachia*-infected male mosquito (M_W) than with a *Wolbachia*-uninfected adult male mosquito (M_U) in the community. Similarly, if $1 + M_U(t) - M_W(t) > 0$, then an adult female mosquito has a higher probability of mating with a *Wolbachia*-uninfected male mosquito (M_U) than with a *Wolbachia*-infected male mosquito (M_W) in the community.

3.2.2 Equations of the Model

Based on the above derivations and assumptions, the two-sex compartmental model for assessing the population-level impact of *Wolbachia* introduction on the population ecology of *Aedes aegypti* mosquitoes and dengue disease in a community is given by the following deterministic system of nonlinear differential equations:

$$
\begin{aligned}
\frac{dA_U}{dt} &= B_{UU} + (1 - v_w)(B_{WU} + B_{WW} + B_{UW}) + B_{DU} - \sigma_m A_U - \mu_a A_U, \\
\frac{dA_W}{dt} &= v_w(B_{WU} + B_{WW} + B_{UW}) + B_{DW} - \sigma_m A_W - \mu_a A_W, \\
\frac{dF_U}{dt} &= b_f \sigma_m A_U - \left(\frac{a_V \beta_V I_H}{N_H}\right) F_U - q\left(\frac{M_W}{1 + M_U + M_W}\right) F_U - \mu_{uf} F_U, \\
\frac{dF_W}{dt} &= b_f \sigma_m A_W + q\left(\frac{M_W}{1 + M_U + M_W}\right) F_U - \theta_w \mu_{uf} F_W, \\
\frac{dM_U}{dt} &= (1 - b_f)\sigma_m A_U - \mu_{um} M_U, \\
\frac{dM_W}{dt} &= (1 - b_f)\sigma_m A_W - \mu_{um} M_W, \\
\frac{dF_D}{dt} &= \left(\frac{a_V \beta_V I_H}{N_H}\right) F_U - \mu_{uf} F_D, \\
\frac{dS_H}{dt} &= \Pi_H - \left(\frac{a_V \beta_H S_H}{N_H}\right) F_D - \mu_H S_H, \\
\frac{dE_H}{dt} &= \left(\frac{a_V \beta_H S_H}{N_H}\right) F_D - \sigma_H E_H - \mu_H E_H,
\end{aligned}
\tag{3.2.5}
$$

$$\frac{dI_H}{dt} = \sigma_H E_H - \gamma_H I_H - \mu_H I_H,$$
$$\frac{dR_H}{dt} = \gamma_H I_H - \mu_H R_H.$$

In the model (3.2.5), the birth functions B_{UU}, B_{WU}, B_{UW},B_{DU} and B_{DW} are defined as before. The parameter $0 < v_w < 1$ is the proportion of offsprings of *Wolbachia*-infected adult female mosquitoes that are born infected with *Wolbachia* (via vertical transmission). The parameter σ_m models the development rate of immature mosquitoes to adulthood, with $0 < b_f < 1$ representing the proportion of new adult mosquitoes that are female. Natural death occurs in all aquatic mosquito stages at a rate μ_a. Adult female (male) mosquitoes die naturally at a rate μ_{uf} (μ_{um}). It is assumed that both *Wolbachia*-uninfected and *Wolbachia*-infected immature mosquitoes mature to adulthood at the same rate σ_m.

Wolbachia-uninfected adult female mosquito acquire dengue infection, following an effective bite on a dengue-infected human (by a susceptible adult female mosquitoes) at a rate $a_V\beta_V$, where a_V is the *per capita* biting rate of F_U mosquito from infectious human (I_H) and β_V is the probability of transmission (from I_H to F_U *per* bite). Further, *Wolbachia*-uninfected adult female mosquito acquire *Wolbachia* infection following successful mating with *Wolbachia*-infected adult male mosquitoes at a rate $\frac{qM_W}{1+M_U+M_W}$, where, q is the rate of horizontal *Wolbachia* transmission (following mating between a *Wolbachia*-infected adult male and a *Wolbachia*-uninfected adult female mosquito). The modification parameter θ_w accounts for the assumed increase of natural mortality rate of *Wolbachia*-infected adult female mosquitoes, in comparison to *Wolbachia*-uninfected adult female mosquitoes (i.e., due to fitness cost of *Wolbachia* infection) [188; 189].

Recruitment into the human population (by birth or immigration) occurs at *per capita* rate Π_H. Susceptible humans acquire dengue infection at a rate $a_V\beta_H$, where β_H is the probability of infection *per* bite from a dengue-infected adult female mosquito.

Exposed humans develop clinical symptoms of dengue at a rate σ_H. Infectious humans recover at a rate γ_H, and humans in all epidemiological compartments are assumed to die naturally at a rate μ_H (no dengue-induced mortality is assumed).

The main assumptions made in the formulation of the model (3.2.5) are:

(i) The eggs laid by *Wolbachia*-uninfected adult female mosquito (F_U) that has successfully mated with a *Wolbachia*-infected adult male mosquito (M_W) will not hatch into larvae due to perfect cytoplasmic incompatibility (CI) effect [20; 113].

(ii) *Wolbachia*-infected adult female mosquitoes (F_W) do not acquire dengue infection. This is owing to the fact that *Wolbachia* blocks the RNA of dengue virus, making dengue transmission in the *Wolbachia*-infected adult female mosquitoes impossible [20; 185]. In other words, *Wolbachia*-infected adult female mosquito has a fitness advantage of not acquiring dengue infection, as against *Wolbachia*-uninfected adult female mosquito.

(iii) *Wolbachia*-infected adult female mosquitoes have a shorter lifespan ($\theta_w > 1$), in comparison to *Wolbachia*-uninfected adult female female mosquitoes. This is a fitness cost in favour of *Wolbachia*-uninfected adult female mosquitoes. It should be mentioned that such heterogeneity (between *Wolbachia*-infected and *Wolbachia*-uninfected adult female mosquitoes) in lifespan is not assumed in the adult male mosquito population [113; 185].

(iv) No heterogeneity in natural mortality rate (μ_a) and maturation rate (σ_m) in the aquatic stage of the mosquito lifecycle is assumed.

(v) *Wolbachia* male-killing effect (i.e., feminization) is not accounted for. This is a simplifying assumption [143; 158].

(vi) No vertical transmission of dengue disease is assumed. Numerous earlier modeling studies, including the study by Taghikhani and Gumel [175], have shown that

vertical transmission has no significant effect on dengue transmission dynamics [67; 154].

Table 3.1. Description of the State Variables of the Model (3.2.5)

State Variables	**Description**
A_U (A_W)	Number of *Wolbachia*-uninfected (infected) immature mosquitoes
F_U (F_W)	Number of *Wolbachia*-uninfected (infected) adult female mosquitoes
M_U (M_W)	Number of *Wolbachia*-uninfected (infected) adult female mosquitoes
F_D	Number of dengue-infected adult female mosquitoes
S_H	Number of susceptible humans
E_H	Number of exposed (infected but not infectious) humans
I_H	Number of symptomatically-infected (infectious) humans
R_H	Number of recovered humans

Table 3.2. Description of the Parameters of the Model (3.2.5)

Parameters	**Description**
K_A	Carrying capacity of aquatic stage of mosquitoes
Π_H	Recruitment rate of humans (*via* birth or immigration)
σ_m	Development rate of immature mosquitoes in aquatic stage
b_f	Proportion of new adult mosquitoes that are female
q	Rate of horizontal transmission of *Wolbachia* from *Wolbachia*-infected adult male mosquitoes to *Wolbachia*-uninfected adult female mosquitoes
c_i	Fraction of unviable offsprings due to cytoplasmic incompatibility
ϕ_u	*Per capita* egg laying rate by *Wolbachia*-free mosquitoes
ψ_u	Probability of successful mating between uninfected adult female and uninfected adult male mosquitoes
ϕ_w	*Per capita* egg laying rate by *Wolbachia*-infected mosquitoes
ψ_w	Probability of successful mating between *Wolbachia*-infected mosquitoes
μ_a	*Per capita* mortality rate of aquatic stage of mosquitoes
μ_{uf}	*Per capita* mortality rate of uninfected adult female mosquitoes
μ_{um}	*Per capita* mortality rate of adult male mosquitoes
v_w	Proportion of offsprings of *Wolbachia*-infected adult female mosquitoes that are born with *Wolbachia* infection
a_V	Biting rate of *Wolbachia*-free mosquitoes
β_H	Probability of infection of a susceptible human *per* bite by an infected mosquito
β_V	Probability of infection of a susceptible mosquito *per* bite by an infected human
σ_H	Rate of development of clinical symptoms of disease by exposed humans
γ_H	Recovery rate for humans
θ_w	Modification parameter for the assumed increase in the mortality rate of *Wolbachia*-infected adult female mosquitoes, in comparison to *Wolbachia*-uninfected adult female mosquitoes

The model (3.2.5) is an extension of numerous *Wolbachia*-infected mosquitoes models that include vertical transmission in the vector population (such as those in [2; 39; 56; 61; 67; 77; 85; 197] by (*inter ralia*) :

- adding the dynamics of dengue disease in the human and mosquito populations (this was not included in the models in [56; 105; 106; 146; 197]);
- allowing for horizontal transmission of *Wolbachia* infection (this was not considered in the models in [56; 85; 105; 106; 125; 146; 197]).

Table 3.3. Ranges and Baseline Values of the Parameters of the Model (3.2.5).

Parameter	**Range**	**Baseline**	**Reference**
b_f	[0.5-0.57]	0.5	[107]
ϕ_u	[0-75]	50	[43]
ψ_u	[0-1]	0.8	[200]
ϕ_w	[0-70]	47	[85; 196]
ψ_w	[0-1]	0.8	–
μ_a	[0.01-0.04]	0.02	[83; 114]
μ_{uf}	[1/21-1/14]	1/17	[113; 172]
μ_m	[1/14-1/7]	1/11	[113; 172]
v_w	[0.89-1]	0.95	[185]
β_H	[0.1-0.75]	0.2	[196; 82]
β_V	[0.05-0.35]	0.1	[196; 82]
σ_H	[0.07-0.3]	0.15	[61]
γ_H	[0.09-0.25]	0.2	[61]
θ_w	[1-1.7]	1.1	[85; 196]
a_V	[0-1]	0.12	[7]

3.2.3 Basic Qualitative Analysis of the Model

In this section, the basic qualitative features of the model (3.2.5) will be explored. The aim is to assess the well-posedness of the model (with respect to positivity and boundedness of solutions of the model). We claim the following result.

Theorem 3.2.1 *Let* $\mathbf{X}(t) = (A_U(t),\ A_W(t),\ F_U(t),\ M_U(t),\ F_W(t),\ M_W(t), F_D(t),\ S_H(t),\ E_H(t),\ I_H(t)\ , R_H(t))^T$ *be solutions of the model* (3.2.5) *at time* t. *If initial data* $\mathbf{X}(0)$ *of the model be strictly positive, then, all solutions of the model remain non-negative and bounded in* $\mathbb{R}^{11}_+$ *for all time* $t > 0$.

Proof of Theorem 3.2.1 is given in Appendix D.

3.3 Analysis of Model Without Cytoplasmic Incompatability

Numerous laboratory studies [20; 113] have shown that the phenomenon of Cytoplasmic Incompatability (CI) is almost perfect (i.e., it is about 95% to 100% effective in preventing these eggs from hatching). Hence, it is instructive to analyse the dynamics of the model (3.2.5) in the absence of CI. It should be recalled that cytoplasmic incompatability causes the eggs produced by *Wolbachia*-unifected adult female mosquito that has mater with a *Wolbachia*-infected adult male mosquito not to hatch. The proportion of these eggs was denoted by the parameter c_i in the formulation of the model (3.2.5). Assuming perfect cytoplasmic incompatability in the model (3.2.5) gives the following reduced model (obtained by setting $c_i = 1$ in (3.2.5), so that $B_{UW}(t) = B_{DW}(t) = B_{DW} = 0$ in (3.2.5)):

$$
\begin{aligned}
\frac{dA_U}{dt} &= B_{UU} + (1-v_w)(B_{WU} + B_{WW}) + B_{DU} - \sigma_m A_U - \mu_a A_U,\\
\frac{dA_W}{dt} &= v_w(B_{WU} + B_{WW}) - \sigma_m A_W - \mu_a A_W,\\
\frac{dF_U}{dt} &= b_f\sigma_m A_U - \left(\frac{a_V\beta_V I_H}{N_H}\right)F_U - q\left(\frac{M_W}{1+M_U+M_W}\right)F_U - \mu_{uf}F_U,\\
\frac{dF_W}{dt} &= b_f\sigma_m A_W + q\left(\frac{M_W}{1+M_U+M_W}\right)F_U - \theta_w\mu_{uf}F_W,\\
\frac{dM_U}{dt} &= (1-b_f)\sigma_m A_U - \mu_{um}M_U,\\
\frac{dM_W}{dt} &= (1-b_f)\sigma_m A_W - \mu_{um}M_W,\\
\frac{dF_D}{dt} &= \left(\frac{a_V\beta_V I_H}{N_H}\right)F_U - \mu_{uf}F_D,\\
\frac{dS_H}{dt} &= \Pi_H - \left(\frac{a_V\beta_H S_H}{N_H}\right)F_D - \mu_H S_H,\\
\frac{dE_H}{dt} &= \left(\frac{a_V\beta_H S_H}{N_H}\right)F_D - \sigma_H E_H - \mu_H E_H,\\
\frac{dI_H}{dt} &= \sigma_H E_H - \gamma_H I_H - \mu_H I_H,
\end{aligned}
\tag{3.3.6}
$$

$$\frac{dR_H}{dt} = \gamma_H I_H - \mu_H R_H.$$

3.3.1 Existence and Asymptotic Stability of Equilibria

The reduced model (3.3.6) will now be analysed for the existence and asymptotic stability of its disease-free (i.e., dengue-free) equilibria.

3.3.1.1 Existence of Disease-free Equilibria

It is convenient, first of all, to define the following quantities

$$\mathcal{R}_U = (\phi_u \psi_u) \left(\frac{\sigma_m}{\sigma_m + \mu_a} \right) (b_f) \left(\frac{1}{\mu_{uf}} \right). \tag{3.3.7}$$

The quantity $\mathcal{R}_U$ represents the average number of new *Wolbachia*-uninfected adult female *Aedes* mosquitoes produced by a *Wolbachia*-uninfected adult female *Aedes* mosquito during its lifetime. Ecologically-speaking, it is product of the eggs laying rate of *Wolbachia*-uninfected adult *Aedes* female mosquitoes ($\phi_u \psi_u$), the probability that these eggs survived to become adult mosquitoes $\left(\frac{\sigma_m}{\sigma_m+\mu_a}\right)$, the proportion of new adult mosquitoes that are females (b_f), and the average lifespan of *Wolbachia*-uninfected adult female mosquitoes $\left(\frac{1}{\mu_{uf}}\right)$. The model (3.3.6) has the following disease-free and boundary equilibria (dengue-present).

3.3.1.2 Trivial (mosquito-free and dengue-free) equilibrium ($\mathcal{T}_0$)

$$\begin{aligned} \mathcal{T}_0 &= (A_U^*, A_W^*, F_U^*, F_W^*, M_U^*, M_W^*, F_D^*, S_H^*, E_H^*, I_H^*, R_H^*) \\ &= (0, 0, 0, 0, 0, 0, 0, \frac{\Pi_H}{\mu_H}, 0, 0, 0). \end{aligned}$$

This equilibrium is ecologically unrealistic (since mosquitoes always exist, and will not be considered in the analysis of the model).

3.3.1.3 Wolbachia-free and Dengue-free Equilibrium ($\mathcal{T}_1$)

$$\begin{aligned}\mathcal{T}_1 &= (A_U^*, A_W^*, F_U^*, F_W^*, M_U^*, M_W^*, F_D^*, S_H^*, E_H^*, I_H^*, R_H^*)\\ &= (A_U^*, 0, \frac{b_f\sigma_m A_U^*}{\mu_{uf}}, 0, \frac{(1-b_f)\sigma_m A_U^*}{\mu_{um}}, 0, 0, \frac{\Pi_H}{\mu_H}, 0, 0, 0),\end{aligned}$$

with $A_U^* = K_A(1 - \frac{1}{\mathcal{R}_U})$. Clearly, this equilibrium exists if and only if $\mathcal{R}_U > 1$ (since $A_U^* > 0$ if and only if $\mathcal{R}_U > 1$).

3.3.2 Existence of Wolbachia-free and Dengue-present Boundary Equilibrium ($\mathcal{T}_2$)

.

$$\begin{aligned}\mathcal{T}_2 &= (A_U^*, A_W^*, F_U^*, F_W^*, M_U^*, M_W^*, F_D^*, S_H^*, E_H^*, I_H^*, R_H^*)\\ &= \left(A_U^*, 0, \frac{\mu_H\mu_{uf}F_D^*}{a_V\beta_V I_H^*}, 0, \frac{(1-b_f)\sigma_m A_U^*}{\mu_{um}}, 0, F_D^*, S_H^*, \frac{a_V\beta_H F_D^* S_H^*}{N_H^*(\sigma_H+\mu_H)}, \frac{\sigma_H E_H^*}{\gamma_H+\mu_H}, \frac{\gamma_H I_H^*}{\mu_H}\right),\end{aligned}$$

where,

$$A_U^* = \frac{K_A\phi_u\psi_u(F_U^*+F_D^*)}{\phi_u\psi_w + K_A(\sigma_m+\mu_a)}, \quad F_D^* = \frac{A-B-C}{D}, \quad \text{and} \quad S_H^* = \frac{\Pi_H\mu_H}{a_V\beta_H F_D^* + \mu_H N_H^*},$$

with,

$$\begin{aligned}A &= \sigma_m\, K_A\Pi_H a_V^2 b_f\beta_H\beta_V\phi_u\psi_u\sigma_H,\\ B &= \phi_u\psi_u N_H^2\mu_H\,(\mu_H+\sigma_H)\,(\gamma_H+\mu_H)\,\mu_{uf}^2,\\ C &= \Pi_H a_V^2 K_A\sigma_H\beta_V\beta_H\,(\sigma_m+\mu_a)\,\mu_{uf},\\ D &= a_V\,(N_H\,(\mu_H+\sigma_H)\,(\gamma_H+\mu_H)\,\mu_{uf} + \Pi_H a_V\beta_V\sigma_H)\,\phi_u\beta_H\mu_{uf}\psi_u.\end{aligned}$$

It follows that this equilibrium ($\mathcal{T}_2$) exists (i.e., $F_D^* > 0$) if and only if

$$\frac{\sigma_m K_A \Pi_H {a_V}^2 b_f \beta_H \beta_V \phi_u \psi_u \sigma_H}{\phi_u \psi_u {N_H}^2 \mu_H (\mu_H + \sigma_H)(\gamma_H + \mu_H) {\mu_{uf}}^2 + \Pi_H {a_V}^2 K_A \sigma_H \beta_V \beta_H (\sigma_m + \mu_a) \mu_{uf}} > 1. \tag{3.3.8}$$

The results above are summarized below.

Theorem 3.3.1 *The model* (3.3.6) *has the following equilibria:*

(i) *A trivial mosquito-free and dengue-free equilibrium ($\mathcal{T}_0$), which always exists.*

(ii) *A Wolbachia-free and dengue-free equilibrium ($\mathcal{T}_1$), which exists if and only if* $\mathcal{R}_U > 1$.

(iii) *A Wolbachia-free and dengue-present boundary equilibrium ($\mathcal{T}_2$), which exists whenever Inequality* (3.3.8) *holds.*

It should be mentioned that the model (3.3.6) has at least one co-existence equilibrium (where both *Wolbachia*-uninfected and *Wolbachia*-infected mosquitoes are present, as well as humans and dengue). However, expressing this equilibrium in closed form is difficult (and not given here).

3.3.3 Asymptotic Stability of Disease-free Equilibria

In this section, the local asymptotic stability of the disease-free equilibria $\mathcal{T}_0$ and $\mathcal{T}_1$ will be explored.

3.3.3.1 Asymptotic Mosquito-free and Dengue-free Equilibrium ($\mathcal{T}_0$)

The linear stability of the trivial equilibrium ($\mathcal{T}_0$) can be established by linearizing the model (3.3.6) around $\mathcal{T}_0$. In particular, the Jacobian of the linearized system (3.3.6)

around $\mathcal{T}_0$ is given by

$$\mathcal{J}(\mathcal{T}_0) = \begin{bmatrix} j_{1,1} & 0 & \phi_u\psi_u & j_{1,4} & 0 & 0 & 0 & 0 & 0 & 0 & 0 \\ 0 & j_{2,2} & 0 & v_w\phi_w\psi_w & 0 & 0 & 0 & 0 & 0 & 0 & 0 \\ b_f\lambda & 0 & -\mu_{uf} & 0 & 0 & 0 & 0 & 0 & 0 & 0 & 0 \\ 0 & b_f\lambda & 0 & -\theta_w\mu_{uf} & 0 & 0 & 0 & 0 & 0 & 0 & 0 \\ j_{5,1} & 0 & 0 & 0 & -\mu_{um} & 0 & 0 & 0 & 0 & 0 & 0 \\ 0 & j_{6,2} & 0 & 0 & 0 & -\mu_{um} & 0 & 0 & 0 & 0 & 0 \\ 0 & 0 & 0 & 0 & 0 & 0 & -\mu_{uf} & 0 & 0 & 0 & 0 \\ 0 & 0 & 0 & 0 & 0 & 0 & -a_V\beta_H & -\mu_H & 0 & 0 & 0 \\ 0 & 0 & 0 & 0 & 0 & 0 & a_V\beta_H & 0 & j_{9,9} & 0 & 0 \\ 0 & 0 & 0 & 0 & 0 & 0 & 0 & 0 & \sigma_H & j_{10,10} & 0 \\ 0 & 0 & 0 & 0 & 0 & 0 & 0 & 0 & 0 & \gamma_H & -\mu_H \end{bmatrix},$$

where, $j_{1,1} = j_{2,2} = -(\sigma_m + \mu_a)$, $j_{1,4} = (1 - v_w)\,\phi_w\psi_w$, $j_{5,1} = (1 - b_f)\,\sigma_m$, $j_{6,2} = (1 - b_f)\,\sigma_m$, $j_{9,9} = -(\sigma_H + \mu_H)$, $j_{10,10} = -(\gamma_H + \mu_H)$. The associated eigenvalues of $\mathcal{J}(\mathcal{T}_0)$ are given by

$$\begin{aligned}
\lambda_1 &= -\frac{1}{2}\left[\theta_w\mu_{uf} + \sigma_m + \mu_a + \sqrt{(\sigma_m + \mu_a - \theta_w\mu_{uf})^2 + 4\,b_f\sigma_m\,\phi_w\psi_w v_w}\right], \\
\lambda_2 &= -\frac{1}{2}\left[\theta_w\mu_{uf} + \sigma_m + \mu_a - \sqrt{(\sigma_m + \mu_a - \theta_w\mu_{uf})^2 + 4\,b_f\sigma_m\,\phi_w\psi_w v_w}\right], \\
\lambda_3 &= -\frac{1}{2}\left[\mu_{uf} + \sigma_m + \mu_a + \sqrt{(\sigma_m + \mu_a - \mu_{uf})^2 + 4\,b_f\sigma_m\,\phi_u\psi_u}\right], \\
\lambda_4 &= -\frac{1}{2}\left[\mu_{uf} + \sigma_m + \mu_a - \sqrt{(\sigma_m + \mu_a - \mu_{uf})^2 + 4\,b_f\sigma_m\,\phi_u\psi_u}\right], \\
\lambda_5 &= -\mu_{uf},\ \lambda_6 = \lambda_7 = -\mu_{um},\ \lambda_8 = \lambda_9 = -\mu_H,\ \lambda_{10} = -(\sigma_H + \mu_H), \\
\lambda_{11} &= -(\gamma_H + \mu_H).
\end{aligned} \tag{3.3.9}$$

It follows from (3.3.9) that the eigenvalues λ_1, λ_3, λ_5, λ_6, λ_7, λ_8, λ_9, λ_{10} and λ_{11} all have negative real part. Furthermore, it can be seen that the eigenvalue $\lambda_2 < 0$ if and

only if

$$\mathcal{R}_W = \frac{v_w b_f \sigma_m \phi_w \psi_w}{\theta_w \mu_{uf}(\sigma_m + \mu_a)} < 1. \tag{3.3.10}$$

Similarly, the eigenvalue $\lambda_4 < 1$ if and only if

$$\mathcal{R}_U = \frac{b_f \sigma_m \phi_u \psi_u}{\mu_{uf}(\sigma_m + \mu_a)} < 1. \tag{3.3.11}$$

These results are summarized below.

Theorem 3.3.2 *The trivial equilibrium ($\mathcal{T}_0$) of the model* (3.3.6) *is locally-asymptotically stable whenever $\mathcal{R}_U < 1$ and $\mathcal{R}_W < 1$, and unstable if $\mathcal{R}_U > 1$ or $\mathcal{R}_W > 1$.*

The ecological implication of Theorem 3.3.2 is that a small influx of mosquitoes (both wild and *Wolbachia*-infected) into the community will not lead to the persistence of the mosquito population whenever both $\mathcal{R}_U$ and $\mathcal{R}_W$ are less than unity. In other words, for small initial number of mosquitoes (both wild and *Wolbachia*-infected), the mosquito population will go extinct whenever $\mathcal{R}_U$ and $\mathcal{R}_W$ are less than unity.

3.3.3.2 Asymptotic Stability of Wolbachia-free and Dengue-free Equilibrium ($\mathcal{T}_1$)

The *Wolbachia*-free and dengue-free equilibrium ($\mathcal{T}_1$) is the more realistic (in nature) of the disease-free (i.e., dengue-free) equilibria discussed above. Hence, it will be solely considered for the asymptotic stability analysis of the model (3.3.6). The *next generation operator* method [46; 182] will be used for the analysis. Using the notation in van den Driessche and Watmough [182], the associated matrices F and V, for the

new infection and transmission terms, respectively, are given by

$$F = \begin{bmatrix} 0 & v_m\phi_w\psi_w\left(1-\frac{A_U^*}{K_A}\right) & 0 & 0 & 0 & 0 & 0 \\ 0 & 0 & \frac{qF_U^*}{(1+M_U^*)} & 0 & 0 & 0 & 0 \\ 0 & 0 & 0 & 0 & 0 & 0 & 0 \\ 0 & 0 & 0 & 0 & 0 & \frac{a_V\beta_V F_U^*}{N_H^*} & 0 \\ 0 & 0 & 0 & \frac{a_V\beta_H S_H^*}{N_H^*} & 0 & 0 & 0 \\ 0 & 0 & 0 & 0 & 0 & 0 & 0 \\ 0 & 0 & 0 & 0 & 0 & 0 & 0 \end{bmatrix},$$

$$V = \begin{bmatrix} \sigma_m+\mu_a & 0 & 0 & 0 & 0 & 0 & 0 \\ -\sigma_m\, b_f & \mu_{uf}\theta_w & 0 & 0 & 0 & 0 & 0 \\ -\left(1-b_f\right)\sigma_m & 0 & \mu_{um} & 0 & 0 & 0 & 0 \\ 0 & 0 & 0 & \mu_{uf} & 0 & 0 & 0 \\ 0 & 0 & 0 & 0 & \sigma_H+\mu_H & 0 & 0 \\ 0 & 0 & 0 & 0 & -\sigma_H & \gamma_H+\mu_H & 0 \\ 0 & 0 & 0 & 0 & 0 & -\gamma_H & \mu_H \end{bmatrix}.$$

It follows that the *reproduction number* of the model (3.3.6), denoted by $\mathcal{R}_0$, is given by (where, ρ is the spectral radius; that is, ρ is the dominant eigenvalue of FV^{-1})

$$\mathcal{R}_0 = \rho(FV^{-1}) = \max\{\mathcal{R}_{0W}, \mathcal{R}_{0D}\}, \tag{3.3.12}$$

where,

$$\mathcal{R}_{0W} = \frac{1}{2}\left[\frac{\mathcal{R}_W}{\mathcal{R}_U} + \sqrt{\left(\frac{\mathcal{R}_W}{\mathcal{R}_U}\right)^2 + 4\frac{K_A q\sigma_m(1-b_f)(\mathcal{R}_U-1)\mathcal{R}_W}{\mu_{uf}\left[\mu_{um}\mathcal{R}_U + K_A\sigma_m(1-b_f)(\mathcal{R}_U-1)\right]\mathcal{R}_U}}\right], \tag{3.3.13}$$

and,

$$\mathcal{R}_{0D} = \sqrt{\frac{a_V^2 K_A b_f \beta_H \beta_V \sigma_m \sigma_H \mu_H\left(\mathcal{R}_U - 1\right)}{\Pi_H \mu_{uf}^2(\sigma_H+\mu_H)(\sigma_H+\mu_H)\mathcal{R}_U}}, \tag{3.3.14}$$

with $\mathcal{R}_U$ and $\mathcal{R}_W$ are defined in Equations (3.3.7) and (3.3.10), respectively.

The quantity $\mathcal{R}_{0W}$ represents the average number of *Wolbachia*-infected mosquitoes produced by one *Wolbachia*-infected adult female mosquito introduced into a mosquito population with only the wild adult mosquitoes present (near to the *Wolbachia*-free and dengue-free equilibrium $\mathcal{T}_1$). Similarly, $\mathcal{R}_{0D}$ is the average number of new dengue cases generated by one dengue-infected human (dengue-infected and *Wolbachia* - uninfected adult female mosquito) introduced into a population of susceptible adult female *Wolbachia*-uninfected mosquitoes (susceptible humans) near the *Wolbachia*-free and dengue-free equilibrium $\mathcal{T}_1$. The result below follows from Theorem 2 of [182].

Theorem 3.3.3 *Consider the model* (3.3.6) *with* $\mathcal{R}_U > 1$. *The Wolbachia-free and dengue-free equilibrium* $\mathcal{T}_1$ *is locally-asymptotically stable whenever* $\mathcal{R}_0 < 1$, *and unstable if* $\mathcal{R}_0 > 1$.

The epidemiological implication of Theorem 3.3.3 is that releasing small number of *Wolbachia* or dengue-infected mosquitoes into the wild mosquito population will not lead to the persistence (or dominance) of the *Wolbachia*-infected mosquitoes or dengue disease in the community when $\mathcal{R}_U > 1$ and $\mathcal{R}_0 < 1$.

The result of Theorem 3.3.3 is numerically-illustrated by simulating the model (3.3.6) using various combinations of $\mathcal{R}_{0W}$ and $\mathcal{R}_{0D}$ (here, various combinations of

$\mathcal{R}_0$). The results obtained are tabulated in Table 3.4. Items (i) and (iii) of Table 3.4 suggest the possibility of backward bifurcation in the model (3.3.6) (see [24; 27] and some of the references therein). This is owing to the fact that these two items show that *Wolbachia*-infected mosquitoes may die out or persist when $\mathcal{R}_0 < 1$. Backward bifurcation is a dynamic phenomenon associated with the co-existence of multiple asymptotically-stable equilibrium (namely, the locally-asymptotically stable $\mathcal{T}_1$ and a locally-asymptotically stable co-existence equilibrium) when $\mathcal{R}_{0W} < 1$ [24; 27]. In particular, Figure 3.1 shows such persistence (Figure 3.1a) or decay (Figure 3.1b) of *Wolbachia*-infected mosquitoes when $\mathcal{R}_0 < 1$ for two different sets of initial conditions.

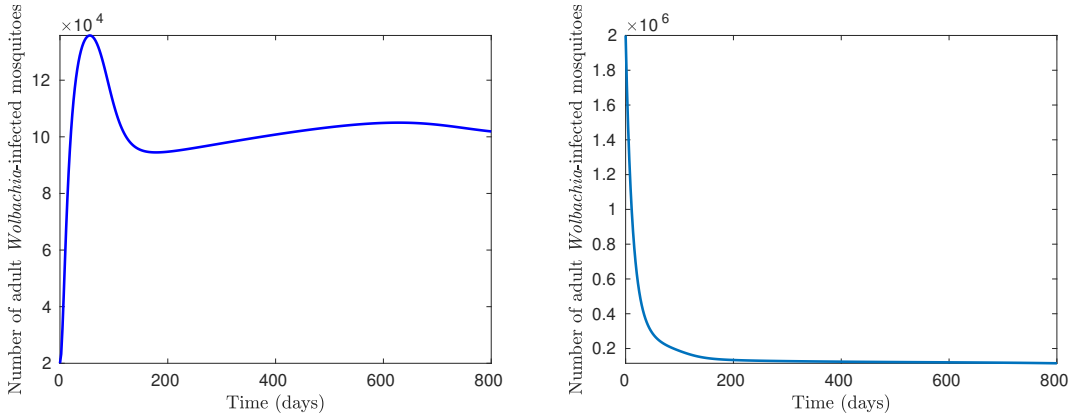

Figure 3.1: Simulation of the Model (3.3.6) Showing the Persistence or Decay of the Total Population of Adult *Wolbachia*-infected Mosquitoes ($F_W + M_W$) as a Function of Time, Using Two Different Set of Initial Conditions. Parameter Values Used Are: $\sigma_m = 0.25$, $q = 0.1$, $K_A = 120000$, $b_f = 0.5$, $\mu_a = 0.001$, $\mu_{uf} = 1/18$, $\mu_{um} = 1/11$, $v_w = 0.5$, $\phi_u = 3$, $\psi_u = 0.8$, $\phi_w = 3$, $\psi_w = 0.6$, $\theta_w = 1.1$, $a_V = 0.3$, $\beta_H = 0.8$, $\beta_V = 0.8$, $\sigma_H = 0.15$, $\gamma_H = 0.2$, $\Pi_H = 100$, and $\mu_H = 0.00005$, such that $\mathcal{R}_U = 21.51$, $\mathcal{R}_{\mathcal{W}} = 7.82$, $\mathcal{R}_{0W} = 0.95$ and $\mathcal{R}_{0D} = 0.94$. The initial values used are: **(a)** $A_U(0) = 100$, $A_W(0) = 0$, $F_U(0) = 10,000$, $F_W(0) = 10,000$, $M_U(0) = 100$, $M_W(0) = 10,000$, $F_D(0) = 1,000$, $S_H(0) = 100,000$, $E_H(0) = 10$, $I_H(0) = 2$, and $R_H(0) = 0$. **(b)** $A_U(0) = 10,000$, $A_W(0) = 1,000$, $F_U(0) = 10,000$, $F_W(0) = 100,000$, $M_U(0) = 10,000$, $M_W(0) = 1,000,000$, $F_D(0) = 1,000$, $S_H(0) = 100,000$, $E_H(0) = 10$, $I_H(0) = 2$, and $R_H(0) = 0$.

Table 3.4. Possible Outcomes Based on Values of the Reproduction Number.

Item	$\mathcal{R}_{0W}$	$\mathcal{R}_{0D}$	$\mathcal{R}_0$	outcome
(i)	< 1	< 1	< 1	*Wolbachia* dies out or persists
(ii)	> 1	< 1	$\mathcal{R}_{0W}$	*Wolbachia* persists
(iii)	< 1	> 1	$\mathcal{R}_{0D}$	*Wolbachia* dies out or persists
(iv)	$1 < \mathcal{R}_{0W} < \mathcal{R}_{0D}$	> 1	$\mathcal{R}_{0D}$	*Wolbachia* dies out or persists
(v)	> 1	$1 < \mathcal{R}_{0D} < \mathcal{R}_{0W}$	$\mathcal{R}_{0W}$	*Wolbachia* persists
(vi)	$\mathcal{R}_{0W} = \mathcal{R}_{0D} > 1$	$\mathcal{R}_{0W} = \mathcal{R}_{0D} > 1$	$\mathcal{R}_{0W}$ or $\mathcal{R}_{0D}$	*Wolbachia* persists

The epidemiological implication of backward bifurcation is that the classical requirement of having $\mathcal{R}_0 < 1$, while necessary, is no longer sufficient for the effective control of mosquitoes in the community [24; 27]. In such a backward bifurcation scenario (in the context of the model (3.3.6)), the effective control of mosquitoes and dengue disease (including the persistence of *Wolbachia*-infected mosquitoes) depend on the initial size of the sub-populations of the model (3.3.6). The presence of the phenomenon of backward bifurcation is now explored rigorously for a special case of the model (3.3.6).

3.3.4 Backward Bifurcation Analysis

For simplicity, the phenomenon of backward bifurcation will be explored for a special case of the model (3.3.6) with mosquitoes only (i.e., no humans and dengue disease). This special case of the model (3.3.6) is given by (where the expressions for $B_{UU}(t)$, $B_{WU}(t)$ and $B_{WW}(t)$, given in Section 3.2.1, are used now)

$$\begin{aligned}
\frac{dA_U}{dt} &= B_{UU} + (1-v_w)(B_{WU}+B_{WW}) - \sigma_m A_U - \mu_a A_U,\\
\frac{dA_W}{dt} &= v_w(B_{WU}+B_{WW}) - \sigma_m A_W - \mu_a A_W,\\
\frac{dF_U}{dt} &= b_f\sigma_m A_U - \left(\frac{a_V\beta_V I_H}{N_H}\right)F_U - q\left(\frac{M_W}{1+M_U+M_W}\right)F_U - \mu_{uf}F_U,\\
\frac{dF_W}{dt} &= b_f\sigma_m A_W + q\left(\frac{M_W}{1+M_U+M_W}\right)F_U - \theta_w\mu_{uf}F_W,\\
\frac{dM_U}{dt} &= (1-b_f)\sigma_m A_U - \mu_{um}M_U,\\
\frac{dM_W}{dt} &= (1-b_f)\sigma_m A_W - \mu_{um}M_W.
\end{aligned} \tag{3.3.15}$$

The model (3.3.15) will be studied in the following invariant region:

$$\mathcal{D} = \{(A_U, A_W, F_U, F_W, M_U, M_W) \in \mathbb{R}^6_+ | A_U, A_W, F_U, F_W, M_U, M_W < K_A\}.$$

For the model (3.3.15), the equilibria $\mathcal{T}_0$ and $\mathcal{T}_1$ now, respectively, reduce to

$$\mathcal{T}_{0\diamond} = (A_U^*, A_W^*, F_U^*, F_W^*, M_U^*, M_W^*) = (0, 0, 0, 0, 0, 0),$$

and,

$$\mathcal{T}_{1\diamond} = (A_U^*, A_W^*, F_U^*, F_W^*, M_U^*, M_W^*) = (A_U^*, 0, \frac{b_f \sigma_m A_U^*}{\mu_{uf}}, 0, \frac{(1-b_f)\sigma_m A_U^*}{\mu_{um}}, 0),$$

with $A_U^* = K_A(1 - \frac{1}{\mathcal{R}_U})$. The equilibrium $\mathcal{T}_{1\diamond}$ exists if and only if $\mathcal{R}_U > 1$. We claim the following result for the trivial equilibrium $\mathcal{T}_{0\diamond}$ of the model (3.3.15).

Theorem 3.3.4 *The trivial equilibrium ($\mathcal{T}_{0\diamond}$) of the model* (3.3.15) *is locally-asymptotically stable whenever $\mathcal{R}_U < 1$ and $\mathcal{R}_W < 1$, and unstable if $\mathcal{R}_U > 1$ or $\mathcal{R}_W > 1$.*

The proof of Theorem 3.3.4, based on using standard linearization, is given in Appendix E. Further, we claim the the following result.

Theorem 3.3.5 *The model* (3.3.15) *with $\mathcal{R}_U > 1$ undergoes a backward bifurcation at $\mathcal{R}_{0W} = 1$ whenever a certain bifurcation coefficient, denoted by $a(\phi_w^*)$ and defined in Equation* (.0.6)*, is positive.*

The proof of Theorem 3.3.5, based on using Center Manifold theory [27; 30], is given in Appendix F. Figure 3.2 depicts the backward bifurcation diagram of the model (3.3.15). It is worth mentioning that some earlier studies for *Wolbachia*-dengue dynamics, such as those in [2; 39; 56; 61; 67; 77; 85; 197], have illustrated the presence of backward bifurcation numerically.

As stated earlier, the presence of backward bifurcation in the transmission dynamics of a disease emphasize the importance of initial conditions in determining the disease outcome when the reproduction number of the model is less than unity. In other words, the presence of backward bifurcation phenomenon makes the effective disease control

more difficult. Consequently, it is instructive to explore the mechanism(s) that cause the presence of backward bifurcation in the model (3.3.15). This is explained below.

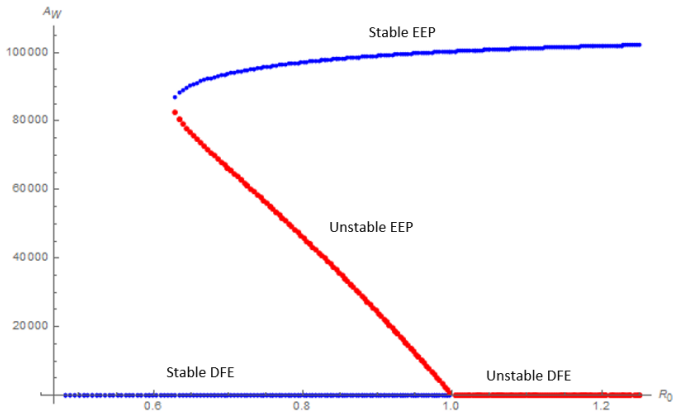

Figure 3.2: Backward Bifurcation Diagram of the Model (3.3.15), Showing a Plot of A_W^* as a Function of the Reproduction Number $\mathcal{R}_{0W}$. Parameter Values Used to Generate This Bifurcation Diagram Are: $\sigma_m = 1/5, q = 0.26, K_A = 120000, b_f = 1/2, \mu_a = 0.001, \mu_{uf} = 1/18, \mu_{um} = 1/9, \phi_u = 17, v_w = 0.88076, \psi_u = 1, \psi_w = 0.42, \theta_w = 0.997$ and $\phi_w = 8$ (so that $a = 2.9496711 \times 10^{-6}$, $\mathcal{R}_0 = 1$). Red and blue lines indicate unstable and stable endemic equilibrium points (EEP), respectively.

It is convenient to consider the special case of the model (3.3.15) with $q = 0$ (no horizontal transmission of *Wolbachia*) and with fixed mating probabilities $\frac{M_W}{1+M_U+M_W}$ and $\frac{1+M_U}{1+M_U+M_W}$. That is, let $q = 0$ in (3.3.15) and

$$m_w = \frac{M_W}{1 + M_U + M_W} = \bar{m}_w, \text{ and } \quad m_u = 1 - m_w = \frac{1 + M_U}{1 + M_U + M_W} = \bar{m}_u,$$

with $\bar{m}_u \in (0,1]$ and $\bar{m}_w \in [0,1)$. Using constant values of m_u and m_w (given by $\bar{m}_u$ and $\bar{m}_w$ above, respectively) in the model (3.3.15), it follows that the equilibria $\mathcal{T}_{0\diamond}$ and $\mathcal{T}_{1\diamond}$ now have the forms:

$$\mathcal{T}_{0c} = (A_U^*, A_W^*, F_U^*, F_W^*, M_U^*, M_W^*) = (0, 0, 0, 0, 0, 0),$$

and,

$$\mathcal{T}_{1c} = (A_U^*, A_W^*, F_U^*, F_W^*, M_U^*, M_W^*) = (A_U^*, 0, \frac{b_f \sigma_m A_U^*}{\mu_{uf}}, 0, \frac{(1 - b_f)\sigma_m A_U^*}{\mu_{um}}, 0),$$

with $A_U^* = K_A(1 - \frac{1}{\bar{m}_u \mathcal{R}_U})$. Furthermore, let

$$\tilde{\mathcal{R}}_{0W} = \frac{\mathcal{R}_W}{\bar{m}_u \mathcal{R}_U},$$

be the associated reproduction number of the model (3.3.15). We claim the following result.

Theorem 3.3.6 *Consider the model* (3.3.15) *with* $m_w = \bar{m}_w \in [0, 1)$, $m_u = \bar{m}_u \in (0, 1]$ *and* $q = 0$. *The trivial equilibrium* $\mathcal{T}_{0c}$ *of the model* (3.3.15) *is locally-asymptotically stable if* $\mathcal{R}_W < 1$ *and* $\bar{m}_w > 1 - \frac{1}{\mathcal{R}_U}$.

The proof of Theorem 3.3.6, based on using standard linearization, is given in Appendix G. We claim the following result.

Theorem 3.3.7 *Let* $\mathcal{R}_U > 1$. *The model* (3.3.15) *with* $m_w = \bar{m}_w$, $m_u = \bar{m}_u$ *and* $q = 0$ *does not undergo a backward bifurcation at* $\tilde{\mathcal{R}}_{0W} = 1$ *whenever* $\bar{m}_w < 1 - \frac{1}{\mathcal{R}_U}$.

The proof of Theorem 3.3.7, based on using Center Manifold theory [27; 30], is given in Appendix H. Theorem 3.3.7 guarantees the non-existence of backward bifurcation in the model (3.3.15) when $\mathcal{R}_U > 1$, $m_w = \bar{m}_w$, $m_u = \bar{m}_u$ and $q = 0$. Thus, this study identifies two main mechanisms that cause the presence of backward bifurcation in the model (3.3.6), namely

(i). horizontal transmission of *Wolbachia* from a *Wolbachia*-infected male mosquito to a *Wolbachia*-uninfected female mosquito (i.e., $q \neq 0$);

(ii). variable mating probabilities for *Wolbachia*-infected (m_w) and *Wolbachia*-uninfected (m_u) adult male mosquitoes. In particular, as shown in the proof of Theorem 3.3.7 (Appendix H), backward bifurcation does not exist at $\tilde{\mathcal{R}}_{0W} = 1$ if $\bar{m}_w < 1 - \frac{1}{\mathcal{R}_U}$.

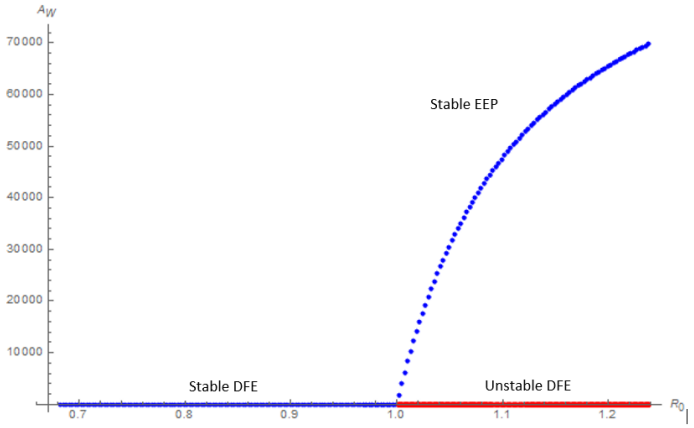

Figure 3.3: Transcritical (Forward) Bifurcation Diagram of the Special Case of the Model (3.3.15), With $m_w\bar{m}_w$, $m_u = \bar{m}_u$ and $q = 0$. Parameter Values Used to Generate This Bifurcation Diagram Are: $\sigma_m = 1/5$, $K_A = 120000$, $b_f = 1/2$, $\mu_a = 0.001$, $\mu_{uf} = 1/17$, $\mu_{um} = 1/9$, $\phi_u = 17$, $\psi_u = 1$, $\psi_w = 0.42$, $\theta_w = 0.997$, $\bar{m}_u = 0.5$, $\bar{m}_w = 0.5$, $v_w = .88076$ and $\phi_w = 25.2$ (so that $a = -5.565182480 \times 10^{-7}$, $\bar{\mathcal{R}}_{0W} = 1$, $w_2 = 1$ and $v_2 = 1$). Red and Blue Lines Indicate Unstable and Stable Endemic Equilibrium, Respectively.

It is instructive to explore whether or not the *Wolbachia*-free equilibrium of the model (3.3.15), given by $\mathcal{T}_{1c}$, is globally-asymptotically stable when the aforementioned conditions for backward bifurcation are relaxed (i.e., when $q = 0$, $m_u = \bar{m}_u$ and $m_w = \bar{m}_w$). This is done below. We claim the following result.

Theorem 3.3.8 *Consider the model* (3.3.15) *with* $m_w = \bar{m}_w$, $m_u = \bar{m}_u$, $q = 0$ *and* $\mathcal{R}_U > 1$. *The Wolbachia-free equilibrium of the model* (3.3.15), *given by* $\mathcal{T}_{1c}$, *is globally-asymptotically stable in* $\mathcal{D}\backslash\{\mathcal{T}_{0\diamond}\}$ *whenever* $\tilde{\mathcal{R}}_{0W} \leq \frac{1}{\mathcal{R}_U(1-\bar{m}_w)} < 1$.

The proof of Theorem 3.3.8, based on using Lyapunov function theory, is given in Appendix I. The epidemiology implication of Theorem 3.3.8 is that the *Wolbachia*-infected mosquito population will not survive in the community regardless of the initial number of *Wolbachia*-infected mosquitoes released into the wild mosquito population (if $\tilde{\mathcal{R}}_{0W} < \frac{1}{\mathcal{R}_U(1-\bar{m}_w)}$ and $\bar{m}_w < 1 - \frac{1}{\mathcal{R}_U}$).

3.3.5 Periodic Release of *Wolbachia*-infected Mosquitoes

To allow for the impulsive/periodic release of mosquitoes in the reduced model (3.3.6), the equations for dynamics of the *Wolbachia*-infected females (F_W) and males (M_W) will now be re-defined as [84; 167]

$$\begin{aligned}
\frac{dF_W}{dt} &= b_f\sigma_m A_W + q\left(\frac{M_W}{1+M_U+M_W}\right)F_U - \theta_w\mu_{uf}F_W, \quad t \neq n\tau,\\
\frac{dM_W}{dt} &= (1-b_f)\sigma_m A_W - \mu_{um}M_W, \qquad\qquad\qquad\quad t \neq n\tau,\\
F_W(n\tau^+) &= F_W(n\tau^+) + W_{Rf}, \qquad\qquad\qquad\quad t = n\tau,\\
M_W(n\tau^+) &= M_W(n\tau^+) + W_{Rm}, \qquad\qquad\qquad\quad t = n\tau,\\
F_W(0^+) &\geq 0, \;\; M_W(0^+) \geq 0,
\end{aligned} \tag{3.3.16}$$

where, $\tau > 0$ is the time lag between successive releases of adult *Wolbachia*-infected mosquitoes (either males or females or both), $n\tau^+$ is the moment immediately after the nth *Wolbachia*-infected mosquitoes release and W_{Rf} and W_{Rm} denote for the number of *Wolbachia*-infected female and male mosquitoes released, respectively, at each release time $n\tau$.

3.3.5.1 Release effect statistic

Following White *et al* [190], we define the *release effect statistic*, denoted by $R(t)$, given by

$$R(t) = \frac{\int_\tau^{t+\tau} N_1(s)ds}{\int_\tau^{t+\tau} N_0(s)ds}, \tag{3.3.17}$$

where, N_1 is the total abundance of uninfected adult female mosquitoes over a period of time with the release of *Wolbachia*-infected mosquitoes and N_0 is the total abundance of un-infected adult female mosquitoes over that same period without the

release of *Wolbachia*-infected mosquitoes. The time-dependent measure $R(t)$ in Equation (3.3.17) gives the relative effect of the *Wolbachia*-infected mosquitoes release at different time points in the population cycle of the wild-type mosquitoes [190]. Equation (3.3.17) gives the following three ecological explanation for the release statistic R [190]:

1. If $R = 1$, then there is no relative effect of the control strategy on the wild-type mosquito population.

2. If $R < 1$, then the release have a negative (desirable) effect on the wild-type mosquito population.

3. If $R > 1$, then the release have a positive (not desirable) effect on the wild-type mosquito population.

3.3.5.2 Simulations: effect of periodic release of *Wolbachia*-infected mosquitoes

The model (3.3.6), with (3.3.16), will now be simulated, using the baseline values tabulated in Table 3.3 (unless otherwise stated), to assess the population-level impact of the release of certain quantities of adult *Wolbachia*-infected mosquitoes on the population abundance of the local wild adult mosquitoes. The model (3.3.6), with (3.3.16), will, first of all, be simulated in the absence of the release of *Wolbachia*-infected mosquitoes (i.e., $A_W = F_W = M_W = 0$), for a period of two year, to determine the baseline worse-case abundance of the local wild adult mosquito population (Figure 3.4). The adult *Wolbachia*-infected mosquitoes are then released periodically for a one year duration.

The model (3.3.6), with (3.3.16), is now simulated to assess the impact of the periodic release of *Wolbachia*-infected mosquitoes on the population abundance of the wild adult mosquitoes. In particular, the model will be simulated using a frequency release period of three weeks (i.e., $\tau = 21$ days) and various values of W_{Rf} and W_{Rm}.

The chosen 3-week release period is consistent with what was done in Australia during the period 2014-2017 [155].

Releasing $10,000$ Wolbachia-infected female and male mosquitoes (i.e., $W_{Rf} = W_{Rm} = 10,000$), for the 3-week release period for a one-year duration (Figure 3.5), shows that the implementation of *Wolbachia*-based mosquito control resulted in a significant decrease in the wild adult mosquito population (in comparison to the baseline worse-case scenario, Figure 3.4). In particular, Figure 3.5 shows that the populations of un-infected adult female (F_U) and adult male (M_U) mosquitoes decreased by 85% and 70%, respectively, in comparison to the worst-case scenario in Figure 3.4. It should be mentioned that, for the number of *Wolbachia*-infected mosquitoes released and frequency of release in this simulation (i.e., $W_{Rf} = W_{Rm} = 10,000$ and $\tau = 21$ days), the associated release effect statistic of the model is $R = 0.79$ (from which it follows that the release of *Wolbachia*-infected mosquitoes will lead to the effective control or elimination of the wild mosquitoes[190]) .

When the number of *Wolbachia*-infected adult mosquitoes released is increased to $100,000$ (i.e., $W_{Rf} = W_{Rm} = 100,000$), for the same 3-week ($\tau = 21$ days) release period and the same one year duration, the results obtained (depicted in Figure 3.6) show a decrease of 93% (from the baseline worse-case scenario) for the un-infected adult female mosquitoes (F_U) and 73% for the un-infected adult male mosquitoes (M_U). The corresponding larger release effect statistic of the model is $R = 0.66 < 1$.

Finally, when the number of *Wolbachia*-infected mosquitoes released is increased to $200,000$ (i.e., $W_{Rf} = W_{Rm} = 200,000$, with the same $\tau = 21$ days frequency of release and one year duration), our simulations show an increase in the reduction in the in the wild adult mosquito population (Figure 3.7). In particular, the populations of un-infected adult female and male mosquitoes decreased by 96% and 76%, respectively. For this case, the corresponding release effect statistic of the model is $R = 0.64 < 1$.

The model (3.3.6), with (3.3.16), is further simulated for the case where *Wolbachia*-infected mosquitoes of one gender are released. In particular, when $200,000$ *Wolbachia*-infected male mosquitoes are released (i.e., $W_{Rm} = 200,000$) and no Wolbachia-infected female mosquitoes are released (i.e., $W_{Rf} = 0$), our simulations (for the 3-week release period over a one-year duration) show a reduction (from their baseline values) of 95% and 75% in the population of adult wild mosquitoes, respectively (Figure 3.8).

Similarly, when only $200,000$ adult female mosquitoes are released, and no adult male mosquitoes are released ($W_{Rf} = 200,000$ and $W_{Rm} = 0$), the simulation results obtained, depicted in Figure 3.9, show a reduction (from baseline) of 90% and 70% in the population of the wild adult mosquitoes. Thus, this study shows that releasing adult male *Wolbachia*-infected mosquitoes is more beneficial than releasing adult female Wolbachia-infected mosquitoes. For these simulations, the release effect statistic (R) is given by $R = 0.65$ if only adult male Wolbachia-infected mosquitoes are released, and 0.68 if only adult females are released. This result can be ecologically explained based on the fact that the *Wolbachia*-infected adult male mosquitoes significantly affect the cytoplasmic incompatibility aspect of *Wolbachia* implementation [188; 189] (thereby reducing the population abundance of the wild mosquitoes).

It is worth stating that if the release frequency is increased, for instance from the default release frequency of every three weeks to weekly (i.e., τ is decreased from $\tau = 21$ days to $\tau = 7$ days), the simulation results obtained for the case with $W_{Rf} = W_{Rm} = 100,000$ (depicted in Figure 3.10) show similar dynamics as those obtained in Figure 3.7. Thus, increasing the frequency of release from the default value of every three weeks to weekly does not significantly affect the effectiveness of the *Wolbachia*-based control program in curtailing the local abundance of the wild mosquitoes. This is contrary to other studies for biological control of mosquitoes, such as sterile insect technology, where the effectiveness of the intervention increase with more frequent releases [16; 28; 177].

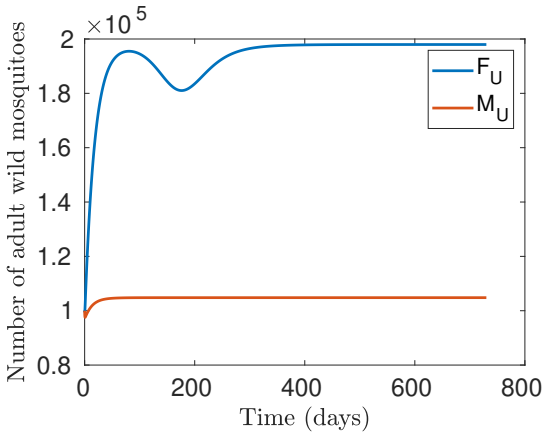

Figure 3.4: Simulations of the Model (3.3.6), with (3.3.16), Showing the Dynamics of Wild Adult Wild Male and Female Mosquitoes, in the Absence of the Release of *Wolbachia*-infected Mosquitoes, over a Two-year Period (This Is Needed to Generate Baseline Values for the Number of Wild Mosquitoes Prior to the Release of Wolbachia-infected Mosquitoes). Parameter Values Used Are as given in Table 3.3 (with This Set of Parameter Values, the Reproduction Number ($\mathcal{R}_0$) Takes the Value $\mathcal{R}_0 = 1.24$).

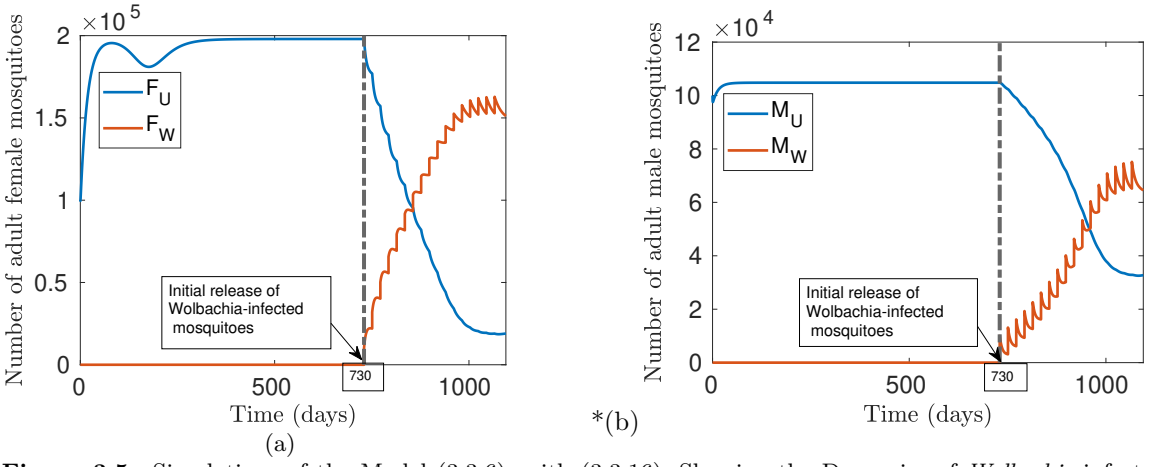

Figure 3.5: Simulations of the Model (3.3.6), with (3.3.16), Showing the Dynamics of *Wolbachia*-infected and *Wolbachia*-uninfected (Wild) Adult Mosquitoes. The Simulations Were Ran for Two Years Without the Release of the *Wolbachia*-infected Mosquitoes, Following Which the *Wolbachia*-infected Mosquitoes Are Released Every Three Weeks (I.E., $\tau = 21$ Days) for a Period of One Year. A Total of 10,000 *Wolbachia*-infected Female ($W_{Rf} = 10,000$) and Male ($W_{Rm} = 10,000$) Mosquitoes Are Released *per* Release Period. Parameter Values Used Are as given in Table **??**. Notation: The Dashed Vertical Lines Represent the Time for the Onset of the Release of the *Wolbachia*-infected Mosquitoes.

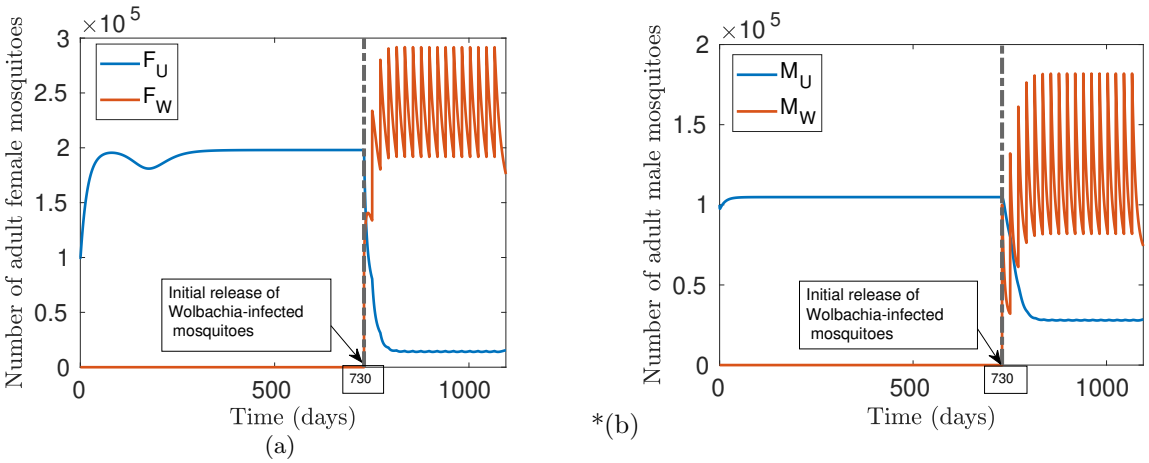

Figure 3.6: Simulations of the Model (3.3.6), with (3.3.16), Showing the Dynamics of *Wolbachia*-infected and *Wolbachia*-uninfected (Wild) Adult Mosquitoes. The Simulations Were Ran for Two Years Without the Release of the *Wolbachia*-infected Mosquitoes, Following Which the *Wolbachia*-infected Mosquitoes Are Released Every Three Weeks (I.E., $\tau = 21$ Days) for a Period of One Year. A Total of 100,000 *Wolbachia*-infected Female ($W_{Rf} = 100,000$) and Male ($W_{Rm} = 100,000$) Mosquitoes Are Released *per* Release Period. Parameter Values Used Are as given in Table 3.3. Notation: The Dashed Vertical Lines Represent the Time for the Onset of the Release of the *Wolbachia*-infected Mosquitoes.

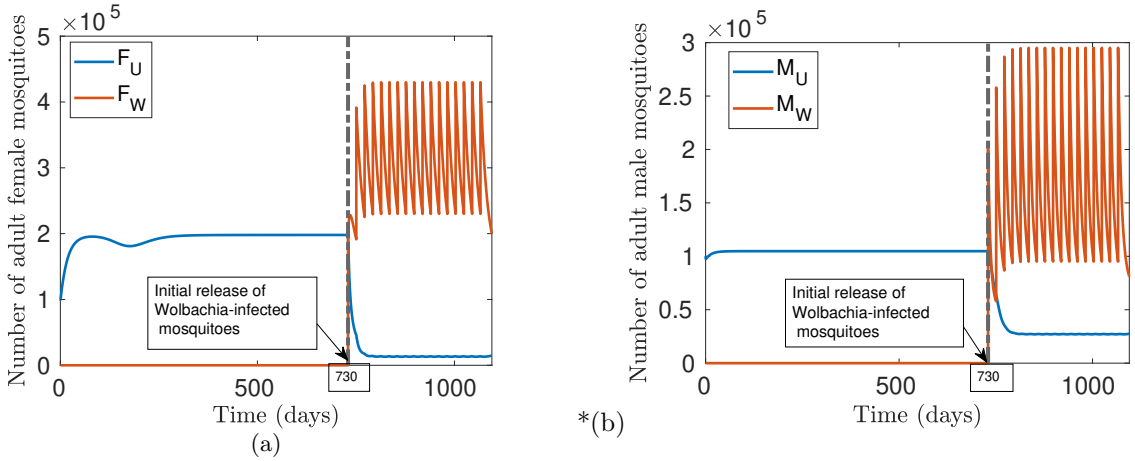

Figure 3.7: Simulations of the Model (3.3.6), with (3.3.16), Showing the Dynamics of *Wolbachia*-infected and *Wolbachia*-uninfected (Wild) Adult Mosquitoes. The Simulations Were Ran for Two Years Without the Release of the *Wolbachia*-infected Mosquitoes, Following Which the *Wolbachia*-infected Mosquitoes Are Released Every Three Weeks (I.E., $\tau = 21$ Days) for a Period of One Year. A Total of 200,000 *Wolbachia*-infected Female ($W_{Rf} = 200,000$) and Male ($W_{Rm} = 200,000$) Mosquitoes Are Released *per* Release Period. Parameter Values Used Are as given in Table 3.3. Notation: The Dashed Vertical Lines Represent the Time for the Onset of the Release of the *Wolbachia*-infected Mosquitoes.

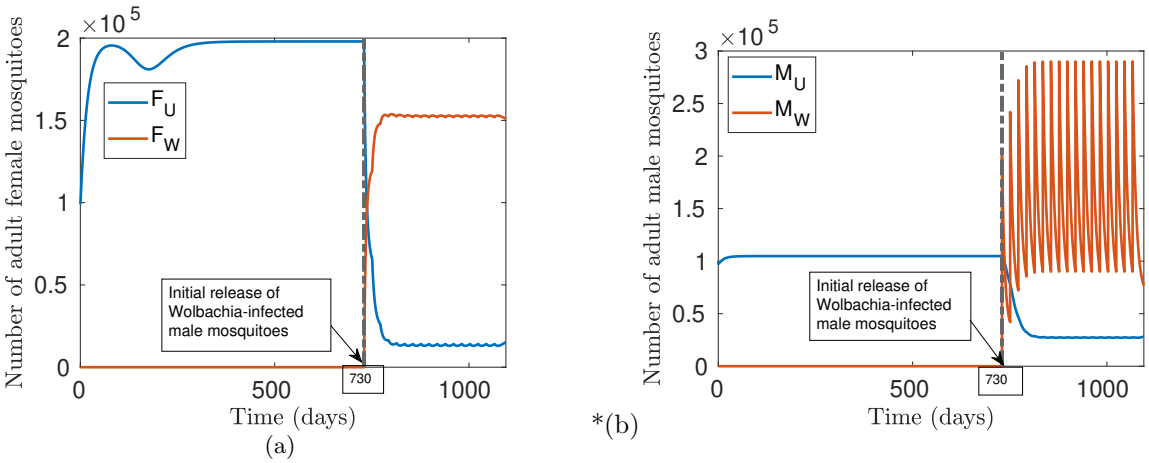

Figure 3.8: Simulations of the Model (3.3.6), with (3.3.16), Showing the Dynamics of *Wolbachia*-infected and *Wolbachia*-uninfected (Wild) Adult Mosquitoes. The Simulations Were Ran for Two Years Without the Release of the *Wolbachia*-infected Mosquitoes, Following Which the *Wolbachia*-infected Mosquitoes Are Released Every Three Weeks (I.E., $\tau = 21$ Days) for a Period of One Year. A Total of 200,000 Only *Wolbachia*-infected Male Mosquitoes ($W_{Rm} = 200,000$ and $W_{Rf} = 0$) Are Released *per* Release Period. Parameter Values Used Are as given in Table 3.3. Notation: The Dashed Vertical Lines Represent the Time for the Onset of the Release of the *Wolbachia*-infected Mosquitoes.

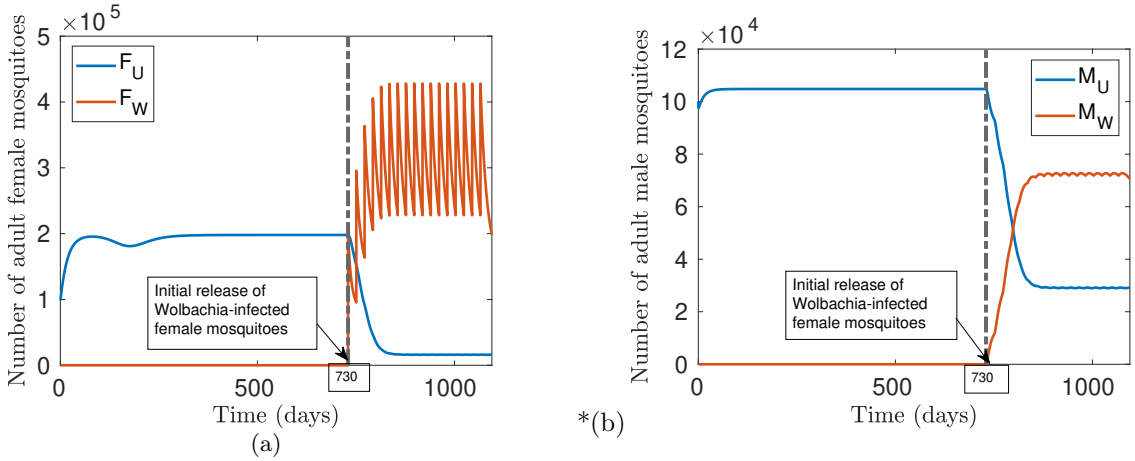

Figure 3.9: Simulations of the Model (3.3.6), with (3.3.16), Showing the Dynamics of *Wolbachia*-infected and *Wolbachia*-uninfected (Wild) Adult Mosquitoes. The Simulations Were Ran for Two Years Without the Release of the *Wolbachia*-infected Mosquitoes, Following Which the *Wolbachia*-infected Mosquitoes Are Released Every Three Weeks (I.E., $\tau = 21$ Days) for a Period of One Year. A Total of 200,000 Only *Wolbachia*-infected Female Mosquitoes ($W_{Rf} = 200,000$ and $W_{Rm} = 0$) Are Released *per* Release Period. Parameter Values Used Are as given in Table 3.3. Notation: The Dashed Vertical Lines Represent the Time for the Onset of the Release of the *Wolbachia*-infected Mosquitoes.

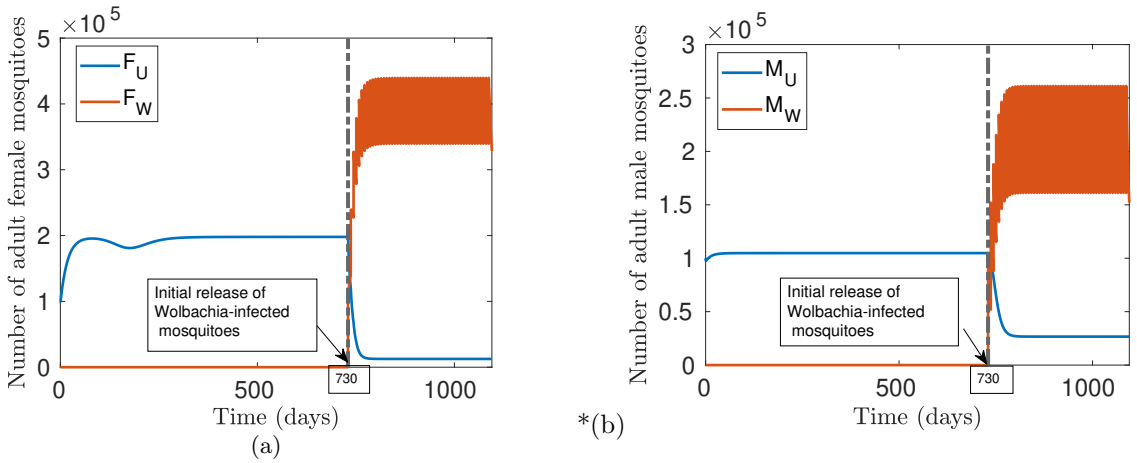

Figure 3.10: Simulations of the Model (3.3.6), with (3.3.16), Showing the Dynamics of *Wolbachia*-infected and *Wolbachia*-uninfected (Wild) Adult Mosquitoes. The Simulations Were Ran for Two Years Without the Release of the *Wolbachia*-infected Mosquitoes, Following Which the *Wolbachia*-infected Mosquitoes Are Released Every One-week (I.E., $\tau = 7$ Days) for a Period of One Year. A Total of 100,000 *Wolbachia*-infected Female ($W_{Rf} = 100,000$) and Male ($W_{Rm} = 100,000$) Mosquitoes Are Released *per* Release Period. Parameter Values Used Are as given in Table 3.3. Notation: The Dashed Vertical Lines Represent the Time for the Onset of the Release of the *Wolbachia*-infected Mosquitoes.

3.3.6 Simulations for Effect of Cytoplasmic Incompatibility (CI)

In this section, the full model (3.2.5) (with $c_i \neq 1$), together with with (3.3.16), will now be simulated to assess the community-wide impact of CI on the effectiveness of the *Wolbachia*-based mosquito control strategy. In particular, the full model (3.2.5), with (3.3.16), is simulated using the baseline parameter values tabulated in Table 3.3. The specific objective is to assess the community-wide impact of CI on the population abundance of the local wild (i.e., *Wolbachia*-uninfected adult female and male) adult mosquitoes. We first considered the case where CI is at a low level. In particular, we first simulated the model (3.2.5), with (3.3.16), where CI is set at 10% (i.e., $c_i = 0.1$). This means 90% of the eggs laid by the *Wolbachia*-uninfected adult female mosquito that mated with a *Wolbachia*-infected adult male mosquito will hatch into larvae. For this simulation, $100,000$ *Wolbachia*-infected adult female and male mosquitoes are released for the 3-week release period (i.e., we set $W_{Rf} = W_{Rm} = 100,000$, $\tau = 21$) for a one-year duration.

The simulation results obtained, depicted in Figure 3.11, show a dramatic decrease in the local abundance of the *Wolbachia*-uninfected adult mosquito population (by about 92% for the adult female and 72% for the adult male mosquitoes, from the baseline worse-case scenario shown in Figure 3.4, respectively). It should, however, be recalled that almost exactly the same dramatic reductions in the population abundance of the *Wolbachia*-uninfected adult mosquito population were achieved for the same scenario but with perfect CI (Figure 3.6). In other words, this simulation shows that CI (at the low level of $c_i = 0.1$) has no significant effect on the effectiveness of *Wolbachia*-based mosquito control strategy.

Additional simulation was carried out, for the same setting (i.e., the model (3.2.5) with $W_{Rf} = W_{Rm} = 100,000$, $\tau = 21$) but with CI increased to 50% (i.e., $c_i = 0.5$). The simulation results obtained show a 93% and 73% reduction in the population abundance of the *Wolbachia*-uninfected adult female and male mosquitoes, respectively. Again, these numbers are similar to those recorded in Figure 3.6 with perfect CI. In summary, our simulations clearly show (by comparing Figures 3.11 and 3.12, where CI is set at 10% and 50%, respectively, with Figure 3.6, where CI is set at 100%) that CI has no significant effect on the effectiveness of *Wolbachia* introduction to curtail the local abundance of the wild adult mosquito population in the community.

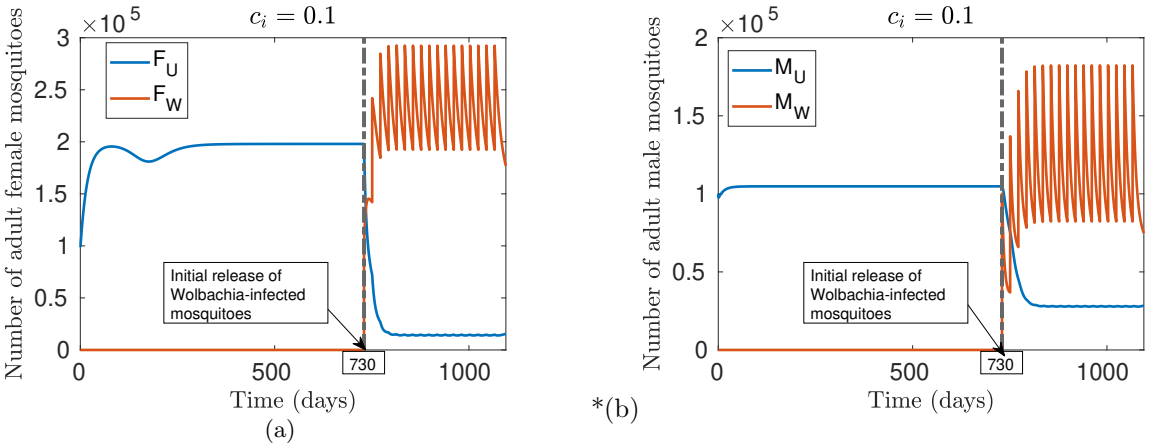

Figure 3.11: Simulations of the Model (3.3.6), With (3.3.16), Showing the Dynamics of *Wolbachia*-infected and *Wolbachia*-uninfected (Wild) Adult Mosquitoes. The Simulations Were Ran for Two Years Without the Release of the *Wolbachia*-infected Mosquitoes, Following Which the *Wolbachia*-infected Mosquitoes Are Released Every Three Weeks (I.E., $\tau = 21$ Days) for a Period of One Year. A Total of 100,000 *Wolbachia*-infected Female ($W_{Rf} = 100,000$) and Male ($W_{Rm} = 100,000$) Mosquitoes Are Released *Per* Release Period With $c_i = 0.1$. Parameter Values Used Are As Given in Table 3.3. Notation: The Dashed Vertical Lines Represent the Time for the Onset of the Release of the *Wolbachia*-infected Mosquitoes.

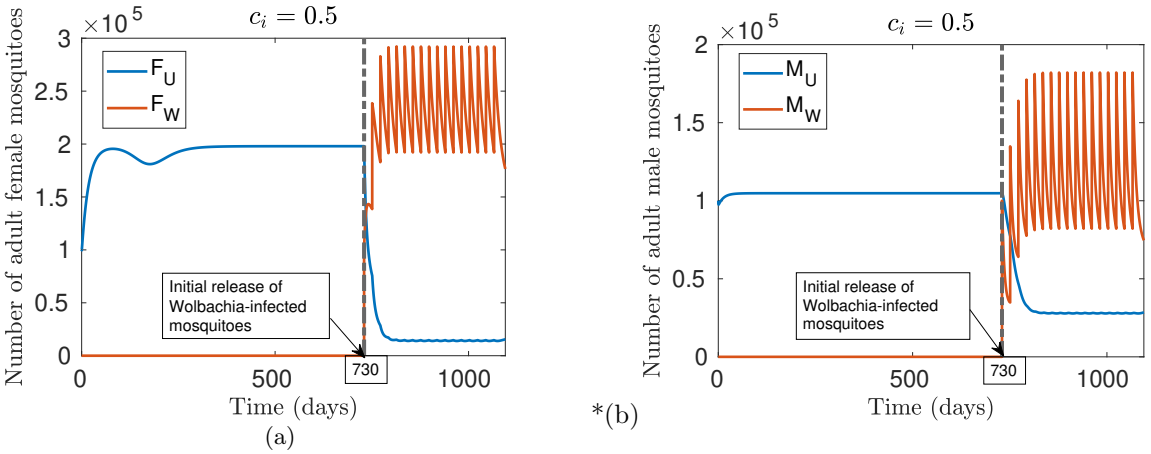

Figure 3.12: Simulations of the Model (3.3.6), with (3.3.16), Showing the Dynamics of *Wolbachia*-infected and *Wolbachia*-uninfected (Wild) Adult Mosquitoes. The Simulations Were Ran for Two Years Without the Release of the *Wolbachia*-infected Mosquitoes, Following Which the *Wolbachia*-infected Mosquitoes Are Released Every Three Weeks (I.E., $\tau = 21$ Days) for a Period of One Year. A Total of 100,000 *Wolbachia*-infected Female ($W_{Rf} = 100,000$) and Male ($W_{Rm} = 100,000$) Mosquitoes Are Released *per* Release Period with $c_i = 0.5$. Parameter Values Used Are as given in Table 3.3. Notation: The Dashed Vertical Lines Represent the Time for the Onset of the Release of the *Wolbachia*-infected Mosquitoes.

3.4 Discussion and Conclusions

Dengue fever is one of the most important vector-borne diseases affecting mankind. The disease, which is spread between humans *via* the bite of adult female *Aedes*

mosquitoes (its main vector), affects over one-third of the world's population (particularly those residing in the tropical and sub-tropical regions) [100; 191]. In general, there are no safe and effective vaccine or drug therapy for use against diseases caused by mosquitoes, such as dengue. Consequently, control measures against mosquito-borne diseases are mostly limited to implementing strategies that target the mosquito population. The traditional methods for controlling mosquito population abundance, such as the use of chemical insecticides to kill immature and adult mosquitoes, the use of long-lasting insecticidal nets (LLINs), insect repellents etc. Unfortunately, the widespread use of these insecticides in endemic areas has resulted in the emergence of insecticide resistance in the adult mosquito population [10; 117]. Consequently, other alternative methods for mosquito control are needed. One of such methods is the implementation of biological measures, such as the release of *Wolbachia*-infected mosquitoes in the endemic areas [16; 28; 177]).

This chapter presents a new sex-structured mathematical model for assessing the community-wide impact of the release of *Wolbachia*-infected mosquitoes on the population abundance of the local wild (i.e., *Wolbachia*-uninfected) *Aedes* mosquitoes, as well as on the transmission dynamics of dengue disease. The model developed in this chapter incorporates many of the many pertinent aspects of *Wolbachia* transmission in mosquito populations. Rigorous analysis of the special case of the model, where the assumption for incomplete cytoplasmic incompatability is relaxed, showed that the *Wolbachia*-free and dengue-free equilibrium of the model is locally-asymptotically stable whenever a certain epidemiological threshold, known as the *reproduction number* of the model, is less than unity.

Furthermore, using Center Manifold theory, it was shown that the model undergoes the dynamic phenomenon of backward bifurcation (when this threshold is less than unity). This bifurcation is characterized by the co-existence of the locally- asymptotically stable *Wolbachia*-free and dengue-free equilibrium with a locally-asymptotically

stable endemic equilibrium. The epidemiological implication of this phenomenon is that the effective control of the wild mosquito population (using the *Wolbachia*-based control intervention) will depend on the initial size of the sub-populations of the model. In other words, the presence of the phenomenon of backward bifurcation makes the prospects for the effective control of the wild mosquito population, using *Wolbachia*-based control, more difficult. This (to the authors', knowledge) is the first time this phenomenon is rigorous established for a two-sex model for the transmission dynamics of a mosquito-borne disease that employs a *Wolbachia*-based anti-mosquito intervention.

Numerous numerical simulations were carried out to assess the population-level impact of the number of *Wolbachia*-infected mosquitoes released into the wild, as well as the frequency of such releases. Based on the reasonable set of parameter values used in the numerical simulations, The simulations carried out in this chapter show, for instance, that releasing 10,000 each of *Wolbachia*-infected adult male and adult female mosquitoes every three weeks for a one year duration can lead to a dramatic reduction of up to 85% and 70% of the local wild adult female and male mosquito populations, respectively. These reductions increase to 93% for adult female and 73%, respectively, for adult male mosquitoes if the number of *Wolbachia*-infected mosquitoes is increased to 100,000 each for adult female and adult male mosquitoes. Further reductions (by 96% for adult female and 76% for adult male) are achieved if the number of *Wolbachia*-infected mosquitoes released is increased to 200,000 for each gender.

We observed (generally) qualitatively similar results when the release frequency is decreased from every three weeks to every two weeks or even weekly. Thus, these simulations show that the *Wolbachia*-based intervention can significantly reduce the local population abundance of the wild adult *Aedes* mosquitoes if the number of *Wolbachia*-infected mosquitoes periodically released into the wild is high enough. In particular, our study shows that up to 90%-95% of the local wild adult female *Aedes* mosquito

population can be eliminated using the aforementioned *Wolbachia*-based intervention. Reducing such a huge number of the local wild adult female *Aedes* mosquitoes certainly imply a great reduction in the burden of dengue disease in the community.

The simulations in this chapter further showed that if only *Wolbachia*-infected mosquitoes of one gender (e.g., only males or only females) can be released, it is more beneficial if *Wolbachia*-infected male mosquitoes, rather than *Wolbachia*-infected female mosquitoes, are released into the wild. This is intuitive ecologically, since the *Wolbachia*-infected adult male mosquitoes significantly affect the cytoplasmic incompatibility property of the *Wolbachia* implementation (thereby reducing the population abundance of the wild mosquitoes in the community). We further showed that cytoplasmic incompatability (CI) does not significantly affect the effectiveness of the *Wolbachia*-based strategy to reduce the local population abundance of the wild mosquito population.

In summary, this chapter aimed to provide insight into the effectiveness of the *Wolbachia*-based biological control strategy in combating the population abundance of the targeted mosquito population (i.e., wild adult *Aedes* mosquitoes) in the community. This was achieved *via* the development, analysis and simulations of a novel, two-sex, mathematical model for the population dynamics of the *Aedes* mosquito (both immature and adult) in a community. In addition to incorporating many relevant features of the mosquito population dynamics (such as vertical and horizontal transmission in *Wolbachia*-infected mosquito population), the model developed in this study also incorporated the effect of cytoplasmic incompatibility (CI) in the mosquito dynamics (to account for the fact CI significantly affects the population abundance of the local wild mosquito population [150; 178]). We showed the that the prospect for the effective control (or elimination) of dengue disease in a community using *Wolbachia*-based mosquito control are promising provided a relatively large number of the *Wolbachia*-infected mosquitoes (both males and females) are released into the wild at reasonable

frequency (e.g., every three weeks or biweekly, or even weekly). We further showed that if resources are limited, and only *Wolbachia*-infected mosquitoes of one gender (e.g., only males or only females) can be released, then releasing male *Wolbachia*-infected mosquitoes is more beneficial. Some of the relevant computer codes for this chapter are given in Appendix J.

Although the model we developed in this chapter contains numerous aspects of mosquito-*Wolbachia* dynamics, as well as the dynamics of dengue disease in the mosquito and the human host, the model can be extended to account for some of its limitations. For instance, the model can be extended to incorporate the spatial heterogeneity of the vector (i.e., mosquito dispersal/diffusion). This may also entail using a patch (metapopulation) modeling framework to account for the dispersal of the mosquitoes within various patches. The model can also be extended to include the effect of climate factors (such as temperature and rainfall) on the population biology of both the wild and *Wolbachia*-infected mosquitoes. Furthermore, the assumption of lumping all three aquatic stages into one can be relaxed (so that the full immature lifecycle can be incorporated; this will allow, for instance, the assessment of the impact density-dependent larval mortality on the mosquito dynamics). The effects of land use changes and human mobility (i.e., immigration and migration) can also be incorporated.

BIBLIOGRAPHY

[1] A. Abdelrazec, J. Bélair, C. Shan, and H. Zhu, *Modeling the spread and control of dengue with limited public health resources*, Math Biosci., 271 (2008), pp. 136–145.

[2] B. Adams and M. Boots, *How important is vertical transmission in mosquitoes for the persistence of dengue? insights from a mathematical model*, Epidemics, 2 (2010), pp. 1–10.

[3] L. Alphey, M. Benedict, R. Bellini, G. G. Clark, D. A. Dame, M. W. Service, , and S. L. Dobson, *Sterile-Insect methods for control of mosquito-borne diseases: an analysis*, Vector Borne Zoonotic Dis, 10 (2010), pp. 295–311.

[4] B. Alto and D. Bettinardi, *Temperature and dengue virus infection in mosquitoes: Independent effects on the immature and adult stages*, Am J Trop Med Hyg, 88 (2013), pp. 497–505.

[5] L. A.Moreira, I. Ormaetxe, J. A.Jeffery, G. Lu, A. T.Pyke, L. M.Hedges, and et al., *A Wolbachia Symbiont in Aedes aegypti Limits Infection with Dengue, Chikungunya, and Plasmodium*, Cell, 139 (2009), pp. 1268–1278.

[6] R. Anderson and R. eds. May, *Population of Biology of Infectious Diseases*, Springer-Verlag, 1982.

[7] M. Andraud, N. Hensand, C. Marais, and P. Beutels, *Dynamic epidemiological models for dengue transmission: a systematic review of structural approaches*, PLoS One, 7 (2012).

[8] B. Angel and V. Joshi, *Distribution and seasonality of vertically transmitted dengue viruses in aedes mosquitoes in arid and semi-arid areas of Rajasthan, India*, J Vector Borne Dis, 45 (2008), pp. 56–59.

[9] M. Ashfaq, P. D. N. Hebert, J. H. Mirza, A. M. Khan, Y. Zafar, and M. S. Mirza, *Analyzing Mosquito (Diptera: Culicidae) Diversity in Pakistan by DNA Barcoding*, PLOS, 9 (2014), pp. 1–12.

[10] B. AW, *Insecticide resistance in mosquitoes: a pragmatic review*, American Mosquito Control Association, 2 (1986), pp. 123–140.

[11] N. Bacaër, *Approximation of the basic reproduction number $\mathcal{R}_0$ for vector-borne diseases with a periodic vector population*, Bull Math Biol, 69 (2007), pp. 1067–1091.

[12] N. Bacaër and X. Abdurahman, *Resonance of the epidemic threshold in a periodic environment*, J Math Biol, 57 (2008), pp. 649–673.

[13] N. Bacaër and R. Ouifki, *Growth rate and basic reproduction number for population models with a simple periodic factor*, Math Biosci, 210 (2007), pp. 647–65.

[14] S. Baqar, C. Hayes, J. Murphy, and D. Watts, *Vertical transmission of west nile virus by culex and aedes species mosquitos*, Am. J. Trop. Med. Hyg, 48 (1993), pp. 757–762.

[15] M. Batty, *Cities and Complexity: Understanding Cities with Cellular Automata*, The MIT Press, 2007.

[16] G. Benelli, C. Jeries, and T. Walker, *Biological control of mosquito vectors:past, present, and future*, Insects, 7 (2016), pp. 1–18.

[17] D. Bernoulli, *Essai d'une nouvelle analyse de la mortalite causee par la petite verole*, Mem. Math. Phys. Acad. Roy, 1 (1766).

[18] S. Bhatt, P. W. Gething, O. J. Brady, J. P. Messina, A. W. Farlow, C. L. Moyes, and et al., *The global distribution and burden of dengue*, Nature, 496 (2013), pp. 504–507.

[19] G. Bian, Y. Xu, P. Lu, Y. Xie, and Z. Xi, *The endosymbiotic bacterium Wolbachia induces resistance to dengue virus in Aedes aegypti*, PLoS Pathog, 6 (2010), pp. 1–10.

[20] M. S. C. Blagrove, C. Arias-Goeta, A.-B. Failloux, and S. P. Sinkins, *Wolbachia strain wMel induces cytoplasmic incompatibility and blocks dengue transmission in Aedes albopictus*, PNAS, 109 (2012), pp. 255–260.

[21] S. M. Blower and H. Dowlatabadi, *Sensitivity and uncertainty analysis of complex models of disease transmission: an HIV model, as an example*, Int. Stat. Rev., 2 (1994).

[22] C. F. Bosio, R. E. Thomas, P. R. Grimstad, and K. S. Rai, *Variation in the efficiency of vertical transmission of dengue-1 virus by strains of aedes albopictus (diptera:culicidae)*, J. Am. Mosq. Control Assoc, 29 (1992), pp. 985–989.

[23] J. Bouyer and T. Lefrancois, *Boosting the sterile insect technique to control mosquitoes*, Trends in Parasitology, 30 (2014), pp. 271–273.

[24] F. Brauer, *Backward bifurcation in simple vaccination models*, Mathematical Analysis and Application, 298 (2004), pp. 418–431.

[25] Bureau of Epidemiology, Thailand, *Diseases Survellance (Report 506).* `http://203.157.15.110/boeeng/index.php`. [Online; accessed february 2015].

[26] C. Castillo-Chavez, K. Cooke, W. Huang, and S. A. Levin, *Results on the dynamics for models for the sexual transmission of the human immunodeficiency virus*, Appl. Math. Lett., 2 (1989), pp. 327–331.

[27] C. Castillo-Chavez and B. Song, *Dynamical models of tuberculosis and their applications*, Math. Biosci. Eng, 1 (2004), pp. 361–404.

[28] L. Cai, A. Shangbing, and J. Li, *Dynamics of mosquitoes population with different strategies for releasing sterile mosquitoes*, SIAM, 74 (2014), pp. 1786–1809.

[29] J. Cariboni, , D. Gatelli, R. Liska, and A. Saltelli, *The role of sensitivity analysis in ecological modeling. ecological modeling*, Ecological modeling, 203 (2007), pp. 167–182.

[30] J. Carr, *Applications of Centre Manifold Theory*, Springer-Verlag, New York, 1981.

[31] E. CASPARI and G. S. WATSON, *On the evolutionary importance of cytoplasmic sterility in mosquitoes*, Evolution, 13 (1959), pp. 568–570.

[32] CDC, *Mosquito Bites: Everyone is at Risk*, 2017.

[33] Centers for Diseas Contorl and Prevention, *Dengue.* `http://www.cdc.gov/dengue/`. [Online;accessed 14 May 2016].

[34] M. Chen and et al., *Effects of extreme precipitation to the distribution of infectious diseases in taiwan, 1994-2008*, PLos One, 6 (2012), pp. 1–8.

[35] N. Chitnis, J. M. Cushing, and J. M. Hyman, *Bifurcation analysis of a mathematical model for malaria transmission*, SIAM J. Appl. Math., 67 (2006), pp. 24–45.

[36] City population, *CHIANG MAI.* `https://www.citypopulation.de/php/thailand-prov-admin.php?adm2id=50`. [Online; accessed:March 2017].

[37] N. Clements, *The Biology of Mosquitoes: Sensory, Reception, and Behaviour*, CABI Publishing. Eastbourne., 1999.

[38] C. Cosner, J. C. Beier, R. S. Cantrell, D. Impoinvil, L. Kapitanski, M. D. Potts, A. Troyo, and S. Ruan, *The effects of human movement on the persistence of vector-borne diseases*, Theoretical Biology, 258 (2009), pp. 550–560.

[39] F. Coutinho, M. Burattini, L. Lopez, and E. Massad, *Threshold conditions for a non-autonomous epidemic system describing the population dynamics of dengue*, Bull. Math. Biol, 68 (2006), pp. 2263–2282.

[40] D. J. Gubler, *Aedes aegypti and aedes aegypti-borne disease control in the 1990s: top down or bottom up*, The American journal of tropical medicine and hygiene, 40 (1989), pp. 571–578.

[41] ——, *Dengue and dengue hemorrhagic fever*, Clinical microbiology reviews, 11 (1998), pp. 480–496.

[42] ——, *Resurgent vector-borne diseases as a global health problem*, Emerg Infect Dis, 4 (1998), pp. 442–450.

[43] H. Delatte, G. Gimonneau, A. Triboire, and D. Fontenille, *Influence of temperature on immature development, survival, longevity, fecundity, and gonotrophic cycles of aedes albopictus, vector of chikungunya and dengue in the indian ocean*, J. Med. Entomol, 46 (2009), pp. 33–41.

[44] M. Diallo, J. Thonnon, and D. Fontenille, *Vertical transmission of the yellow fever virus by aedes aegypti (diptera, culicidae): dynamics of infection in f-1 adult progeny of orally infected females*, Am. J. Trop. Med. Hyg, 62 (2000), pp. 251–156.

[45] O. B. Dick, J. L. S. Martín, R. H. Montoya, and et al., *The history of dengue outbreaks in the americas*, The American Society of Tropical Medicine and Hygiene, (2012).

[46] O. Diekmann, J. Heesterbeek, and J. Metz, *On the definition and the computation of the basic reproduction ratio R_0 in models for infectious diseases in hetero- geneous populations*, Math. Biol., 28 (1990), pp. 365–382.

[47] R. Edelman, *Dengue and dengue vaccines*, Infectious Diseases, 191 (2005), pp. 650–653.

[48] Entomology Department at Purdue University, *Mosquitoes*. `https://extension.entm.purdue.edu/publichealth/insects/mosquito.html`. [Online; accessed:March 2017].

[49] L. Esteva and C. Vargas, *Influence of vertical and mechanical transmission on the dynamics of dengue disease*, Mathematical Biosciences, 167 (2000), pp. 51–64.

[50] European Centre for Disease Prevention and Control, *Geographical distribution of dengue cases reported worldwide, 2019*, 2017.

[51] O. Evans, E. P. Caragata, C. J. McMeniman, M. Woolfit, D. C. Green, C. R. Williams, and et al., *Increased locomotor activity and metabolism of Aedes aegypti infected with a life-shortening strain of Wolbachia pipientis*, J Exp Biol, 212 (2009), pp. 1436–1441.

[52] D. Ewing and et al., *Modelling the effect of temperature on the seasonal population dynamics of temperate mosquitoes*, J Theoretical Biology, 400 (2016), pp. 65–79.

[53] F. B. Agusto and A. B. Gumel and P. E. Parham, *Qualitative assessment of the role of temperature variations on malaria transmission dynamics*, J. Biol. Syst., 23 (2015), pp. 1–34.

[54] K. Fatima and N. I. Syed, *Dengvaxia controversy: impact on vaccine hesitancy*, J Glob Health, 8 (2018), pp. 1–3.

[55] Z. Feng and X. Jorge, *Competitive exclusion in a vector-host model for the dengue fever*, J. Math. Biol., 35 (1997), pp. 523–5244.

[56] N. M. Ferguson, D. Kien, H. Clapham, R. Aguas, V. Trung, T. Chau, and et al, *Modeling the impact on virus transmission of wolbachia-mediated blocking of dengue virus infection of aedes aegypti*, Sci Transl Med, 7 (2015), pp. 1–28.

[57] J. E. Freier and L. Rosen, *Vertical transmission of dengue viruses by mosquitoes of the aedes scutellaris group*, Am. J. Trop. Med. Hyg, 37 (1987), pp. 640–647.

[58] F. D. Frentiu, J. Robinson, P. R. Young, E. A. McGraw, and S. L. ÓNeill, *Wolbachia-Mediated Resistance to Dengue Virus Infection and Death at the Cellular Level*, PLOS, 5 (2009), pp. 1–8.

[59] F. D. Frentiu, T. Zakir, T. Walker, J. Popovici, A. T. Pyke, A. van, and et al, *Limited Dengue Virus Replication in Field-Collected Aedes aegypti Mosquitoes Infected with Wolbachia*, PLOS neglected tropical diseases, 6 (2012), pp. 1–10.

[60] G. Fu, R. S. Lees, D. Nimmo, D. Aw, L. Jin, P. Gray, and T. U. Berendonk, *Female-specific flightless phenotype for mosquito control*, PNAS, 107 (2010), pp. 4550–4554.

[61] S. M. Garba, A. B. Gumel, and M. R. A. Bakar, *Backward bifurcation in dengue transmission dynamics*, Math. Biosci., 215 (2008), pp. 11–25.

[62] R. Gibbons and D. Vaughn, *Dengue: An escalating problem*, BMJ, 324 (2002), pp. 1563–1566.

[63] R. V. Gibbons and D. W. Vaughn, *Dengue: an escalating problem*, BMJ: British Medical Journal, 324 (2002).

[64] A. K. Githeko, S. W. Lindsay, U. E. Confalonieri, and J. A. Patz, *Climate change and vec-tor-borne diseases: a regional analysis*, Bull. World Health Organ, 78 (2000), pp. 1136–47.

[65] N. G. Gratz, *Emerging and resurging vector-borne diseases*, Annual review of entomology, 44 (1999), pp. 51–75.

[66] N. G. Gratz and A. B. Knudsen, *The rise and spread of dengue, dengue haemorrhagic fever and its vectors: a historical review (up to 1995)*, WHO, 1996.

[67] M. Grunnill and M. Boots, *How important is vertical transmission of dengue viruses by mosquitoes (diptera: Culicidae)?*, J Med Entomol., 53 (2016), pp. 1–19.

[68] D. Gubler and D. Trent, *Emergence of epidemic dengue/dengue hemorrhagic fever as a public health problem in the Americas*, Infectious Agents Diseases, 2 (1994), pp. 383–393.

[69] D. J. Gubler, *Insects in Disease Transmission*, Saunders, 1991.

[70] D. J. Gubler, *Dengue and dengue hemorrhagic fever*, Clin Microbiol Rev., 11 (1998), pp. 480–496.

[71] ——, *Resurgent Vector-Borne Diseases as a Global Health Problem*, Emerging Infectious Diseases, 4 (1998), pp. 442–450.

[72] ——, *Epidemic dengue/dengue hemorrhagic fever as a public health, social and economic problem in the 21st century*, Trends Microbiol, 10 (2002), pp. 100–103.

[73] A. Gumel, *Causes of backward bifurcations in some epidemiological models*, J. Math. Anal. Appl., 395 (2012), pp. 355–365.

[74] X. Guo, T. Zhao, Y. Dong, and B. Lu, *Survival and replication of dengue-2 virus in diapausing eggs of aedes albopictus (diptera: Culicidae)*, J. Med. Entomol., 44 (2007), pp. 492–497.

[75] H. Thieme, *Convergence result and a poincaré-bendixon trichotomy for asymptotical autonomous differential equations*, J Math Biol, 30 (1992), pp. 755–763.

[76] W. M. Haddad and V. S. Chellaboina, *Nonlinear Dynamical Systems and Control: a Lyapunov-based approach*, Princeton University Press, 2008.

[77] H. Halide and P. Ridd, *A predictive model for dengue hemorrhagic fever epidemics*, Int. J. Environ Health Res, 18 (2008), pp. 253–265.

[78] S. B. Halstead, *Pathogenesis of dengue: Challenges to molecular biology*, Science, 239 (1988), pp. 476–481.

[79] P. Hancock, S. Sinkins, and H. Godfray, *Population dynamic models of the spread of Wolbachia*, Amer Nat, 177 (2011), pp. 323–333.

[80] M. Helinski and B. Knols, *The influence of late-stage pupal irradiation and increased irradiated: un-irradiated male ratio on mating competitiveness of the malaria mosquito Anopheles arabiensis Patton*, Bull Entomol Res, 99 (2009), pp. 317–322.

[81] H. M. Hethcote, *The mathematics of infectious diseases*, SIAM Rev., 42 (2000), pp. 599–653.

[82] A. Hoffmann, B. Montgomery, J. Popovici, I. Iturbe-Ormaetxe, P. Johnson, F. Muzzi, and et al., *Successful establishment of wolbachia in aedes populations to suppress dengue transmission*, Nature, 476 (2011), pp. 454–7.

[83] A. A. Hoffmann, I. Iturbe-Ormaetxe, A. G. Callahan, B. L. Phillips, K. Billington, J. K. Axford, and et al., *Stability of the wmel wolbachia infection following invasion into aedes aegypti populations*, PLoS Negl Trop Dis, 8 (2014), pp. 1–9.

[84] M. Huang, X. Song, and J. Li, *Modelling and analysis of impulsive releases of sterile mosquitoes. Journal of Biological Dynamics*, Journal of Biological Dynamics, 11 (2016), pp. 147–171.

[85] H. Hughes and N. Britton, *Modelling the use of wolbachia to control dengue fever transmission*, Bull Math Biol, 75 (2013), pp. 796–818.

[86] J. C. Kamgang and G. Sallet, *Global asymptotic stability for the disease free equilibrium for epidemiological models*, CRAS Serie I, 341 (2005), pp. 433–438.

[87] J. C. Kamgang and G. Sallet, *Computation of threshold conditions for epidemiological models and global stability of the disease-free equilibrium (DFE)*, Math. Biosci., 213 (2008), pp. 1–12.

[88] A. A. James, *Gene drive systems in mosquitoes: rules of the road*, Trends Parasitol, 21 (2005), pp. 64–67.

[89] F. Jiggins, *The spread of Wolbachia through mosquito populations*, PLoS Biol., 15 (2017), pp. 1–6.

[90] Joon K. Chye, Chin T. Lim, and Kwee B. Ng, *Vertical transmission of dengue*, Clin Infect Dis, 25 (1997), pp. 1374–7.

[91] V. Joshi, D. T. Mourya, and R. C. Sharma, *Persistence of dengue-3 virus through transovarial transmission passage in successive generations of aedes aegypti mosquitoes*, Am. J. Trop. Med. Hyg, 67 (2002), pp. 158–161.

[92] V. Joshi, R. Sharma, Y. Sharma, S. Adha, K. Sharma, H. Singh, A. Purohit, and M. Singhi, *Importance of socioeconomic status and tree holes in distribution of aedes mosquitoes (diptera: Culicidae) in jodhpur, rajasthan, india*, J. Med. Entomol, 43 (2006), pp. 330–336.

[93] T. Karl and N. Plummer, *Trends in high-frequency climate variability in the twentieth century*, Nature, 377 (1995), pp. 217–220.

[94] W. O. Kermack and A. G. McKendrick, *A contribution to the mathematical theory of epidemic*, Proc. Roy. Soc. A., 115 (1927), pp. 700–721.

[95] E. D. Kilbourne, *The emergence of emerging diseases: a lesson in holistic epidemiology*, The Mount Sinai journal of medicine, 63 (1996), pp. 159–166.

[96] S. C. Kliks, A. Nisalak, W. E. Brandt, L. Wahl, and D. S. Burke, *Antibody-dependent enhancement of dengue virus growth in human monocytes as a risk factor for dengue hemorrhagic fever*, The American journal of tropical medicine and hygiene, 40 (1989), pp. 444–451.

[97] J. Koiller, M. A. da Silva, M. O. Souza, C. Codeco, A. Iggidr, and G. Sallet, *Aedes, Wolbachia and dengue*, Hal Inria, (2014), pp. 1–47.

[98] C. Y. Kow, L. L. Koon, and P. F. Yin, *Detection of dengue viruses in field caught male aedes aegypti and aedes albopictus (diptera: Culicidae) in singapore by type-specific pcr*, J. Med. Entomol, 38 (2001), pp. 475–479.

[99] M. Kraemer, M. Sinka, K. Duda, A. Mylne, F. Shearer, and C. Barker, *The global distribution of the arbovirus vectors Aedes aegypti and Ae. albopictus*, Elife, 4 (2015), pp. 1–18.

[100] J. Kyle and E. Harris, *Global spread and persistence of dengue*, Annu. Rev. Microbiol., 62 (2008), pp. 71–92.

[101] K. Lafferty, *The ecology of climate change and infectious diseases*, Ecology, 90 (2009), pp. 888–900.

[102] Z. Lam, D. Burke, M. Capeding, and C. Chong, *Preparing for introduction of a dengue vaccine: recommendations from the 1st Dengue v2V Asia-Pacific Meeting*, Vaccine, 29 (2011), pp. 9417–9422.

[103] L. Lambrechts, K. Paaijmansb, and T. Fansiri, *Impact of daily temperature fluctuations on dengue virus transmission by aedes aegypti*, Proceedings of the National Academy of Sciences of the United States of America, 108 (2011), pp. 7460–7465.

[104] V. Laperriere, K. Brugger, and F. Rubel, *Simulation of the seasonal cycles of bird, equine and human west nile virus cases*, Prev. Vet. Med., 88 (2011), pp. 99–110.

[105] D. Li and H. Wan, *The threshold infection level for wolbachia invasion in a two-sex mosquito population model*, Bulletin of Mathematical Biology, 81 (2019), pp. 2596–2624.

[106] Y. Li and X. Liu, *An impulsive model for wolbachia infection control of mosquito-borne diseases with general birth and death rate functions*, Nonlinear Anal Real World Appl, 37 (2017), pp. 412–432.

[107] W. Lin, T. Burkot, and B. Kay, *Effects of temperature and larval diet on development rates and survival of the dengue vector aedes aegypti in north queensland*, Medical and veterinary entomology, 14 (2000), pp. 13–37.

[108] L. P. Lounibos and R. L. Escher, *Sex ratios of mosquitoes from long-term censuses of florida tree holes*, J Am Mosq Control Assoc, 24 (2008), pp. 11–15.

[109] A. Lutambi, M. Penny, T. Smith, and N. Chitnis, *Weather-driven malaria transmission model with gonotrophic and sporogonic cycles*, Mathematical Biosciences, 241 (2013), pp. 198–216.

[110] G. MacDonald, *The Epidemiology Control of Malaria*, Oxford University Press, 1957.

[111] S. Marino, I. B. Hogue, C. J. Ray, and D. E. Kirschner, *A methodology for performing global uncertainty and sensitivity analysis in systems biology*, J. Theor. Biol., 254 (2008), pp. 178–196.

[112] M. T. Marrelli, C. K. Moreira, D. Kelly, L. Alphey, and M. Jacobs-Lorena, *Mosquito transgenesis: what is the fitness cost?*, Trends Parasitol, 22 (2006), pp. 197–202.

[113] C. J. McMeniman, R. V. Lane, B. N. Cass, A. W. Fong, M. Sidhu, Y.-F. Wang, , and S. L. O'neill, *Stable introduction of a life-shortening wolbachia infection into the mosquito aedes aegypti*, Science, 323 (2009), pp. 141–144.

[114] C. J. McMeniman and S. L. O'Neill, *A virulent wolbachia infection decreases the viability of the dengue vector aedes aegypti during periods of embryonic quiescence*, PLoS Negl Trop Dis, 4 (2010), pp. 1–6.

[115] B. Miller, G. Defoliart, and T. Yuill, *Vertical transmission of la-crosse virus (california encephalitis group)-transovarial and filial infection-rates in aedes triseriatus (diptera culicidae)*, J. Med. Entomol, 14 (1978), pp. 437–440.

[116] C. Mitchell and B. Miller, *Vertical transmission of dengue viruses by strains of aedes albopictus recently introduced into brazil*, J. Am. Mosq. Control Assoc, 6 (1990), pp. 251–253.

[117] J. Mohammed-Awel, F. Agusto, R. E. Mickens, and A. B. Gumel, *Mathematical assessment of the role of vector insecticide resistance and feeding/resting behavior on malaria transmission dynamics: Optimal control analysis*, Infectious Disease Modelling, 3 (2018), pp. 301–321.

[118] T. Monath, F. Heinz, and et al, *Virology*, Lippincott-Raven, Philadelphia, 1996.

[119] E. A. Mordecai, K. P. Paaijmans, L. R. Johnson, C. Balzer, T. Ben-Horin, E. Moor, A. McNally, S. Pawar, S. J. Ryan, T. C. Smith, and et al, *Optimal temperature for malaria transmission is dramatically lower than previously predicted*, Ecology letters, 16 (2013), pp. 22–30.

[120] D. M. Morens, G. K. Folkers, and A. S. Fauci, *The challenge of emerging and re-emerging infectious diseases*, Nature, 430 (2004).

[121] S. S. Morse, *Factors in the emergence of infectious diseases*, In Plagues and politics, (2001), pp. 8–26.

[122] mosquitoturlock, *Life Cycle*, 2017.

[123] L. Mousson, K. Zouache, C. A. Goeta, V. Raquin, P. Mavingui, and A. B. Failloux, *The Native Wolbachia Symbionts Limit Transmission of Dengue Virus in Aedes albopictus*, LoS Neglected Trop. Dis., 6 (2012), pp. 1–10.

[124] J. Nayar, L. Rosen, and J. Knight, *Experimental vertical transmission of saint louis encephalitis-virus by florida mosquitos*, Am. J. Trop. Med. Hyg, 35 (1986), pp. 1296–1301.

[125] M. Ndii, R. Hickson, D. Allingham, and G. Mercer, *Modelling the transmission dynamics of dengue in the presence of wolbachia*, Math Biosci, 262 (2015), pp. 157–166.

[126] T. Nguyen, H. Nguyen, T. Nguyen, S. Vu, N. Tran, T. Le, and et al., *Field evaluation of the establishment potential of wMelPop Wolbachia in Australia and Vietnam for dengue control*, Parasites and Vectors, 8 (2015), pp. 1–14.

[127] P. Novosel and et al, *Dengue virus infection in croatia: seroprevalence and entomological study*, New Microbiol, 38 (2015), pp. 97–100.

[128] O. Sharomi and A. B. Gumel, *Re-infection-induced backward bifurcation in the transmission dynamics of chlamydia trachomatis*, J. Math. Anal. Appl., 365 (2009), pp. 96–118.

[129] O. Sharomi and C.N. Podder and A.B. Gumel and E.H. Elbasha and J. Watmough, *Role of incidence function in vaccine-induced backward bifurcation in some hiv models*, Math. Biosci, 210 (2007), pp. 436–463.

[130] K. Okuneye, S. Eikenberry, and A. B. Gumel, *Weather-driven malaria transmission model with gonotrophic and sporogonic cycles*, In review, (2018).

[131] A. Ong, M. Sandar, M. I. Chen, and L. Y. Sin, *Fatal dengue hemorrhagic fever in adults during a dengue epidemic in singapore*, Journal of Infectious Diseases, 11 (2007), pp. 263–267.

[132] I. Ormaetxe, T. Walker, and S. L. O. Neill, *Wolbachia and the biological control of mosquito-borne disease*, Embo Rep, 12 (2011), pp. 508–518.

[133] S. L. O'Neill, *The use of wolbachia by the world mosquito program to interrupt transmission of aedes aegypti transmitted viruses*, Institute Vector Borne Disease, (2018), pp. 355–360.

[134] K. P. Paaijmans, M. O. Wandago, A. K. Githeko, and W. Takken, *Unexpected high losses of anopheles gambiae larvae due to rainfall*, PLoS One, 2 (2007).

[135] G. Pachecoa, L. Estevab, and C. Vargasc, *Seasonality and outbreaks in west nile virus infection*, Bull. Mathematical Biology, 71 (2009), pp. 1378–1393.

[136] R. M. Packard, *The fielding h. garrison lecture:"break-bone" fever in Philadelphia, 1780: Reflections on the history of disease*, Bulletin of the History of Medicine, 90 (2016), pp. 193–221.

[137] Pan American Sanitary Bureau, *Health Conditions in the Americas*, Cientificas (Washington, D.C.), 1994.

[138] Pan American Sanitary Bureau, *Dengue and dengue hemorrhagic fever in the Americas: guidelines for prevention and control*, Cientificas (Washington, D.C.), 1995.

[139] P. E. Parham and E. Michael, *Modeling the effects of weather and climate change on malaria transmission*, Environmental health perspectives, 118 (2010), pp. 620–626.

[140] L. Perko, *Differential Equations and Dynamical Systems*, Springer Texts in Applied Mathematics 7, 1991.

[141] J. E. Peter and J. Peccoud, *Quantitative modeling of stochastic systems in molecular biology by using stochastic petri nets*, PNAS, pp. 6750–6755.

[142] P. Pongsiri and et al., *Changing pattern of dengue virus serotypes in thailand between 2004 and 2010*, J. Health Popul. Nutr, 30 (2012), pp. 366–370.

[143] J. Popovici, L. A. Moreira, A. Poinsignon, I. Iturbe-Ormaetxe, D. McNaughton, and S. L. ÓNeill, *Assessing key safety concerns of a Wolbachia-based strategy to control dengue transmission by Aedes mosquitoes*, Mem Inst Oswaldo Cruz, 105 (2010), pp. 957–964.

[144] Z. QU and J. M. HYMAN, *Generating a hierarchy of reduced models for a system of differential equations modeling the spread of Wolbachia in mosquitoes*, SIAM J. A PPL . M ATH ., 79 (2019), pp. 1675–1699.

[145] Z. Qu, L. Xue, , and J. M. Hyman, *Modeling the transmission of Wolbachia in mosquitoes for controlling mosquito-borne diseases*, SIAM J. A PPL . M ATH ., 78 (2018), pp. 826–852.

[146] Z. QU, L. XUE, and J. M. HYMAN, *Modeling the transmission of wolbachia in mosquitoes for controlling mosquito-borne diseases*, SIAM J. A PPL . M ATH, 78 (2018), pp. 826–852.

[147] R. S. Varga, *Factorization and normalized iterative methods, boundary problems in differential equations (R. E. Langer, ed.)*, University of Wisconsin Press, (1960), pp. 121–142.

[148] R. S. Varga, *Matrix Iterative Analysis, Analysis Prentice Hall Series in Automatic Computation*, 1962.

[149] P. Reiter and D. J. Gubler, *Surveillance and control of urban dengue vectors. in d. j. gubler and g. kuno (eds.), dengue and dengue hemorrhagic fever*, Wallingford: CABI Publishing, 241 (2001).

[150] M. Riegler, M. Sidhu, W. J. Miller, and S. L. ÓNeill, *Evidence for a global wolbachia replacement in drosophila melanogaster*, Curr. Biol, 15 (2005), pp. 1428–33.

[151] J. G. Rigau-Perez, G. G. Clark, D. J. Gubler, P. Reiter, E. J. Sanders, and A. V. Vorndam, *Dengue and dengue haemorrhagic fever*, The Lancet, 352 (1998), pp. 971–977.

[152] R.M. Anderson and R.M. eds. May, *Infectious Diseases of Humans:Dynamics and Control*, Oxford Univ, 1991.

[153] D. J. Rogers and S. Hay, *The climatic suitability for dengue transmission in continental europe*, european center for disease prevention and control, (2012).

[154] L. Rosen, D. A. Shroyer, R. B. Tesh, J. E. Freier, and J. C. Lien, *Transovarial transmission of dengue viruses by mosquitoes: Aedes albopictus and aedes aegypti*, Am. J. Trop. Med. Hyg, 32 (1983), pp. 1108–1119.

[155] P. A. Ryan, A. P. Turley, G. Wilson, T. P. Hurst, K. Retzki, and J. Brown-Kenyon, *Establishment of wMel Wolbachia in Aedes aegypti mosquitoes and reduction of local dengue transmission in Cairns and surrounding locations in northern Queensland, Australia*, Gates Open Research, 3 (2019), pp. 1329–1339.

[156] S. B. Halstead, *Safety issues from a phase 3 clinical trial of a live-attenuated chimeric yellow fever tetravalent dengue vaccine*, Human vaccines and immunotherapeutics, 14 (2018), pp. 2158–2162.

[157] Samui Times, *Thailand is experiencing its largest dengue epidemic in more than two decades.* `http://www.samuitimes.com/thailand-experiencing-largest-dengue-epidemic-two-decades/`. [Online; accessed: December 2017].

[158] A. Saridaki and K. Bourtzis, *Wolbachia: more than just a bug in insects genitals*, Current Opinion in Microbiology, 13 (2010), pp. 67–72.

[159] T. Scott, P. Amerasinghe, and A. Morrison, *Longitude studies of aedes aegypti (diptera:culicidae) in thailand and puerto rico: blood feeding frequency*, Journal of Medical Entomology, 37 (2000), pp. 89–101.

[160] T. W. Scott, W. Takken, B. G. J. Knols, and C. Boëte, *The Ecology of Genetically Modified Mosquitoes*, Science, 298 (2002), pp. 117–119.

[161] J. L. Scully, *The xxth century dengue pandemic: Need for surveillance and research*, World Health Stat Q, 45 (1992), pp. 292–298.

[162] ——, *What is a disease?*, EMBO Rep, 5 (2004), pp. 650–653.

[163] M. Segoli, A. A. Hoffmann, J. Lloyd, G. J. Omodei, and S. A. Ritchie, *The Effect of Virus-Blocking Wolbachia on Male Competitiveness of the Dengue Vector Mosquito, Aedes aegypti*, PLOS, 8 (2014), pp. 1–10.

[164] D. A. Shroyer, *Vertical maintenance of dengue-1 virus in sequential generations of aedes albopictus*, J. Am. Mosq. Control Assoc, 6 (1990), pp. 312–314.

[165] Z. Shuai, J. A. P. Heesterbeek, and P. V. den Driessche, *Extending the type reproduction number to infectious disease control targeting contacts between types*, Math. Biol., 67 (2013), pp. 1067–1082.

[166] Z. Shuai, J. A. P. Heesterbeek, and P. van den Driessche, *Extending the type reproduction number to infectious disease control targeting contacts between types*, J. Math. Biol., 67 (2013), pp. 1067–1082.

[167] P. S. Simeonov, V. Lakshmikantham, and D. Bainov, *Theory of Impulsive Dierential Equations*, World Scientific, 1989.

[168] C. P. Simmons, J. J. Farrar, N. van Vinh Chau, and B. Wills, *Dengue*, New England, 366 (2012), pp. 1423–1432.

[169] H. Smith, *Monotone dynamical systems: an introduction to the theory of competitive and cooperative systems*, American Mathematical Society, 1995.

[170] R. Soss, *On some peculiar pigmented cells found in two mosquitoes fed on malarial blood*, BMJ, pp. 1786–1788.

[171] J. Spitzen and W. Takken, *Keeping track of mosquitoes: a review of tools to track, record and analyse mosquito flight*, Parasites and Vectors, 11 (2018).

[172] L. M. Styer, S. L. Minnick, A. K. Sun, , and T. W. Scott, *Mortality and reproductive dynamics of aedes aegypti (diptera: Culicidae) fed human blood*, Vector-borne and zoonotic diseases, 7 (2007), pp. 86–98.

[173] N. Sullivan, *Antibody-mediated enhancement of viral disease*, Curr Top Microbiol Immunol, 260 (2001), pp. 145–169.

[174] C. systems biology: a network modeling perspective, *Cancer systems biology: a network modeling perspective*, Carcinogenesis, pp. 2–8.

[175] R. Taghikhani and A. B. Gumel, *Mathematics of dengue transmission dynamics: Roles of vector vertical transmission and temperature fluctuations*, Infectious Disease Modelling, 3 (2018), pp. 266–292.

[176] Thai Meteorological Department, *Thailand Weather*. `https://www.tmd.go.th/en/thailand.php`. [Online; accessed:March 2017].

[177] R. Thome, H. Yang, and L. Esteva, *Optimal control of aedes aegypti mosquitoes by sterile insect technique and insecticide*, Journal of Math. Biosci, 223 (2010), pp. 12–23.

[178] M. Turelli and A. A. Hoffmann, *Rapid spread of an inherited incompatibility factor in california drosophila*, Nature, 353 (1991), pp. 440–2.

[179] M. Turelli and A. A. Hoffmann, *Cytoplasmic Incompatibility in Drosophila Simulans: Dynamics and Parameter Estimates from Natural Populations*, Genetics, 140 (1995), pp. 1319–1338.

[180] E. A. Undurraga, F. E. Edillo, J. N. V. Erasmo, M. T. P. Alera, I. Yoon, F. M. Largo, and D. S. Shepard, *Disease burden of Dengue in the philippines: Adjusting for underreporting by comparing active and passive dengue surveillance in Punta Princesa, Cebu city*, The American journal of tropical medicine and hygiene, 96 (2017), pp. 887–898.

[181] United Nations and Department of Economic and Social Affairs and Population Division, *World Population Prospects, the 2010 Revision*. `http://www.un.org/`. [Online; accessed:March 2017].

[182] P. van den Driessche and J. Watmough, *Reproduction numbers and sub-threshold endemic equilibria for compartmental models of disease transmission*, Math. Biosci, 180 (2002), pp. 29–48.

[183] K. S. Vannice, A. Durbin, , and J. Hombach, *Status of vaccine research and development of vaccines for dengue*, Health policy and planning, 7 (1992), pp. 342–351.

[184] D. W. Vaughn, *Dengue viremia titer, antibody response pattern, and virus serotype correlate with disease severity*, J. Infectious Diseases, 181 (2000), pp. 1–8.

[185] T. Walker, P. Johnson, L. Moreira, I. Iturbe-Ormaetxe, F. Frentiu, and C. McMeniman, *The wMel wolbachia strain blocks dengue and invades caged aedes aegypti populations*, Nature, 476 (2011), pp. 450–453.

[186] W. Wang and X. Zhao, *Threshold dynamics for compartmental epidemic models in periodic environments*, J. Dyn. Diff. Equat., 20 (2008), pp. 699–717.

[187] R. T. Watson, M. C. Zinyowera, and R. H. Moss, *The Regional Impacts of Climate Change. An Assessment of Vulnerability. A Special Report of IPCC Working Group II.*, Cambridge University Press, Oxford, 1998.

[188] A. R. Weeks, M. Turelli, W. R. Harcombe, K. T. Reynolds, and A. A. Hoffmann, *Rapid evolution of wolbachia in natural populations of drosophila*, PLoS Biol, 5 (2007), pp. 997–1005.

[189] J. H. Werren, *Biology of wolbachia*, Annu Rev Entomol, 42 (1997), pp. 587–609.

[190] S. White, P. Rohani, and S. Sait, *Modelling pulsed releases for sterile insect techniques: fitness costs of sterile and transgenic males and the effects on mosquito dynamics*, Appl. Ecol, 47 (2010), pp. 1329–1339.

[191] WHO, *Dengue and severe dengue*. `https://www.who.int/news-room/fact-sheets/detail/dengue-and-severe-dengue`. [Online; accessed: December 2019].

[192] S. Wiggins, *Introduction to Applied Nonlinear Dynamical Systems and Chaos*, Springer-Verlag, New York, 1983.

[193] World Health Organization, *Updated Questions and Answers related to the dengue vaccine Dengvaxia and its use*. `http://www.who.int/immunization/diseases/dengue/q_and_a_dengue_vaccine_dengvaxia_use/en/`. [Online; accessed: December 2019].

[194] world health Organization, *Vector-borne Diseases*. `http://www.who.int/mediacentre/factsheets/fs387/en/`, 2017. [Online; accessed:March 2017].

[195] ——, *Vector-borne Diseases*, 2020.

[196] L. Xue, X. Fang, and J. M. Hyman, *Comparing the effectiveness of different strains of wolbachia for controlling chikungunya, dengue fever, and zika*, PLoS Negl Trop Dis, 12 (2018), pp. 1–24.

[197] L. Xue, C. Manore, P. Thongsripong, and J. Hyman, *Two-sex mosquito model for the persistence of wolbachia*, J Biol Dyn, 11 (2017), pp. 216–237.

[198] H. Yang, M. Macoris, and K.Galvani, *Assessing the effects of temperature on the population of aedes aegypti, the vector of dengue*, Epidemiology and Infection, 137 (2009), pp. 1188–1202.

[199] J. Yu, L. Hu, and B. Zheng, *Qualitative analysis for a wolbachia infection model with diffusion*, Science China Mathematics, 59 (2016), pp. 1249–1266.

[200] B. Yuval and A. Bouskila, *Temporal dynamics of mating and predation in mosquito swarms*, Oecologia, 95 (1993), pp. 65–69.

[201] C. Zhang and et al., *Severe dengue outbreak in yunnan, china, 2013*, Journal of Infectious Diseases, 27 (2014), pp. 4–6.

[202] F. Zhang and X. Zhao, *A periodic epidemic model in a patchy environment*, J Math Anal Appl, 325 (2007), pp. 496–516.

[203] B. ZHENG, M. TANG, and J. YU, *Modeling wolbachia spread in mosquitoes through delay differential equations*, SIAM J. APPL. MATH., 74 (2014), pp. 743–770.

[204] B. Zheng, M. Tang, J. Yu, and J. Qiu, *Wolbachia spreading dynamics in mosquitoes with imperfect maternal transmission*, Mathematical Biology, 76 (2018), pp. 235–263.

APPENDIX A

TABLE OF DATA

Monthly dengue incidence data in Chiang Mai province of Thailand [25; 33]

Table A1. Average monthly DENV incidence in Chiang Mai, Thailand, for the period of 2005-2016.

Month	2005	2006	2007	2008	2009	2010	2011	2012	2013	2014	2015	2016	Average (*per* 100,000)
January	4	8	1	21	87	44	29	19	138	12	17	80	3.8
February	12	4	3	21	44	30	7	23	90	9	13	28	2.3
March	9	8	3	27	34	44	11	5	175	2	7	42	3.5
April	21	18	12	74	54	45	12	20	573	5	25	61	7.5
May	164	95	32	227	151	158	87	65	1293	19	173	109	21.4
June	168	301	99	591	314	525	142	170	3120	89	400	277	51.63
July	148	217	160	987	322	1850	93	252	3146	150	400	1074	73.33
August	103	137	156	971	287	2304	96	335	1691	184	826	1624	72.61
September	79	47	98	561	177	1153	49	332	818	168	1067	868	45.14
October	56	35	48	383	144	283	22	373	240	83	889	303	23.82
November	35	16	43	270	133	69	40	215	106	40	911	215	17.44
December	9	9	10	128	44	41	13	129	42	25	363	73	7.38

Table A2. Full monthly DENV incidence in Chiang Mai, Thailand, for the period of 2005-2016 [25; 33].

Month 2005-2016	Temp (°C)	Rain (mm)	Dengue cases
2005			
1	22.6	0	4
2	25.5	0	12
3	27.2	24.7	9
4	29.8	57.2	21
5	29.6	104.7	164
6	29	193.5	168
7	28.4	179.1	148
8	27	155.2	103
9	26.9	436.3	79
10	26.8	192	56
11	25.5	22.8	35
12	22.6	27.9	9
2006			
1	22.4	0	8
2	25.1	0	4
3	28	18	8
4	29.2	206.7	18
5	26.4	219.5	95
6	28.6	180.4	301
7	26.3	269.3	217
8	26	341.4	137
9	26.6	194.8	47
10	25.7	69.9	35
11	23.9	0	16
12	21.8	0	9
2007			
1	21	0	1
2	23.3	0	3
3	26.5	0	3
4	29.5	56	12
5	26.4	393.5	32

6	27.8	130.1	99
7	26.9	74.6	160
8	26.9	153.2	156
9	26.8	179.8	98
10	25.7	64.6	48
11	23	73.5	43
12	21.8	0	10
2008			
1	22.2	16.6	21
2	24.5	13.8	21
3	27.7	9.4	27
4	29.8	57.2	74
5	27.3	158.7	227
6	27.9	147.1	591
7	27.7	101.6	987
8	27.2	170.9	971
9	26.9	236.4	561
10	26.6	188.1	383
11	24.2	34.1	270
12	21.5	7.1	128
2009			
1	21.3	0	87
2	25.3	0	44
3	27	16.7	34
4	29.5	97.9	54
5	28.4	142	151
6	27.6	140.2	314
7	27.7	124	322
8	27.9	126.8	287
9	27.9	191.7	177
10	27.3	223.4	144
11	25	0	133
12	22.4	7.5	44
2010			
1	24.1	21.7	44
2	24.4	0	30
3	26.9	0	44
4	31.5	3.9	45
5	31.3	46.4	158
6	29.6	122.7	525
7	28.5	114.5	1850
8	27	470.6	2304
9	27.4	196.2	1153
10	26.8	169.6	283
11	24.7	0	69
12	23.4	6.1	41
2011			
1	22.6	2.6	29
2	24.4	0.8	7

3	25.3	60.4	11
4	27.2	92.6	12
5	27.2	292.7	87
6	27.7	216.8	142
7	27.6	191.2	93
8	26.8	260.5	96
9	27.1	254.9	49
10	26.4	69.7	22
11	24.9	6.7	40
12	23	0.6	13
2012			
1	23	11	19
2	25.1	0	23
3	27.4	8.3	5
4	29.3	75.9	20
5	28.5	216.4	65
6	28.1	55.9	170
7	27.5	106	252
8	27.6	185.4	335
9	27.6	179.6	332
10	27.3	80.1	373
11	26.9	38.8	215
12	24.2	1	129
2013			
1	23.2	25	138
2	26.9	31.6	90
3	27.6	17.1	175
4	31.2	1.2	573
5	29.8	89.9	1293
6	28.9	39.7	3120
7	27.9	272.9	3146
8	27.3	299.4	1691
9	27.4	275.6	818
10	26.2	123.4	240
11	26.4	85.4	106
12	21	26.8	42
2014			
1	21.3	0	12
2	24.3	0	9
3	27.7	5.9	2
4	29.6	34.9	5
5	29.1	236.1	19
6	28.8	58.2	89
7	28	175.2	150
8	27.4	231.3	184
9	27.6	177.5	168
10	27.3	129.3	83
11	25.8	16	40
12	23.5	0	25

2015			
1	22.3	78.9	17
2	24.3	0	13
3	27.9	27.5	7
4	29.7	53.8	25
5	30.4	76.5	173
6	29.9	15.2	400
7	28.2	120.2	613
8	28.2	143	826
9	28.2	139.4	1067
10	27.3	93.2	889
11	26.8	79.2	911
12	24.5	4.9	363
2016			
1	21.6	34.2	80
2	24.2	45.3	28
3	29.4	0	42
4	32.4	17.7	61
5	31.1	85.7	109
6	28.1	236.1	277
7	27.6	162.1	1074
8	27.7	132.1	1624
9	27.6	213.1	868
10	27.6	141.7	303
11	26.3	105.3	215
12	24	6	73

Appendix B

PROOF OF THEOREM 2.3.3

Proof. Let $\mathtt{r}_0 > 1$ and $\mathbb{R}_G < 1$. The proof is based on using the approach in [86; 87]. In particular, the following theorem will be used (where a dot represents differentiation with respect to time t).

Theorem .0.1 *[86; 87] Let $\mathcal{D} \setminus \{\mathbf{0}\} \subset \mathbb{R}^6_+ \times \mathbb{R}^6_+$, $\mathcal{D}$ the compact subset defined in page 30. The system (2.2.1) is C^1 class defined on $\mathcal{D}$. If*

1. *D is positively invariant relative to (2.2.1);*
2. *The autonomous case of the model (2.2.1) reduced to the disease-free sub-manifold $D \cap (\mathbb{R}^6_+ \times \{\mathbf{0}\}) : \dot{x}_S = A_1(x_S, \mathbf{0})(x_S - x_S^\dagger)$ is GAS at $x_S^\dagger$;*
3. *For any $x \in D$, the matrix $A_2(x)$ is Metzler irreducible;*
4. *There exists a matrix $\bar{A}_2$, which is an upper bound of the set $M = \{A_2(x) \in \mathcal{M}_6(\mathbb{R}) \mid x \in \mathcal{D}\}$ with the property that if $\bar{A}_2 \in M$, for any $\bar{x} \in \mathcal{D}$, such that $A_2(\bar{x}) = \bar{A}_2$, then $\bar{x} \in \mathbb{R}^6 \times \{\mathbf{0}\}$;*
5. *The stability modulus of $\bar{A}_2$ satisfies $\mathrm{Re}(\rho(\bar{A}_2)) \leq 0$.*

Then DFE $(x_S^\dagger, \mathbf{0})$ is GAS in $\mathcal{D}$.

Let $x(t) = (x_S(t), x_I(t))$, where, $x_S(t) = (S_E(t), S_L(t), S_P(t), S_M(t), S_H(t), R_H(t))$, $x_I(t) = (I_E(t), I_L(t), I_P(t), I_M(t), E_H(t), I_H(t))$. Following [86], it is convenient to re-write the autonomous case of the model (2.2.1) as:

$$\begin{aligned} \dot{x}_S &= A_1(x)(x_S - x_S^\dagger) + A_{12}(x)x_I, \\ \dot{x}_I &= A_2(x)x_I, \end{aligned} \tag{.0.1}$$

where,

$$A_1(x) = \begin{bmatrix} -g_1 & 0 & 0 & a_{1,4} & 0 & 0 \\ \sigma_E & -g_2 & 0 & 0 & 0 & 0 \\ 0 & \sigma_L & -g_3 & 0 & 0 & 0 \\ 0 & 0 & f_V\sigma_P & -\mu_V & 0 & 0 \\ 0 & 0 & 0 & 0 & -\mu_H & 0 \\ 0 & 0 & 0 & 0 & 0 & -\mu_H \end{bmatrix}, A_{12}(x) = \begin{bmatrix} 0 & 0 & 0 & b_{1,4} & 0 & 0 \\ 0 & 0 & 0 & 0 & 0 & 0 \\ 0 & 0 & 0 & 0 & 0 & 0 \\ 0 & 0 & 0 & 0 & b_{4,5} & 0 \\ 0 & 0 & 0 & b_{5,4} & 0 & 0 \\ 0 & 0 & 0 & 0 & 0 & \gamma_H \end{bmatrix},$$

$$A_2(x) = \begin{bmatrix} -g_E & 0 & 0 & c_{1,4} & 0 & 0 \\ \sigma_E & -g_L & 0 & 0 & 0 & 0 \\ 0 & \sigma_L & -g_P & 0 & 0 & 0 \\ 0 & 0 & f_V\sigma_P & -\mu_V & 0 & \frac{a_V\beta_H S_H}{N_H} \\ 0 & 0 & 0 & \frac{a_V\beta_H S_H}{N_H} & -g_5 & 0 \\ 0 & 0 & 0 & 0 & \sigma_H & -g_6 \end{bmatrix},$$

with $a_{1,4} = \phi_V\left(1 - \frac{S_M + S_M^\dagger}{K_V}\right)$, $b_{1,4} = \phi_V\left[\frac{S_M(r-2)}{K_V} + (1-r)\left(1 - \frac{S_M^\dagger}{K_V}\right)\right]$, $b_{4,5} = -\frac{a_V\beta_V S_M}{N_H}$, $b_{5,4} = -\frac{a_V\beta_H S_H}{N_H}$, $c_{1,4} = r\phi_V\left(1 - \frac{S_M + I_M}{K}\right)$.

It can be seen that the eigenvalues of $A_1(x)$ are negative. Therefore, $\dot{x}_S = A_1(x_S, \mathbf{0})(x_S - x_S^\dagger)$ is GAS at $x_S^\dagger$. Furthermore, following [147; 148], the matrix $A_2(x)$ can be written as $A_2(x) = \Lambda + B(x)$, where

$$\Lambda = \begin{bmatrix} -g_1 & 0 & 0 & 0 & 0 & 0 \\ \sigma_E & -g_2 & 0 & 0 & 0 & 0 \\ 0 & \sigma_L & -g_3 & 0 & 0 & 0 \\ 0 & 0 & f_V\sigma_P & -\mu_V & 0 & 0 \\ 0 & 0 & 0 & 0 & -g_5 & 0 \\ 0 & 0 & 0 & 0 & \sigma_H & -g_6 \end{bmatrix}, B(x) = \begin{bmatrix} 0 & 0 & 0 & d_{1,4} & 0 & 0 \\ 0 & 0 & 0 & 0 & 0 & 0 \\ 0 & 0 & 0 & 0 & 0 & 0 \\ 0 & 0 & 0 & 0 & 0 & \frac{a_V\beta_V S_M}{N_H} \\ 0 & 0 & 0 & \frac{a_V\beta_H S_H}{N_H} & 0 & 0 \\ 0 & 0 & 0 & 0 & 0 & 0 \end{bmatrix},$$

with $d_{1,4} = \phi_V r\left(1 - \frac{S_M + S_M^\dagger}{K_V}\right)$. Since Λ is a Metzler matrix and $B(x)$ is a positive and bounded matrix, it follows [87; 147; 148] that the matrix $A_2(x)$ has all eigenvalues with negative real part if and only if [87]

$$\mathbb{R}_G = \rho(-B\Lambda^{-1}) = \frac{1}{2}\left[r\mathtt{r}_0 + \sqrt{r\mathtt{r}_0^2 + 4\mathbb{R}_0}\right] < 1. \tag{.0.2}$$

Furthermore, it can be seen that if $\mathbb{R}_G < 1$, then $\mathbb{R}_{0V} < 1$ (since $\mathbb{R}_{0V} \leq \mathbb{R}_G$). □

Appendix C

PROOF OF THEOREM 2.4.2

Proof. Consider the special case of the non-autonomous model (2.2.1). The model (2.2.1) can be re-written as (for infected compartments)

$$\begin{aligned}
\frac{dI_E(t)}{dt} &\leq r\phi_V(t)\left[1-\frac{S^*_{nM}(t)}{K_V(t)}\right]I_M-[\sigma_E(t)+\mu_E(t)]\,I_E,\\
\frac{dI_L(t)}{dt} &\leq \sigma_E(t)I_E-[\sigma_L(t)+\mu_L(t)]\,I_L,\\
\frac{dI_P(t)}{dt} &= \sigma_L(t)I_L-[\sigma_P(t)+\mu_P(t)]\,I_P,\\
\frac{dI_M(t)}{dt} &\leq f_V\sigma_P(t)I_P+\frac{a_V(t)\beta_V(t)S^*_{nM}(t)}{S^*_{nH}(t)}I_H-\mu_V(t)I_M,\\
\frac{dE_H(t)}{dt} &\leq a_V(t)\beta_V(t)I_M-(\sigma_H+\mu_H)E_H,\\
\frac{dI_H(t)}{dt} &\leq \sigma_H E_H-(\gamma_H+\mu_H)I_H,\\
\frac{dR_H(t)}{dt} &= \gamma_H I_H-\mu_H R_H. \qquad (.0.1)
\end{aligned}$$

The equation (.0.1), with equality used in place of the inequality, can be re-written in terms of the matrices $F(t)$ and $V(t)$, as follows

$$\frac{dW}{dt}=[F(t)-V(t)]W. \qquad (.0.2)$$

It follows from Lemma 2.1 in [202] that there exists a positive ω-periodic function $w(t)=\left(\underline{I_E(t)},\underline{I_L(t)},\underline{I_P(t)},\underline{I_M(t)},\underline{E_H(t)},\underline{I_H(t)},\underline{R_H(t)}\right)^T$ such that

$$W(t)=\mathrm{e}^{\theta t}w(t),\quad \text{with}\quad \theta=\frac{1}{\omega}\ln\rho[\phi_{F-V}(\omega)],$$

is a solution of the equation given by (.0.2). Furthermore, the assumption $\mathcal{R}_{0n}<1$ implies that $\rho\left(\phi_{F-V}(\omega)\right)<1$ (by Theorem 2.2 in [186]). Hence, θ is a negative constant. Thus, $W(t)\to 0$ as $t\to\infty$. Therefore, the unique disease-free solution of the linear system (.0.2) given by $W(t)=0$ is GAS.

For any non-negative initial solution $w(0)=\left(\underline{I_E(0)},\underline{I_L(0)},\underline{I_P(0)},\underline{I_M(0)},\underline{E_H(0)},\underline{I_H(0)},\underline{R_H(0)}\right)^T$ of the system (.0.2), there exists a sufficiently large $M^*>0$ such that

$$(I_E(0),I_L(0),I_P(0),I_M(0),E_H(0),I_H(0),R_H(0))<M^*w(0).$$

Thus, by comparison theorem [169], it follows that

$$(I_E(t),I_L(t),I_P(t),I_M(t),E_H(t),I_H(t),R_H(t))<M^*W(t),\ \text{ for all }\ t\geq 0,$$

where, $M^*W(t)$ is also a solution of (.0.2). Hence,
$(I_E(t),I_L(t),I_P(t),I_M(t),E_H(t),I_H(t),R_H(t))\to 0$ as $t\to 0$. Finally, it follows from Theorem 1.2 in [75] that
$(S_E(t),S_L(t),S_P(t),S_M(t),S_H(t))\ \to\ (S^*_{nE}(t),S^*_{nL}(t),S^*_{nP}(t),S^*_{nM}(t),S^*_{nH}(t))$, where,

$(S^*_{nE}(t), S^*_{nL}(t), S^*_{nP}(t), S^*_{nM}(t), S^*_{nH}(t))$ satisfies (2.4.19). Thus, for $\mathcal{R}_{0n} < 1$, $(S_E(t), I_E(t), S_L(t), I_L(t), S_P(t), I_P(t), S_M(t), I_M(t), S_H(t), E_H(t), I_H(t), R_H(t)) \to \varepsilon_{0n}(t)$ as $t \to \infty$. □

Appendix D

PROOF OF THEOREM 3.2.1

Proof. We first show the non-negativity of the state variables $S_H(t)$ and $N_H(t)$ for all $t > 0$. Let $S_H(t_1) = 0$ for some $t = t_1 > 0$. Then, it follows from the eighth equation of (3.2.5) that (noting that all parameters of the model are assumed to be non-negative)

$$\frac{dS_H}{dt}|_{t=t_1} = \Pi_H > 0.$$

Hence, the solution $S_H(t)$ is increasing at $t = t_1$. Thus, $S_H(t)$ cannot decrease below zero. This shows that $S_H(t) > 0$ for all $t \geq 0$.

For the non-negativity of $N_H(t)$, it is convenient to consider the equation for the rate of change of the total human population (obtained by adding the last four equations of the model (3.2.5)), given by

$$\frac{dN_H}{dt} = \Pi_H - \mu_H N_H. \tag{.0.1}$$

Let $N_H(t_2) = 0$ for some $t = t_2 > 0$. It follows from (.0.1) that

$$\frac{dN_H}{dt}|_{t=t_2} = \Pi_H > 0,$$

so that (using similar argument as above) $N_H(t) > 0$ for all $t \geq 0$.

To show the non-negativity of the remaining 10 state variables of the model (3.2.5), it is convenient to define

$$t^* = \min_{t>0}\{t|\text{at least one of the remaining 10 state variables of the model (3.2.5) is zero}\}. \tag{.0.2}$$

First of all, the case where no such t^* exists (i.e., when each of the remaining 10 state variables of the model is strictly positive) is the trivial case (and no proof is needed).

Suppose such t^* exists. Further, without loss of generality, let $A_U(t^*) = 0$ and the other remaining state variables of the model (3.2.5) are non-negative at $t = t^*$. Based on the definition of t^* in (.0.2), the assumption $A_U(t^*) = 0$ is equivalent to saying $A_U(t) > 0$ for all $t < t^*$. It follows from the first equation of the model (3.2.5) that

$$\begin{aligned}\frac{dA_U}{dt}|_{t=t^*} &= B_{UU}(t^*) + (1-v_w)(B_{WU}(t^*) + B_{WW}(t^*)) + B_{DU}(t^*) \\ &= \phi_u\psi_u\left(1 - \frac{N_A(t^*)}{K_A}\right)\left(\frac{M_U(t^*)+1}{1+M_U(t^*)+M_W(t^*)}\right)(F_U(t^*)+F_D(t^*)) \\ &+ (1-v_w)\phi_w\psi_w\left(1 - \frac{N_A(t^*)}{K_A}\right)\left(\frac{1}{1+M_U(t^*)+M_W(t^*)}\right)(F_U(t^*)M_U(t^*) \\ &+ M_W(t^*)F_W(t^*)).\end{aligned} \tag{.0.3}$$

To show that $A_U(t) \geq 0$ for all t, we need to show that each of the state variables in (.0.3) (namely $F_U(t)$, $F_W(t)$, $M_U(t)$ and $M_W(t)$) is non-negative at $t = t^*$.

Let $M_W(t^*) = 0$. If $A_W(t^*) > 0$, then it follows from the sixth equation of the model (3.2.5) that, at $t = t^*$,

$$\frac{dM_W}{dt}|_{t=t^*} = (1 - b_f)\sigma_m A_W(t^*) > 0.$$

Since $\frac{dM_W}{dt}|_{t=t^*} > 0$, it follows that $M_W(t)$ is an increasing function at $t = t^*$. Hence, $M_W(t)$ is non-negative in a neighbourhood of t^*.

Next, consider the case where $M_W(t^*) = A_W(t^*) = 0$. Since (in this case) $M_W(t^*) = 0$, it follows that, for any $\epsilon_1 > 0$, there exists a $\delta_1 > 0$ such that, for $|t - t^*| < \delta_1$, the inequality $|M_W(t)| < \frac{\epsilon_1}{\mu_{um}}$ holds. It can be seen from the sixth equation of the model (3.2.5) that the equation for the derivative of $M_W(t)$ in a neighborhood of t^* (where, now, $t \in (t^* - \delta_1, t^*)$ or $(t^*, t^* + \delta_1)$)

$$\frac{dM_W}{dt} \geq (1 - b_f)\sigma_m A_W(t) - \epsilon_1. \tag{.0.4}$$

Since $A_W(t) > 0$ for $t < t^*$, ϵ_1 can be chosen small enough such that $A_W(t) > \frac{\epsilon_1}{(1-b_f)\sigma_m}$ in a neighbourhood of t^*. Therefore, from equation (.0.4), the derivative of M_W is positive in a neighbourhood of t^*. Hence, M_W is an increasing function at $t = t^*$ and $M_W(t) \geq 0$ in an interval of t^* (i.e., sub-interval of $(t^* - \delta_1)$ or $(t^*, t^* + \delta_1)$). Similarly, it can be shown that $M_U(t) \geq 0$ in an interval of t^*.

Next, we show that $I_H(t) \geq 0$ in a neighbourhood of t^*. Let $I_H(t^*) = 0$. Then, for any $\epsilon_2 > 0$, there exists $\delta_2 > 0$ such that for $|t - t^*| < \delta_2$, the inequality $|I_H(t)| < \frac{\epsilon_2}{\gamma_H + \mu_H}$ holds. It follows from the tenth equation of the model (3.2.5) that, in the neighbourhood of t^*,

$$\frac{dI_H}{dt} > \sigma_H E_H - \epsilon_2. \tag{.0.5}$$

Since $E_H(t) > 0$ for $t < t^*$, ϵ_2 can be chosen small enough such that $E_H(t) > \frac{\epsilon_2}{\sigma_H}$, in a neighbourhood of t^*. Hence, it follows from equation (.0.5) that $I_H(t)$ is an increasing function when t is close enough to t^*. Thus, $I_H(t) \geq 0$ in a neighbourhood of t^*. Next we show that $F_U(t) \geq 0$ in a neighbourhood of $t = t^*$. Let $F_U(t^*) = 0$. Then, for any $\epsilon_3 > 0$, there is $\delta_3 > 0$ such that for $|t - t^*| < \delta_3$, the inequality $|F_U(t)| < \epsilon_3$ holds. Since we showed previously that $I_H(t)$, $M_U(t)$ and $M_W(t)$ are all greater or equal to zero in a neighbourhood of $t = t^*$, then it follows from the fourth equation of the model (3.2.5) that (in a neighbourhood of t^*, and recall that $I_H(t) < N_H(t)$ for all t),

$$\frac{dF_U}{dt} > b_f \sigma_m A_U - a_V \beta_V F_U - q F_U - \mu_{uf} F_U. \tag{.0.6}$$

Let $\lambda = \max\{a_V \beta_V, q, \mu_{uf}\}$. Then, equation (.0.6) satisfies

$$\frac{dF_U}{dt} > b_f \sigma_m A_U - 3\lambda F_U > b_f \sigma_m A_U - 3\lambda \epsilon_3. \tag{.0.7}$$

Since $A_U(t) > 0$ for $t < t^*$, then it follows from (.0.7) that ϵ_3 can be chosen small enough such that $A_U(t) > \frac{3\lambda\epsilon_3}{b_f \sigma_m}$ in a neighbourhood of t^*, (i.e., sub-interval of $(t^* - \delta_3, t^*)$ or $(t^*, t^* + \delta_3)$). Hence, $F_U(t)$ is increasing function near t^*. Therefore, $F_U(t) \geq 0$ in a

neighbourhood of t^*. Since we showed $I_H(t) > 0$ and $F_U(t) > 0$ in a neighbourhood of t^*, it can be shown that $F_D(t) > 0$ in a neighbourhood of t^* by the same argument. We have shown that all the state variables on the right-hand side of the equation (.0.3) are positive. Hence, $A_U(t)$ is an increasing function in a neighbourhood of t^*, which implies that $A_U(t)$ cannot be negative.
This proof can be applied for any other state variable of the model (3.2.5) such that the state variable is zero at $t = t^*$ for the first time. Hence, all the state variables of the model (3.2.5) are non-negative if the initial vector $\mathbf{X}(0)$ is positive.

For the boundedness of the solutions of the model, it should first be noted that $A_U(t) < K_V$ for all $t \geq 0$. Suppose this assumption is relaxed and $A_U(t)$ can be equal to K_V. Let t_1 be the first time such that $A_U(t)$ equals K_V. That is, define t_1 such that $A_U(t_1) = K_V$. Thus, it follows from the first equation of (3.2.5) that $\frac{dA_U}{dt}|_{t=t_1} < 0$ (since $\left(1 - \frac{N_A(t_1)}{K_A}\right) < 0$). This implies that $A_U(t)$ is a decreasing function of t in some t_1 neighborhood. Therefore, $A_U(t)$ can not exceed K_V (since $A_U(t)$ is decreasing in a neighbourhood of t_1). Hence, $A_U(t) < K_V$ for all $t > 0$. Using similar argument, it can be shown that $A_W(t) < K_V$ for all $t > 0$.

To show the boundedness for $F_U(t)$, the equation for $\frac{dF_U}{dt}$ in (3.2.5) can be rewritten as (noting that $A_U(t) < K_V$ for all $t > 0$)

$$\frac{dF_U}{dt} < b_f \sigma_m K_V - \mu_{uf} F_U,$$

from which it follows that

$$F_U(t) < \frac{b_f \sigma_m}{\mu_{uf}} K_V + e^{-\mu_{uf} t} \left(F_U(0) - \frac{b_f \sigma_m}{\mu_{uf}} \right).$$

Hence, $F_U(t)$ is bounded for all $t > 0$. Similarly, it can be shown that the remaining mosquito state variables, $F_W(t)$, $M_U(t)$, $M_W(t)$ and F_D are all bounded for all $t > 0$.

For the boundedness of the state variables for the human components of the model (3.2.5), it is convenient to consider the equation for the rate of change of total human population ($N_H(t)$), given by

$$\frac{dN_H}{dt} = \Pi_H - \mu_H N_H,$$

from which it follows that $N_H(t) < \frac{\Pi_H}{\mu_H} + N_H(0)$ for all $t > 0$. Hence, $N_H(t)$ is bounded. Thus, since $N_H(t) = S_H(t) + E_H(t) + I_H(t) + R_H(t)$, it follows that $S_H(t)$, $E_H(t)$, $I_H(t)$ and $R_H(t)$ are bounded for all $t > 0$.

□

APPENDIX E

PROOF OF THEOREM 3.3.4

Proof. Consider the model (3.3.15) with $\mathcal{R}_U < 1$ and $\mathcal{R}_W < 1$. The Jacobian of the model (3.3.15) at the trivial equilibrium $\mathcal{T}_{0\diamond}$ is given by

$$\mathcal{J}(\mathcal{T}_{0\diamond}) = \begin{bmatrix} -\sigma_m - \mu_a & 0 & \phi_u\psi_u & (1-v_w)\,\phi_w\psi_w & 0 & 0 \\ 0 & -\sigma_m - \mu_a & 0 & v_w\phi_w\psi_w & 0 & 0 \\ b_f\sigma_m & 0 & -\mu_{uf} & 0 & 0 & 0 \\ 0 & b_f\sigma_m & 0 & -\theta_w\mu_{uf} & 0 & 0 \\ (1-b_f)\,\sigma_m & 0 & 0 & 0 & -\mu_{um} & 0 \\ 0 & (1-b_f)\,\sigma_m & 0 & 0 & 0 & -\mu_{um} \end{bmatrix}.$$

The associated eigenvalues of the matrix $\mathcal{J}(\mathcal{T}_{0\diamond})$ are

$$\begin{aligned} \lambda_1 &= -\frac{1}{2}\left[\theta_w\mu_{uf} + \sigma_m + \mu_a + \sqrt{(\sigma_m + \mu_a - \theta_w\mu_{uf})^2 + 4\,b_f\sigma_m\,\phi_w\psi_w v_w}\right], \\ \lambda_2 &= -\frac{1}{2}\left[\theta_w\mu_{uf} + \sigma_m + \mu_a - \sqrt{(\sigma_m + \mu_a - \theta_w\mu_{uf})^2 + 4\,b_f\sigma_m\,\phi_w\psi_w v_w}\right], \\ \lambda_3 &= -\frac{1}{2}\left[\mu_{uf} + \sigma_m + \mu_a + \sqrt{(\sigma_m + \mu_a - \mu_{uf})^2 + 4\,b_f\sigma_m\,\phi_u\psi_u}\right], \\ \lambda_4 &= -\frac{1}{2}\left[\mu_{uf} + \sigma_m + \mu_a - \sqrt{(\sigma_m + \mu_a - \mu_{uf})^2 + 4\,b_f\sigma_m\,\phi_u\psi_u}\right], \\ \lambda_5 &= \lambda_6 = -\mu_{um}. \end{aligned} \tag{.0.1}$$

It is clear from (.0.1) that eigenvalues λ_1, λ_3, λ_5 and λ_6 are automatically negative. Furthermore, it can be shown easily, using similar argument as in the proof of Theorem 3.3.2, that the eigenvalue $\lambda_2 < 0$ whenever $\mathcal{R}_W < 1$ and the eigenvalue $\lambda_4 < 0$ whenever $\mathcal{R}_U < 1$. □

APPENDIX F

PROOF OF THEOREM 3.3.5

Proof. Consider the model (3.3.15) with $\mathcal{R}_U > 1$. It is convenient to define the following change of variables for the model (3.3.15), $A_U = x_1$, $A_W = x_2$, $F_U = x_3$, $F_W = x_4$, $M_U = x_5$ and $M_W = x_6$. Furthermore, by using the vector notation $\mathbf{x} = (x_1, x_2, x_3, x_4, x_5, x_6)^T$, the model (3.3.15) can be written in form $\frac{d\mathbf{x}}{dt} = \mathbf{f} = (f_1, f_2, f_3, f_4, f_5, f_6)^T$, as follows,

$$\begin{aligned}
\frac{dx_1}{dt} &= \left(1 - \frac{x_1 + x_2}{K_A}\right)\left[\phi_u\psi_u\left(\frac{1 + x_5}{1 + x_5 + x_6}\right)x_3 + \phi_w\psi_w(1 - v_w)x_4\right] - (\sigma_m + \mu_a)x_1,\\
\frac{dx_2}{dt} &= v_w\phi_w\psi_w\left(1 - \frac{x_1 + x_2}{K_A}\right)x_4 - (\sigma_m + \mu_a)x_2,\\
\frac{dx_3}{dt} &= b_f\sigma_m x_1 - q\left(\frac{x_6}{1 + x_5 + x_6}\right)x_3 - \mu_{uf}x_3,\\
\frac{dx_4}{dt} &= b_f\sigma_m x_2 + q\left(\frac{x_6}{1 + x_5 + x_6}\right)x_3 - \theta_w\mu_{uf}x_4,\\
\frac{dx_5}{dt} &= (1 - b_f)\sigma_m x_1 - \mu_{um}x_5,\\
\frac{dx_6}{dt} &= (1 - b_f)x_2 - \mu_{um}x_6.
\end{aligned} \tag{.0.1}$$

The proof is based on using Center Manifold theory [27; 30]. In particular, the following Theorem from [27] will be used.

Theorem .0.1 ([27]) *Consider a system of ordinary differential equations*

$$\frac{dx}{dt} = f(x, \phi), f : \mathbb{R}^n \times \mathbb{R} \to \mathbb{R}^n \tag{.0.2}$$

with a parameter ϕ, assumed such that:

1. *0 is an equilibrium of the system, $f(0, \phi) = 0$ for all $\phi \in \mathbb{R}$;*
2. *0 is a simple eigenvalue of $\mathcal{J} = D_x f(0, 0) = [\frac{\partial f_i}{\partial x_i}(0, 0)]$ and all other eigenvalues of $\mathcal{J}$ have negative real parts.*

Let $W = [w_1, w_2, \ldots, w_n]^T$ and $V = [v_1, v_2, \ldots, v_n]$ be a right and a left eigenvector matrix $\mathcal{J}$, respectively, associated to eigenvalues 0 and $f_k(x, \phi)$ be the kth component of $f(x, \phi)$. Then the local dynamics of system around the equilibrium point 0 is totally determined by the signs of a and b below:

$$\begin{aligned}
a &= \sum_{k=1}^{n}\sum_{j=1}^{n}\sum_{k=1}^{n} v_k w_i w_j \frac{\partial^2 f_k}{\partial x_i \partial x_j}(0, 0),\\
b &= \sum_{k=1}^{n}\sum_{i=1}^{n} v_k w_i \frac{\partial^2 f_k}{\partial \phi \partial x_i}(0, 0),
\end{aligned}$$

Then local dynamics of (.0.2) around 0 are totally determined by a and b.

(i). $a > 0$, $b > 0$. *When* $\phi < 0$ *with* $|\phi| < 1$, *0 is locally asymptotically stable, and there exists a positive unstable equilibrium; when* $0 < \phi < 1$, *0 is unstable and there exists a negative and locally asymptotically stable equilibrium;*

(ii). $a < 0$, $b < 0$. *When* $\phi < 0$ *with* $|\phi| < 1$, *0 is unstable; when* $0 < \phi < 1$, *0 is locally asymptotically stable, and there exists a positive unstable equilibrium;*

(iii). $a > 0$, $b < 0$. *When* $\phi < 0$ *with* $|\phi| < 1$, *0 is unstable, and there exists a locally asymptotically stable negative equilibrium; when* $0 < \phi < 1$, *0 is stable, and a positive unstable equilibrium appears;*

(iv). $a < 0$, $b > 0$. *When* ϕ *changes from negative to positive, 0 changes its stability from stable to unstable. Correspondingly a negative unstable equilibrium becomes positive and locally-asymptotically stable.*

If $a > 0$ *and* $b > 0$, *then a backward bifurcation occurs at* $\phi = 0$ *for the system* (.0.2).

It can be seen that the Jacobian of the model (.0.1) at $\mathcal{T}_1$ is given by:

$$\mathcal{J}(\mathcal{T}_1) = \begin{bmatrix} j_{11} & -\frac{\phi_u\psi_u F_U^*}{K_A} & j_{13} & j_{14} & 0 & j_{16} \\ 0 & -\sigma_m - \mu_a & 0 & j_{24} & 0 & 0 \\ b_f\sigma_m & 0 & -\mu_{uf} & 0 & 0 & -\frac{qF_U^*}{\left(M_U^*+1\right)} \\ 0 & b_f\sigma_m & 0 & -\theta_w\mu_{uf} & 0 & \frac{qF_U^*}{\left(M_U^*+1\right)} \\ (1-b_f)\,\sigma_m & 0 & 0 & 0 & -\mu_{um} & 0 \\ 0 & (1-b_f)\,\sigma_m & 0 & 0 & 0 & -\mu_{um} \end{bmatrix},$$

where, $j_{11} = -\frac{\phi_u\psi_u F_U^*}{K_A} - \sigma_m - \mu_a$, $j_{13} = \phi_u\psi_u\left(1 - \frac{A_U^*}{K_A}\right)$, $j_{14} = (1-v_w)\,\phi_w\psi_w\left(1 - \frac{A_U^*}{K_A}\right)$, $j_{16} = -\frac{\phi_u\psi_u F_U^*}{\left(M_U^*+1\right)}\left(1 - \frac{A_U^*}{K_A}\right)$, $j_{24} = v_w\phi_w\psi_w\left(1 - \frac{A_U^*}{K_A}\right)$. Consider the case where $\mathcal{R}_{0W} = 1$. Suppose, further, that ϕ_w be chosen as a bifurcation parameter. Solving for ϕ_w from $\mathcal{R}_{0W} = 1$ gives

$$\phi_w^* = \left[v_w\psi_w\left(1 - \frac{A_U^*}{K_A}\right)\left(\frac{\mathcal{R}_U}{\theta_w\phi_u\psi_u} + \frac{q(1-b_f)F_U^*\mathcal{R}_U}{\mu_{um}b_f(1+M_U^*)\theta_w\phi_u\psi_u}\right)\right]^{-1}.$$

Let $\mathbf{w} = [w_1, \ldots, w_6]^T$ and $\mathbf{v} = [v_1, \ldots, v_6]$ be the right and left eigenvectors of $\mathcal{J}(\mathcal{T}_1)$, respectively, given by:

$$\begin{aligned} w_1 &= \frac{w_2(A_1+A_2)}{D}, & w_2 &> 0, \\ w_3 &= \frac{w_2\sigma_m(B_1+B_2)}{\mu_{uf}D}, & w_4 &= \frac{w_2\sigma_m\,(\,M_U^*b_f\mu_{um} - qF_U^*b_f + qF_U^*)}{\theta_w\mu_{um}\mu_{uf}M_U^*}, \\ w_5 &= \frac{\sigma_m\,(b_f-1)\,w_2(C_1+C_2)}{\mu_{um}D}, & w_6 &= \frac{w_2\sigma_m\,(1-b_f)}{\mu_{um}}, \\ v_1 &= 0, & v_2 &> 0, \end{aligned} \tag{.0.3}$$

$$v_3 = 0, \qquad v_4 = \frac{\psi_w \phi_w^* v_w v_2}{\theta_w \mu_{uf} \mathcal{R}_U},$$

$$v_5 = 0, \qquad v_6 = \frac{q\psi_w \phi_w^* v_w v_2 F_U^*}{\theta_w \mu_{um} \mu_{uf} M_U^* \mathcal{R}_U},$$

where,

$$\begin{aligned}
A_1 &= -\sigma_m F_U^* \left(A_U^* - K_A\right)\left(b_f - 1\right)\left(\phi_u \psi_u \theta_w q + q\phi_w^* \psi_w v_w + \phi_u \psi_u \theta_w \mu_{uf} - q\phi_w^* \psi_w\right), \\
A_2 &= \sigma_m M_U^* b_f \mu_{um} \phi_w^* \psi_w \left(A_U^* - K_A\right)\left(v_w - 1\right) - F_U^* M_U^* \mu_{uf} \mu_{um} \phi_u \psi_u \theta_w, \\
B_1 &= \sigma_m M_U^* {b_f}^2 \mu_{um} \phi_w^* \psi_w \left(A_U^* - K_A\right)\left(v_w - 1\right) + \\
&\quad q F_U^* \mu_{uf} \theta_w \left(b_f - 1\right)\left(F_U^* \phi_u \psi_u + \sigma_m K_A + K_A \mu_a\right), \\
B_2 &= -\sigma_m F_U^* b_f \left(A_U^* - K_A\right)\left(b_f - 1\right)\left(q\phi_w^* \psi_w v_w + \phi_u \psi_u \theta_w \mu_{uf} - q\phi_w \psi_w\right) - \\
&\quad F_U^* M_U^* b_f \mu_{uf} \mu_{um} \phi_u \psi_u \theta_w, \\
C_1 &= \sigma_m M_U^* b_f \mu_{um} \phi_w^* \psi_w \left(A_U^* - K_A\right)\left(v_w - 1\right) - F_U^* M_U^* \mu_{uf} \mu_{um} \phi_u \psi_u \theta_w, \\
C_2 &= -\sigma_m F_U^* \left(A_U^* - K_A\right)\left(b_f - 1\right)\left(\phi_u \psi_u \theta_w q + q\phi_w^* \psi_w v_w + \phi_u \psi_u \theta_w \mu_{uf} - q\phi_w^* \psi_w\right) \\
D &= \left(K_A \mu_{uf}\left(\sigma_m + \mu_a\right) + F_U^* \mu_{uf} \phi_u \psi_u - \frac{\sigma_m b_f \phi_u \psi_u}{\mathcal{R}_U}\right) \theta_w \mu_{um} M_U^*.
\end{aligned} \tag{.0.4}$$

Applying Theorem .0.1, it can be shown, by computing the non-zero partial derivatives of $\mathbf{f}$, that the associated backward bifurcation coefficients, a and b, are given, respectively, by

$$a = \sum_{k=1}^{6}\sum_{j=1}^{6}\sum_{k=1}^{6} v_k w_i w_j \frac{\partial^2 f_k}{\partial x_i \partial x_j}(\mathcal{T}_1), \text{ and } b = \sum_{k=1}^{6}\sum_{i=1}^{6} v_k w_i \frac{\partial^2 f_k}{\partial \phi_w \partial x_i}(\mathcal{T}_1), \tag{.0.5}$$

where, (with the eigenvectors w_i and v_i, $i = 1, 2, \ldots, 6$, are as given in (.0.3))

$$\begin{aligned}
a(\phi_w^*) = &\frac{2\psi_w \phi_w^* v_w v_2 w_2^2 \sigma_m \left(M_U^* b_f \mu_{um} - q F_U^* b_f + q F_U^*\right) v_w \phi_w^* \psi_w (A_1 + A_2)}{D\, \theta_w \mu_{um} \mu_{uf} M_U^* K_A} + \\
&\frac{2 v_2 v_w \phi_w^* \psi_w w_2 w_4}{K_A} + \frac{2q(1 - b_f)\, \psi_w \phi_w^* v_w v_2 {w_2}^2 {\sigma_m}^2 (B_1 + B_2)}{D\, \theta_w \mu_{um} \mu_{uf}^2 M_U^* \mathcal{R}_U} - \\
&\frac{2q F_U^*\, \psi_w \phi_w^* v_w v_2 {\sigma_m}^2 \left(b_f - 1\right)^2 {w_2}^2 (C_1 + C_2)}{\theta_w \mu_{uf}\, {\mu_{um}}^2 {M_U^*}^2 \mathcal{R}_U} + \frac{2\psi_w \phi_w^* v_w v_2 {w_2}^2 {\sigma_m}^2 \left(b_f - 1\right)^2 q F_U^*}{\theta_w \mu_{uf}\, {\mu_{um}}^2 {M_U^*}^2 \mathcal{R}_U},
\end{aligned} \tag{.0.6}$$

and, (noting that $0 < b_f < 1$)

$$b(\phi_w^*) = \frac{v_2 w_2 \sigma_m \left(M_U^* b_f \mu_{um} + q F_U^* \left(1 - b_f\right)\right) \phi_w \psi_w}{\theta_w \mu_{um} \mu_{uf} M_U^* \mathcal{R}_U} > 0, \tag{.0.7}$$

where, the expressions for $A_1, A_2, B_1, B_2, C_1, C_2$ are given in (.0.4). Hence, it follows from Theorem .0.1 that, the model (3.3.15) undergoes a backward bifurcation whenever $a(\phi_w^*)$, given in (.0.6), is positive. □

APPENDIX G

PROOF OF THEOREM 3.3.6

Proof. Consider the model (3.3.15) with $\mathcal{R}_W < 1$ and $\bar{m}_w > 1 - \dfrac{1}{\mathcal{R}_U}$. The Jacobian of the model (.0.1) at the trivial equilibrium $\mathcal{T}_{0\diamond}$ is given by

$$\mathcal{J}(\mathcal{T}_{0\diamond}) = \begin{bmatrix} -\sigma_m - \mu_a & 0 & \phi_u\psi_u\bar{m}_u & (1-v_w)\,\phi_w\psi_w & 0 & 0 \\ 0 & -\sigma_m - \mu_a & 0 & v_w\phi_w\psi_w & 0 & 0 \\ b_f\sigma_m & 0 & -\mu_{uf} & 0 & 0 & 0 \\ 0 & b_f\sigma_m & 0 & -\theta_w\mu_{uf} & 0 & 0 \\ (1-b_f)\,\sigma_m & 0 & 0 & 0 & -\mu_{um} & 0 \\ 0 & (1-b_f)\,\sigma_m & 0 & 0 & 0 & -\mu_{um} \end{bmatrix}.$$

The associated eigenvalues of the matrix $\mathcal{J}(\mathcal{T}_{0\diamond})$ are

$$\begin{aligned} \lambda_1 &= -\frac{1}{2}\left[\theta_w\mu_{uf} + \sigma_m + \mu_a + \sqrt{(\sigma_m + \mu_a - \theta_w\mu_{uf})^2 + 4\,b_f\sigma_m\,\phi_w\psi_w v_w}\right], \\ \lambda_2 &= -\frac{1}{2}\left[\theta_w\mu_{uf} + \sigma_m + \mu_a - \sqrt{(\sigma_m + \mu_a - \theta_w\mu_{uf})^2 + 4\,b_f\sigma_m\,\phi_w\psi_w v_w}\right], \\ \lambda_3 &= -\frac{1}{2}\left[\mu_{uf} + \sigma_m + \mu_a + \sqrt{(\sigma_m + \mu_a - \mu_{uf})^2 + 4\,b_f\sigma_m\,\phi_u\psi_u(1-\bar{m}_w)}\right], \\ \lambda_4 &= -\frac{1}{2}\left[\mu_{uf} + \sigma_m + \mu_a - \sqrt{(\sigma_m + \mu_a - \mu_{uf})^2 + 4\,b_f\sigma_m\,\phi_u\psi_u(1-\bar{m}_w)}\right], \\ \lambda_5 &= \lambda_6 = -\mu_{um}. \end{aligned} \tag{.0.1}$$

It is clear from (.0.1) that eigenvalues λ_1, λ_3, λ_5 and λ_6 are automatically negative. Furthermore, it can be shown that the eigenvalue $\lambda_2 < 0$ whenever $\mathcal{R}_W < 1$ and the eigenvalue $\lambda_4 < 0$ whenever $\bar{m}_w > 1 - \frac{1}{\mathcal{R}_U}$. □

APPENDIX H

PROOF OF THEOREM 3.3.7

Proof. Consider the model (3.3.15) with $m_w = \bar{m}_w,\ m_u = \bar{m}_u,\ q = 0$ and $\mathcal{R}_U > 1$. Further, let

$$m_w = \frac{M_W}{1 + M_U + M_W} = \bar{m}_w \in [0, 1), \text{ and } m_u = 1 - m_w = \frac{1 + M_U}{1 + M_U + M_W} = \bar{m}_u \in (0, 1].$$

In this case, the *Wolbachia*-free and dengue-free equilibrium ($\mathcal{T}_{1c}$) is given by

$$\mathcal{T}_{1c} = (A_U^*, A_W^*, F_U^*, F_W^*, M_U^*, M_W^*) = (A_U^*, 0, \frac{b_f \sigma_m A_U^*}{\mu_{uf}}, 0, \frac{(1 - b_f)\sigma_m A_U^*}{\mu_{um}}, 0),$$

with $A_U^* = K_A(1 - \frac{1}{\bar{m}_u \mathcal{R}_U})$. This equilibrium exists if and only if $\bar{m}_u \mathcal{R}_U > 1$ (or, equivalently, $0 \leq \bar{m}_w < \frac{\mathcal{R}_U - 1}{\mathcal{R}_U}$). Let

$$\tilde{\mathcal{R}}_{0W} = \frac{\mathcal{R}_W}{\bar{m}_u \mathcal{R}_U}, \tag{.0.1}$$

be the associated reproduction number of the model (3.3.15), with $m_w = \bar{m}_w,\ m_u = \bar{m}_u$ and $q = 0$. Solving $\tilde{\mathcal{R}}_{0W} = 1$ for ϕ_w (chosen as the bifurcation parameter) gives

$$\phi_w^* = \frac{\bar{m}_u \theta_w \mu_{uf}(\sigma_m + \mu_a)\mathcal{R}_U}{v_w \sigma_m b_f \psi_w}.$$

The Jacobian of the model (3.3.15), with $m_w = \bar{m}_w,\ m_u = \bar{m}_u$ and $q = 0$, at $\mathcal{T}_{1c}$, is given by

$$\mathcal{G}(\mathcal{T}_{1c}) = \begin{bmatrix} g_{11} & -\frac{\phi_u \psi_u (1 - \bar{m}_w) F_U^*}{K_A} & g_{13} & g_{14} & 0 & 0 \\ 0 & -\sigma_m - \mu_a & 0 & j_{24} & 0 & 0 \\ b_f \sigma_m & 0 & -\mu_{uf} & 0 & 0 & 0 \\ 0 & b_f \sigma_m & 0 & -\theta_w \mu_{uf} & 0 & 0 \\ (1 - b_f)\, \sigma_m & 0 & 0 & 0 & -\mu_{um} & 0 \\ 0 & (1 - b_f)\, \sigma_m & 0 & 0 & 0 & -\mu_{um} \end{bmatrix},$$

where, $g_{11} = -\frac{\phi_u \psi_u (1 - \bar{m}_w) F_U^*}{K_A} - \sigma_m - \mu_a$ and $g_{13} = g_{14} = (1 - \bar{m}_w)$. The right and a left eigenvector of the matrix $\mathcal{G}$, are given, respectively, by

$$w_1 = \frac{(B_1 + B_2)\, w_2}{\theta_w \left(K_A \mu_{uf} \left(\sigma_a + \mu_a\right)\left(1 - \bar{m}_u \mathcal{R}_U\right)\right)},\ w_2 > 0,\ w_3 = \frac{\sigma_m w_1}{\mu_{uf}},\ w_4 = \frac{\sigma_a b_f w_2}{\theta_w \mu_{uf}},$$

$$w_5 = 0, w_6 = \frac{\lambda\, (1 - b_f)\, w_2}{\mu_{um}},\ \ v_1 = 0,\ \ v_2 > 0,\ v_3 = 0,\ v_4 = \frac{v_w \phi_w \psi_w v_2}{\theta_w \mu_{uf} \bar{m}_u \mathcal{R}_U} v_5 = 0,\ v_6 = 0, \tag{.0.2}$$

where,

$$B_1 = \frac{K_A b_f \sigma_a \psi_w \phi_w (1 - v_w)}{\bar{m}_u R_U}, \text{ and } B_2 = K_A b_f \phi_u \psi_u \theta_w \mu_{uf} \sigma_a \bar{m}_u \left(1 - \frac{1}{\bar{m}_u \mathcal{R}_U}\right).$$

The associated backward bifurcation coefficients, a and b, are given, respectively, by (where the eigenvectors w_i and v_i, $i = 1, 2, \ldots, 6$, are given in (.0.2))

$$a(\phi_w^*) = \frac{2 v_2 {w_2}^2 \sigma_m b_f v_w \phi_w \psi_w \mathcal{R}_W (1 - v_w)}{\theta_w \mu_{uf} K_A \bar{m}_u \mathcal{R}_U (1 - \mathcal{R}_U (1 - \bar{m}_w))}, \tag{.0.3}$$

and,

$$b = \frac{v_2 w_2 b_f v_w \psi_w \sigma_m}{\theta_w \mu_{uf} (1 - \bar{m_w}) \mathcal{R}_U} > 0.$$

It follows from Equation (.0.3) that, $b > 1$, (since $0 < \bar{m}_w < 1$). Hence, $a(\phi^*) < 0$ whenever $\bar{m}_w < 1 - \frac{1}{\mathcal{R}_U}$. Thus, it follows from item (iv) of Theorem .0.1 [27] that the model (3.3.15) does not undergo a backward bifurcation at $\tilde{\mathcal{R}}_{0W} = 1$ whenever $\mathcal{R}_U > 1$ and $\bar{m}_w < 1 - \frac{1}{\mathcal{R}_U}$. □

APPENDIX I

PROOF OF THEOREM 3.3.8

Proof. Consider the model (3.3.15) with $m_w = \bar{m}_w,\ m_u = \bar{m}_u,\ q = 0$ and $\mathcal{R}_U > 1$. Also, let $\tilde{\mathcal{R}}_{0W} \leq \frac{1}{\mathcal{R}_U(1-\bar{m}_w)} < 1$. Further, consider the Lyapunov function

$$V = b_f\sigma_m A_W + (\sigma_m + \mu_a)F_W.$$

so that the derivative of V with respect to t is given by

$$\begin{aligned}
\frac{dV}{dt} &= b_f\sigma_m\frac{dA_W}{dt} + (\sigma_m+\mu_a)\frac{dF_W}{dt}\\
&= b_f\sigma_m v_w\phi_w\psi_w\left(1-\frac{A_U+A_W}{K_A}\right)F_W - b_f\sigma_m(\sigma_m+\mu_a)F_W\\
&+b_f\sigma_m(\sigma_m+\mu_a)F_W - (\sigma_m+\mu_a)\theta_w\mu_{uf}F_W\\
&< b_f\sigma_m v_w\phi_w\psi_w\left(1-\frac{A_U}{K_A}\right)F_W - (\sigma_m+\mu_a)\theta_w\mu_{uf}F_W\\
&= \theta_w\mu_{uf}(\sigma_m+\mu_a)F_W\left[\frac{b_f\sigma_m v_w\phi_w\psi_w}{\theta_w\mu_{uf}(\sigma_m+\mu_a)}\left(1-\frac{A_U}{K_A}\right)-1\right]\\
&= \theta_w\mu_{uf}(\sigma_m+\mu_a)F_W\left[\frac{b_f\sigma_m\phi_u\psi_u}{\mu_{uf}(\sigma_m+\mu_a)}\frac{v_w\phi_w\psi_w}{\theta_w\phi_u\psi_u}\left(1-\frac{A_U}{K_A}\right)-1\right]\\
&= \theta_w\mu_{uf}(\sigma_m+\mu_a)F_W\left[\bar{\mathcal{R}}_{0W}\mathcal{R}_U(1-\bar{m}_w)\left(1-\frac{A_U}{K_A}\right)-1\right]\\
&< \theta_w\mu_{uf}(\sigma_m+\mu_a)F_W\left[\bar{\mathcal{R}}_{0W}\mathcal{R}_U(1-\bar{m}_w)-1\right] \qquad (.0.1)\\
&= \theta_w\mu_{uf}(\sigma_m+\mu_a)\mathcal{R}_U(1-\bar{m}_w)F_W\left[\bar{\mathcal{R}}_{0W}-\frac{1}{\mathcal{R}_U(1-\bar{m}_w)}\right] \qquad (.0.2)\\
&\leq 0 \ \text{ for } \ \tilde{\mathcal{R}}_{0W} \leq \frac{1}{\mathcal{R}_U(1-\bar{m}_w)} < 1. \qquad (.0.3)
\end{aligned}$$

Thus, $\frac{dV}{dt} \leq 0$ whenever $\bar{\mathcal{R}}_{0W} \leq \frac{1}{\mathcal{R}_U(1-\bar{m}_w)}$ with $\frac{dV}{dt} = 0$ if and only if $F_W = 0$. Let

$$\mathcal{L} = \{\mathbf{x}\in\mathcal{D}|\frac{dV}{dt}(\mathbf{x}) = 0\}\backslash\{\mathcal{T}_{0\diamond}\} = \{\mathbf{x}\in\mathcal{D}|F_W = 0\}\backslash\{\mathcal{T}_{0\diamond}\}.$$

Since V is positive definite function and the set $\mathcal{L}$ does not contain any equilibria of the system besides the equilibria $\mathcal{T}_{1\diamond}$ when $\bar{m}_w < \frac{\mathcal{R}_U-1}{\mathcal{R}_U}$ ($\mathcal{T}_{0\diamond}$ is unstable, by Theorem 3.3.6) then by the LaSalle's invariance principle [76] as $t\to\infty$, then $A_W\to 0$, $F_W\to 0$, $M_W\to 0$, $A_U\to A_U^*$, $F_U\to F_U^*$ and $M_U\to M_U^*$. Hence, the equilibria $\mathcal{T}_{1\diamond}$ is globally asymptotically stable when $\bar{\mathcal{R}}_{0W} \leq \frac{1}{\mathcal{R}_U(1-\bar{m}_w)} < 1$. □

APPENDIX J

CODES

```
#install.packages("deSolve")
#install.packages("sfsmisc")

require("deSolve")
require("sfsmisc")
par(pch=20)

#########################################################
#########################################################
# this function gets passed to the ODEsolve package
#########################################################
zikafunc=function(t,x,vparameters){

  SE=x[1]
  IE=x[2]
  SL=x[3]
  IL=x[4]
  SP=x[5]
  IP=x[6]
  SM=x[7]
  IM=x[8]
  SH=x[9]
  EH=x[10]
  IH=x[11]
  RH=x[12]
  IHC=x[13]

  if(IH<0) IH=0 # this is a cross check to ensure that we always
  have sensical values of I
  if(EH<0) EH=0
  if(IM<0) IM=0
  if(IE<0) IE=0
  if(IL<0) IL=0
  if(IP<0) IP=0



  with(as.list(vparameters),{

      NH=SH+EH+IH+RH
dSE=phiV*(1-(SM+IM)/KV)*(SM+(1-r)*IM)-(sigmaE+muE)*SE
dIE=r*phiV*(1-(SM+IM)/KV)*IM-(sigmaE+muE)*IE
dSL=sigmaE*SE-(sigmaL+muL)*SL
dIL=sigmaE*IE-(sigmaL+muL)*IL
dSP=sigmaL*SL-(sigmaP+muP)*SP
dIP=sigmaL*IL-(sigmaP+muP)*IP
dSM=fV*sigmaP*SP-(betaV*aV*IH/NH)*SM-muV*SM
dIM=fV*sigmaP*IP+(betaV*aV*IH/NH)*SM-muV*IM
dSH=PIH+alphaH*(SH+EH+RH+(1-q)*IH)-(betaH*aV*IM/NH)*SH-muH*SH
 dEH=(betaH*aV*IM/NH)*SH+q*alphaH*IH-(sigmaH+muH)*EH
 dIH=sigmaH*EH-(gammaH+muH+deltaH)*IH
 dRH=gammaH*IH-muH*RH
 dIHC=sigmaH*EH
```

```
out = c(dSE,dIE,dSL,dIL,dSP,dIP,dSM,dIM,dSH,dEH,dIH,dRH,dIHC)
    list(out)
  })
}


################################################
################################################
################################################
zikainf = read.table("Data_dengue.txt",header=F,sep="")
################################################
# Initial Values
################################################
SE_0  =0
IE_0  = 0
SL_0  = 5
IL_0 = 2
SP_0 = 1
IP_0 = 1
SM_0 = 90000
IM_0 =5
SH_0 = 100000
EH_0=5
#IH_0=runif(1,1,10)
RH_0=0
IHC_0=1
# Parameter values
################################################
sigmaE=0.2
muE=0.2
sigmaL=0.2
muL=0.2
sigmaP=0.3
muP=0.2
fV=0.6
#sigmaH=0.3
muH=0.000042
deltaH=0.1
gammaH=0.2
r=0.1
alphaH=0.000041
q=0.1
PIH=50
#betaV=0.4
#phiV=1.80
muV=0.04
# KV=100000
# aV=0.1
# betaH=0.4


vtime = seq(1,360,30)  #
################################################
vsigmaE=numeric(0)
vmuE=numeric(0)
vsigmaL=numeric(0)
vmuL=numeric(0)
```

```
vsigmaP=numeric(0)
vmuP=numeric(0)
vfV=numeric(0)
vsigmaH=numeric(0)
vmuH=numeric(0)
vdeltaH=numeric(0)
vgammaH=numeric(0)
vr=numeric(0)
valphaH=numeric(0)
vq=numeric(0)
vPIH=numeric(0)
vbetaV=numeric(0)
vphiV=numeric(0)
vmuV=numeric(0)
vKV=numeric(0)
vaV=numeric(0)
vbetaH = numeric(0)

SE_bestfit = numeric(0)
IE_bestfit = numeric(0)
SL_bestfit = numeric(0)
IL_bestfit = numeric(0)
SP_bestfit = numeric(0)
IP_bestfit = numeric(0)
SM_bestfit = numeric(0)
IM_bestfit = numeric(0)
SH_bestfit = numeric(0)
EH_bestfit = numeric(0)
IH_bestfit = numeric(0)
RH_bestfit = numeric(0)
IHC_bestfit = numeric(0)


vpearsonsq = numeric(0)
# this will containt the pearson chi
#squared statistic calculated for the

upperbound =1e30 # this control the maximum differences
#between the data and model's outcome


niter = 500 # number of different alphaN and deltaM
#hypotheses we should test
for (iter in 1:niter)
{
  if (iter %%100==0) cat("Doing iteration ",iter," out of ",niter,"\n")
  # inform user the script is doing something, and not hung
  #beta1 = runif(1,0,1)
  #beta2 = runif(1,0,1)



  ##############################################
  ##############################################
  vparameters = c(sigmaE=sigmaE,muE=muE,sigmaL=sigmaL, muL=muL,
                  sigmaP=sigmaP,
```

```
                        muP=muP,muP=muP,
      fV=fV,sigmaH=sigmaH,muH=muH,deltaH=deltaH,gammaH=gammaH,r=r,
      alphaH=alphaH,
      q=q, PIH=PIH,betaV=betaV,phiV=phiV,muV=muV, aV=aV,
      betaH=betaH,KV=KV)
  #I2_0 =I1_0*c;
  inits = c(SE =SE_0,IE=IE_0,SL=SL_0,IL=IL_0,SP=SP_0,IP=IP_0,
            SM=SM_0,IM=IM_0
             ,SH=SH_0,EH=EH_0,IH=IH_0,RH=RH_0,IHC=IHC_0)
  if (vtime<31){
    aV=0.01
     else if (30<vtime<61){
      aV=0.5
}

   betaH = runif(1,0.01,0.5)
  KV = runif(1,91000,100000)     # randomly sample
                                  #alphaN uniformly
  aV = runif(1,0.01,0.2)    # randomly sample PS uniformly
  sigmaH=runif(1,0.1,0.3)
  phiV=runif(1,0.01,5)
  betaV=runif(1,0.01,0.8)
  IH_0=runif(1,1,20)
  zikamodel = as.data.frame(lsoda(inits, vtime,
                                  zikafunc,
                                  vparameters))
  # this numerically solves the SIR model
  # alphaN*Pmin*r
  #alphaM*k
  ######################################

  SE_pred = zikamodel$SE
  IE_pred = zikamodel$IE
  SL_pred = zikamodel$SL
  IL_pred = zikamodel$IL
  SP_pred = zikamodel$SP
  IP_pred = zikamodel$IP
  SM_pred = zikamodel$SM
  IM_pred = zikamodel$IM
  SH_pred = zikamodel$SH
  EH_pred = zikamodel$EH
  IH_pred = zikamodel$IH
  RH_pred = zikamodel$RH
  IHC_pred = zikamodel$IHC

  y_pred=numeric(0)
  Weeks=zikainf[[1]]
  for (i in 1:11){
    y_pred[1] = IHC_pred[1]
    y_pred[i+1]=IHC_pred[i+1]-IHC_pred[i]
  }
  y_pred

  ######################################################
  ##################################################
  # calculate the Pearson chi squares statistic
  ######################################################
```

```
  P_chi_sq    = sum(((y_pred)-zikainf[[2]])^2/(y_pred))

  vsigmaE =append(vsigmaE,sigmaE)
  vmuE=append(vmuE,muE)
  vsigmaL=append(vsigmaL,sigmaL)
  vsigmaP=append(vsigmaP,sigmaP)
  vmuP=append(vmuP,muP)
  vfV=append(vfV,fV)
  vsigmaH=append(vsigmaH,sigmaH)
  vmuH=append(vmuH,muH)
  vdeltaH=append(vdeltaH,deltaH)
  vgammaH=append(vgammaH,gammaH)
  vr=append(vr,r)
  valphaH=append(valphaH,alphaH)
  vq=append(vq,q)
  vPIH=append(vPIH,PIH)
  vbetaV=append(vbetaV,betaV)
  vphiV=append(vphiV,phiV)
  vmuV=append(vmuV,muV)
  vKV=append(vKV,KV)
  vaV=append(vaV,aV)
  vbetaH=append(vbetaH,betaH)

  vpearsonsq = append(vpearsonsq,P_chi_sq)

  if (P_chi_sq < upperbound){
    upperbound = P_chi_sq
    y_bestfit=y_pred
    SE_bestfit  = SE_pred
    IE_bestfit  = IE_pred
    SL_bestfit  = SL_pred
    IL_bestfit  = IL_pred
    SP_bestfit  = SP_pred
    IP_bestfit  = IP_pred
    SM_bestfit  = SM_pred
    IM_bestfit  = IM_pred
    SH_bestfit  = SH_pred
    EH_bestfit  = EH_pred
    IH_bestfit  = IH_pred
    RH_bestfit  = RH_pred
    IHC_bestfit  = IHC_pred


    ##########################################

    par(mfrow=c(1,1))
    plot(zikainf[[1]],zikainf[[2]]
         #,ylim=c(0,1.3*max(zikainf[[3]]))
         ,xlab="Weeks"
         ,ylab="Number of Cases because of Zika"
         ,cex=1)
 lines(zikainf[[1]],y_bestfit,col=2,lwd=3) # overlay the model
 points(zikainf[[1]],zikainf[[2]],cex=1,col=1)
legend("topleft",legend=c("Data","Pearson Chi
            squares best-fit prediction"),col=c(1,2),
lwd=3,bty="n", cex=0.7)
  }
```

```
}

setwd("C:/Users/Rahim/Dropbox/Research-AR/R_files/R_codes")


betagal.abs =read.table("data_dengue_chiang.txt",header=F,sep="")
cell.density = read.table("aV_data_dengue.txt",header=F,sep="")
time = cell.density$V1


## add extra space to right margin of plot within frame
par(mar=c(5, 4, 4, 6) + 0.1)

## Plot first set of data and draw its axis
plot(time, betagal.abs$V3, pch=16, axes=FALSE, xlab="", ylab="",
     type="b",col="black") # main="Mike's test data"
axis(2, ylim=c(0,1),col="black",las=1)  ## las=1 makes horizontal labels
mtext("Dengue cases (per 100,000)",side=2,line=2.5)
box()

## Allow a second plot on the same graph
par(new=TRUE)

## Plot the second plot and put axis scale on right
plot(time, cell.density$V3, pch=15,  xlab="", ylab="",
     axes=FALSE, type="b", col="red",cex.axis=1.2)
## a little farther out (line=4) to make room for labels
mtext("Fitted biting rate",side=4,col="red",line=3)
axis(4, col="red",col.axis="red",las=1,cex.axis=1)

## Draw the time axis
#axis(1,pretty(range(time),10))
axis(1, at=1:12, labels=c("Jan","Feb","Mar", "Apr","May","June","July","
    Aug","Sep","Oct",
                          "Nov","Dec"),cex.axis=1.1)
mtext("",side=1,col="black",line=2)

## Add Legend
legend("topright",legend=c("Ddata","Fitted biting rate"),
       text.col=c("black","red"),pch=c(16,15),col=c("black","red"),cex
           =0.82)

setwd("C:/Users/Rahim/Dropbox/Research-AR/R_files/R_codes")


data1 = read.table("data_dengue_chiang.txt",header=F,sep="")
pred1=read.table("pred_simulation.txt",header=F,sep="")
plot(data1$V1,data1$V3,pch=1,xaxt = 'n',type="b",col="black",xlab="",
     ylab="Average monthly  number of infected humans",cex.lab=1,ylim=c
         (0,90),cex.axis=1.2)
points(pred1$V1,pred1$V3,pch=22,cex=1.2,type="b",col='red')
axis(1, at=1:12, labels=c("Jan","Feb","Mar", "Apr","May","June",
                          "July","Aug","Sep","Oct","Nov","Dec"),cex.axis
                              =1.2)
legend("topright",legend=c("Data","Model"), pch=c(1,22),
       text.col=c("black","red"),col=c("black","red"),cex=1)
```

```
#a = -8/3 ; b <- -10; c <- 28
library(deSolve)

sigmaE=0.3
muE=0.2
sigmaL=0.2
muL=0.2
sigmaP=0.2
muP=0.2
fV=0.5
sigmaH=0.2
muH=0.000042
deltaH=0.15
gammaH=0.4
r=0.1
alphaH=0.000045
q=0.1
PIH=40
KV=100000

# Jan
#T=20 ;aV=0.05
#  yini=c(SE=100,IE=1,SL=50,IL=1,SP=30,IP=1,SM=90000,IM=2,SH=100000,EH=1,
    IH=1,RH=0,IHC=1)
#ICH= 3.187842


#Feb
#T=22.9 ;aV=0.01
#yini=c(SE=67860,IE=1,SL=50661.337,IL=1,SP=26812.0905,IP=1,SM=88217.16,
     IM=2,SH=101208.3,EH=1,IH=1,RH=0,IHC=3)
#ICH=4.318234



#Mar
#T=26 ;aV=0.01
#yini=c(SE=96879.99,IE=1,SL=66446.77,IL=1,SP=30356.20,IP=1,SM=88888.80,
     IM=2,SH=102417.1,EH=1,IH=1,RH=2,IHC=)
#ICH=6.407475


#Apr
#T=28 ;aV=0.09
 #yini=c(SE=100,IE=1,SL=50,IL=1,SP=30,IP=1,SM=90000,IM=2,SH=100000,EH
      =1,IH=1,RH=0,IHC=5)
#ICH=10.85838

#May
#  T=28.1 ;aV=0.15
#  yini=c(SE=119431.57,IE=1,SL=87839.62,IL=1,SP=38536.05,IP=2,SM
    =91210.37,IM=2,SH=100000,EH=1,IH=3,RH=0,IHC=5)
#ICH=19.09147
```

```
#June
# T=27 ;aV=0.12
#yini=c(SE=99000,IE=1,SL=50,IL=1,SP=32543.059,IP=3,SM=102607.86,IM=9,SH
    =100000,EH=9,IH=6,RH=0,IHC=18)
# ICH=58.73268


#July
# T=26 ;aV=0.15
#yini=c(SE=44059.532,IE=10,SL=11637.887,IL=5,SP=5481.911,IP=3,SM=90000,
    IM=12,SH=100000,EH=1,IH=10,RH=0,IHC=35)
#IHC=88.73038


#Aug
#T=26.6; aV=0.1
#yini=c(SE=44059.532,IE=10,SL=11637.887,IL=5,SP=5481.911,IP=3,SM=90000,
    IM=12,SH=100000,EH=1,IH=10,RH=0,IHC=45)
#IHC=76.52697

#Sep
#T=26; aV=0.05
#   yini=c(SE=44059.532,IE=10,SL=11637.887,IL=5,SP=5481.911,IP=3,SM
    =90000,IM=5,SH=100000,EH=2,IH=1,RH=0,IHC=50)
#IHC=58.11852

#Oct
# T=25.8; aV=0.03
#   yini=c(SE=44059.532,IE=10,SL=11637.887,IL=5,SP=5481.911,IP=1,SM
    =90000,IM=2,SH=100000,EH=0,IH=1,RH=0,IHC=30)
#IHC=31.72397

#Nov
#T=23.8 ;aV=0.02
#   yini=c(SE=44059.532,IE=10,SL=11637.887,IL=5,SP=5481.911,IP=1,SM
    =90000,IM=2,SH=100000,EH=0,IH=1,RH=0,IHC=25)
# IHC=25.98196

# Dec
#T=21 ;aV=0.02
# yini=c(SE=44059.532,IE=10,SL=11637.887,IL=5,SP=5481.911,IP=1,SM
    =90000,IM=2,SH=100000,EH=0,IH=1,RH=0,IHC=10)
#IHC=10.73338

#aV=0.0943+0.0043*T # for 21<T<32
 #aV=0.1
betaH=0.001044*T*(T-12.286)*sqrt(32.461-T) # for 12.4<T<32.5
# betaH
betaV=-0.9037+0.0729*T # for 12.4<T<26.1 otherwise 1
#betaV
phiV=-15.837+1.2897*T-0.0163*T^2  # 15<T<30 otherwise 0
#phiV
muV=0.8692-0.159*T+0.01116*T^2-3.408*10^(-4)*T^3+3.809*10^(-6)*T^4 #
    for 10.54<T<33.4
#muV=
```

```
#yini <- c(X = 1, Y = 1, Z = 1)
 #yini=c(SE=0,IE=0,SL=0,IL=0,SP=0,IP=0,SM=90000,IM=2,SH=100000,EH=1,IH
     =1,RH=0,IHC=5)

Lorenz <- function (t, y, parms) {
  with(as.list(y), {
    NH=SH+EH+IH+RH
    dSE=phiV*(1-(SM+IM)/KV)*(SM+(1-r)*IM)-(sigmaE+muE)*SE
    dIE=r*phiV*(1-(SM+IM)/KV)*IM-(sigmaE+muE)*IE
    dSL=sigmaE*SE-(sigmaL+muL)*SL
    dIL=sigmaE*IE-(sigmaL+muL)*IL
    dSP=sigmaL*SL-(sigmaP+muP)*SP
    dIP=sigmaL*IL-(sigmaP+muP)*IP
    dSM=fV*sigmaP*SP-(betaV*aV*IH/NH)*SM-muV*SM
    dIM=fV*sigmaP*IP+(betaV*aV*IH/NH)*SM-muV*IM
    dSH=PIH+alphaH*(SH+EH+RH+(1-q)*IH)-(betaH*aV*IM/NH)*SH-muH*SH
    dEH=(betaH*aV*IM/NH)*SH+q*alphaH*IH-(sigmaH+muH)*EH
    dIH=sigmaH*EH-(gammaH+muH+deltaH)*IH
    dRH=gammaH*IH-muH*RH
    dIHC=sigmaH*EH
    list(c(dSE, dIE, dSL,dIL,dSP,dIP,dSM,dIM,dSH,dEH,dIH,dRH,dIHC))
  })
}
times =seq(from = 1, to = 31, by = 1)
out = ode(y = yini, times = times, func = Lorenz, parms = NULL)
plot(out[,13],pch=21)
out[,14]
IHC=out[31,14];iniIH=out[31,14]-out[30,14]
out
IHC
iniIH

clc;
clear;
global r
global z

% r=linspace(0,1,350/0.1)
% Ysol=zeros(3500,4);

r=linspace(0,1,10);
%Ysol=zeros(10,1);

SE0=10000;
IE0=500;
SL0=5000;
IL0=200;
SP0=3000;
IP0=100;
SM0=150000;
IM0=1000;
SH0=170000;
EH0=600;
IH0=400;
RH0=200;
INTIM0=0;
```

```
INTEH0=0;
y0=[SE0;IE0;SL0;IL0;SP0;IP0;SM0;IM0;SH0;EH0;IH0;RH0;INTIM0;INTEH0]; #NEW


tim=linspace(0,350,10);
for z= 1:length(r)
 [T,Y]=ode45(@denguetemp,tim,y0);
 Ysol(:,z)=Y(:,14);
end
%figure(1)
%plot(T,Ysol(:,4),'r',T,Ysol(:,3),'k',T,Ysol(:,2),'b',T,Ysol(:,2),'g',T,
    Ysol(:,1),'c');
%  set(0, 'DefaultTextInterpreter', 'Latex')
% legend('r=0.5','r=0.333','r=0.166','r=0','location','northeast')
% ylabel('Total number of infected mosquitoes','fontsize',16)
% xlabel('Time (days)','fontsize',16)
%  axis tight
% for j=2:20:100
%  plot(r,Ysol(j,:))
%  hold on
% end
set(0, 'DefaultTextInterpreter', 'Latex')
% plot3(T,r,Ysol(:,1),T,r,Ysol(:,2),T,r,Ysol(:,3), T,r,Ysol(:,4))
%  ylabel('$r$','fontsize',16)
%   xlabel('Time (days) ','fontsize',16)
%    zlabel('Cumulative number of new infected mosquitoes','fontsize',16)
% legend('d','f','h')
% plot(r,Ysol(5,:),'g',r,Ysol(10,:),'c',r,Ysol(15,:),'b',r,Ysol(20,:),'k'
    ,r,Ysol(25,:),'r')
legend('ef','r=0.333','r=0.166','r=0','location','northeast')
A=[Ysol];
plot3(T,r,A)
xlabel('Time (days)')
ylabel('$r$')
title('$T=30^{\circ}$C')
zlabel('Cumulative number of new infected humans','fontsize',15)

function s=LHS_Call(xmin,xmean,xmax,xsd,nsample,distrib,logscale)
% s=latin_hs(xmean,xsd,nsample,nvar)
% LHS from normal distribution, no correlation
% method of Stein
% Stein, M. 1987.
%Large Sample Properties of Simulations Using Latin Hypercube Sampling.
%     Technometrics 29:143-151

if nsample==1
    s=xmean;
    return
end
if nargin<6
    logscale=1e3;
    distrib='unif';
end
if nargin<7
    logscale=1e3;
end
```

```
[sample,nvar]=size(xmean);
if distrib == 'norm' % you only need to specify xmean & xsd
    rand('twister',sum(100*clock));
    ran=rand(nsample,nvar); % rand('twister',sum(100*clock))
    s=zeros(nsample,nvar);
    %method of Stein
    for j=1: nvar
        idx=randperm(nsample);
        P=(idx'-ran(:,j))/nsample; % probability of the cdf
        %SQRT(2) * ERFINV(2*P-1)
        s(:,j) = xmean(j) + sqrt(2)*erfinv(2*P-1).* xsd(j);
% this can be replaced by any inverse distribution function
 %s(:,j) = xmean(j) + ltqnorm(P).* xsd(j);
 % this can be replaced by any inverse distribution function
    end
end


if distrib == 'unif% you only need to specify xmin & xmax
    if xmin==0
        xmin=1e-300;
    end
    nvar=length(xmin);
    %rand('twister',sum(100*clock));
    ran=rand(nsample,nvar);
    s=zeros(nsample,nvar);
    for j=1: nvar
        idx=randperm(nsample);
        P =(idx'-ran(:,j))/nsample;
        xmax(j);
        xmin(j);
        xmax(j)/xmin(j);
 if (xmax(j)<1 & xmin(j)<1) || (xmax(j)>1 & xmin(j)>1)
            'SAME RANGE';
   if (xmax(j)/xmin(j))<logscale%1e3
%% It uses the log scale if the order
%of magnitude of [xmax-xmin] is bigger than 1e2,
                '<1e3: LINEAR SCALE';
               s(:,j) = xmin(j) + P.* (xmax(j)-xmin(j));
       else
                '>=1e3: LOG SCALE';
           s(:,j) = log(xmin(j)) + P.*abs(abs(log(xmax(j)))-abs(log(xmin(
              j))));
            s(:,j) = exp(s(:,j));
            end
        else
            'e- to e+';
    if (xmax(j)/xmin(j))<logscale%1e3
%It uses the log scale if the order of magnitude of [xmax-xmin] is bigger
    than 1e2,
                '<1e3: LINEAR SCALE';
          s(:,j) = xmin(j) + P.* (xmax(j)-xmin(j));
         else
            '>=1e3: LOG SCALE';
    s(:,j) = log(xmin(j)) + P.*abs(log(xmax(j))-log(xmin(j)));
          s(:,j) = exp(s(:,j));
          end
```

```
        end
    end
end
hist(s);
```

Codes for Chapter 2

```
% Code for simulating the effects
of periodic releases of sterile males on a mosquito population
% Modified by Jay Taylor from code by Enahoro Iboi

% Requires an auxiliary file sterile_ODE.m

clear all

global ci z
ci= 0.5;


C_R = [10000,10000];% number of sterile males released at a time
pre = 0.01;      % number of years without sterile male releases (burn-in
    period)
dur = 1;           % number of years with sterile male releases
T_pre = pre*365;      % length of burn-in period in days
T_release = dur*365;   % length of treatment period in days
T_total = T_pre + T_releas % total length of simulated period in days
period = 21;           % days between successive sterile male releases
num_releases = floor(T_release/period);% number of releases in treatment
    period

impulse = zeros(1,14);
impulse([4  6]) = C_R;  % only sterile males are released

% Loop over values of v (or some other parameter to be varied)
for z = 1:length(ci)
    T1=[];    % time vector
    Y1=[];    % solution vector (with periodic releases of sterile males)
    Y0=[];  % solution vector (without periodic releases of sterile males
        )
    I1=[];  % vector for integrated number of females (with releases)
    I0=[]; % vector for integrated number of females (without releases)

IC0=[10000,0,100000,0,100000,0,100,100000,5,4,0,100000,100000,100];
    % initial conditions for ODE's without releases
    IC =IC0;       % initial conditions for ODE's with releases
 %[10000,10000,10000,10000,10000,10000,7,100000,5,4,0]
    % The main loop solving the ODEs starts here:
    for i = 0:num_releases
        if i == 0
            tlb = 0;
            tub = T_pre;
        elseif i==num_releases
            tlb = T_pre + (num_releases-1)*period;
            tub = T_total;
        else
            tlb = T_pre + (i-1)*period;
            tub = T_pre + i*period;
        end
```

```
        tspan1 = [tlb :0.05: tub];

        % solve equations with periodic releases of sterile males
        [T,Y] = ode15s(@sterile_ODE1CI,tspan1,IC);
        IC = Y(end,:)+impulse;
% update initial conditions with sterile male releases
        T1 = [T1;T];      % augment the time vector
        Y1 = [Y1;Y];    % augment the solution vector

        % solve equations without periodic releases of sterile males
        [T,Y] = ode15s(@sterile_ODE1CI,tspan1,IC0);
        IC0 = Y(end,:); % update initial conditions without releases
        Y0 = [Y0;Y]; % augment the solution vector

    end % for i

    % Calculate the release effect function R (White et al. 2010, eqn 5)
    I1par(:,z) = cumtrapz(T1,Y1(:,7));    % with releases
    I0par(:,z) = cumtrapz(T1,Y0(:,7));      % without releases
    Tpre_index = min(find(T_pre <= T1)); % index when releases begin
    eps = 0.000001;     % regularization
    I1par(:,z) = I1par(:,z) - I1par(Tpre_index,z) + eps;
    I0par(:,z) = I0par(:,z) - I0par(Tpre_index,z) + eps;
    R(:,z) = I1par(:,z)./I0par(:,z);

    Y1z(:,:,z) = Y1;% save the complete solution to Y1z (with releases)
    Y0z(:,:,z) = Y0;% save the complete solution to Y0z (without releases
        )

end % for z



% Plot the total number of mated females




% Plot all of the life stages
z = 1;

figure(1)
set(0,'defaulttextinterpreter','latex')

%subplot(1,1,1)
plot(T1,Y1z(:,7,1),T1,Y1z(:,10,1),'LineWidth',2)
set(gca,'FontSize',18);
%title('$c_i=0.5$');
%xl=xline(730 ,'-.','fontsize',10,'LineWidth',3);
ylabel('Number of dengue-infected female mosquitoes and humans',
'fontsize',17);
xlabel('Time (days)','fontsize',18);
legend('F_D','I_H')
%xl.LabelVerticalAlignment = 'bottom';
figure(2)
%subplot(1,1,2)
plot(T1,Y1z(:,5,1),T1,Y1z(:,6,1),'LineWidth',2)
```

```
title('$c_i=0.5$');
set(gca,'FontSize',18);
set(gca,'FontSize',18);
xl=xline(730 ,'-.','fontsize',10,'LineWidth',3);
ylabel('Number of adult male mosquitoes','fontsize',18);
xlabel('Time (days)','fontsize',18);
legend('M_U','M_W')
xl.LabelVerticalAlignment = 'bottom';
%subplot(2,2,3)
figure(3)
plot(T1,Y1z(:,14,1))
ylabel('f total')
figure(4)
plot(T1,Y1z(:,14,1))
ylabel('m total')
%xlabel('Time (days)','fontsize',16);
%ylabel('$M_U$, $M_W$','fontsize',16);
%legend('M_U','M_W')

%subplot(2,2,4)
%plot(T1,Y1z(:,7,1),T1,Y1z(:,10,1))
%xlabel('Time (days)','fontsize',16);
%label('$F_D$, $I_H$','fontsize',16);
%legend('F_D','I_H')

%sterile
function ydot = sterile_ODE1CI(t,x)

global ci z


bf = 1/2; phiu = 8; psiu = 0.5; phiw = 3; psiw = 0.4; mua = 0.1e-2;
muuf = 1/17; muum = 1/9;  betaH = .7; betaV = .7; sigmaH = .15;
gamma1H = .2; sigmam = 1/5; q = .2;  thetaw = 1.1; Ka = 120000; vw=0.75;
pih=100;muh=0.000042; sigmah=0.15;gammah=0.2; aV=0.19;

% x1=Au; x2=Aw; x3=Fu; x4=Fw; x5=Mu; x6=Mw;x7=Fd;x8=Sh;x9=Eh;x10=Ih;x11=
    Rh

Mw=x(6)/(x(5)+x(6)+1);
M_u=x(5)/(x(5)+x(6)+1);
%%%%
Buu=phiu*psiu*M_u*x(3)*(1-(x(1)+x(2))/Ka);
Bdu=phiu*psiu*M_u*x(7)*(1-(x(1)+x(2))/Ka);
Bwu=phiw*psiw*M_u*x(4)*(1-(x(1)+x(2))/Ka);
Bww=phiw*psiw*Mw*x(4)*(1-(x(1)+x(2))/Ka);
Buw=(1-ci)*phiw*psiw*Mw*x(3)*(1-(x(1)+x(2))/Ka);
Bdw=(1-ci)*phiw*psiw*Mw*x(7)*(1-(x(1)+x(2))/Ka);
% vector field for the ODE

ydot=zeros(14,1);
ydot(1)= Buu+(1-vw)*(Bwu+Bww+Buw+Bdw)+Bdu-sigmam*x(1)-mua*x(1);
ydot(2)=vw*(Bwu+Bww+Buw+Bdw)-sigmam*x(2)-mua*x(2);
ydot(3)=bf*sigmam*x(1)-aV*betaV*x(3)*x(10)/(x(8)+x(9)+x(10)+x(11))-q*Mw*x
    (3)-muuf*x(3);
ydot(4)=bf*sigmam*x(2)+q*Mw*x(3)-thetaw*muuf*x(4);
ydot(5)=(1-bf)*sigmam*x(1)-muum*x(5);
```

```
ydot(6)=(1-bf)*sigmam*x(2)-muum*x(6);
ydot(7)=aV*betaV*x(3)*x(10)/(x(8)+x(9)+x(10)+x(11))-muuf*x(7);
ydot(8)=pih-aV*betaH*x(7)*x(8)/(x(8)+x(9)+x(10)+x(11))-muh*x(8);
ydot(9)=aV*betaH*x(7)*x(8)/(x(8)+x(9)+x(10)+x(11))-sigmah*x(9)-muh*x(9);
ydot(10)=sigmah*x(9)-gammah*x(10)-muh*x(10);
ydot(11)=gammah*x(10)-muh*x(11);
ydot(12)=bf*sigmam*x(1);
ydot(13)=(1-bf)*sigmam*x(1);
ydot(14)=(1-bf)*sigmam*x(10);



% Original formulation
% sigmaL1=4*(D-(sigmaE).^(-1)-(sigmaP).^(-1)).^(-1);
% sigmaL2=4*(D-(sigmaE).^(-1)-(sigmaP).^(-1)).^(-1);
% sigmaL3=4*(D-(sigmaE).^(-1)-(sigmaP).^(-1)).^(-1);
% sigmaL4=4*(D-(sigmaE).^(-1)-(sigmaP).^(-1)).^(-1);
```